Undisturbed Sampling of Cohesionless Soil for Evaluation of Mechanical Properties and Micro-structure

by

Kanyembo Katapa

A Thesis Presented in Partial Fulfillment
of the Requirements for the Degree
Master of Science

Approved July 2011 by the
Graduate Supervisory Committee:

Edward Kavazanjian Jr., Chair
Claudia Zapata
Sandra Houston

ARIZONA STATE UNIVERSITY

August 2011

ABSTRACT

As a prelude to a study on the post-liquefaction properties and structure of soil, an investigation of ground freezing as an undisturbed sampling technique was conducted to investigate the ability of this sampling technique to preserve soil structure and properties. Freezing the ground is widely regarded as an appropriate technique to recover undisturbed samples of saturated cohesionless soil for laboratory testing, despite the fact that water increases in volume when frozen. The explanation generally given for the preservation of soil structure using the freezing technique was that, as long as the freezing front advanced uni-directionally, the expanding pore water is expelled ahead of the freezing front as the front advances. However, a literature review on the transition of water to ice shows that the volume of ice expands approximately nine percent after freezing, bringing into question the hypothesized mechanism and the ability of a frozen and then thawed specimen to retain the properties and structure of the soil in situ. Bench-top models were created by pluviation of sand. The soil in the model was then saturated and subsequently frozen. Freezing was accomplished using a pan filled with alcohol and dry ice placed on the surface of the sand layer to induce a unidirectional freezing front in the sample container. Coring was used to recover frozen samples from model containers. Recovered cores were then placed in a triaxial cell, thawed, and subjected to consolidated undrained loading. The stress-strain-strength behavior of the thawed cores was compared to the behavior of specimens created in a split mold by pluviation and then saturated and sheared

without freezing and thawing. The laboratory testing provide insight to the impact of freezing and thawing on the properties of cohesionless soil.

DEDICATION

This thesis is dedicate to my father Mr. Julius M. Katapa who inspired me to pursue engineering and encouraged me to never stop learning.

To my mother Mrs. Loveness K. Katapa who has been a calming influence when everything seems to fall apart.

And to three of the best people in the world:

Tafwachi L. Chamunda, Kasumpa J.Z. Katapa, and Zanga P.K. Katapa

ACKNOWLEDGMENTS

I would like to express my sincere gratitude to my advisor, Dr. Edward Kavazanjian, Jr. for the opportunity to study under his instruction and leadership and for his guidance throughout my graduate school studies at Arizona State University. I want to thank 'Ed' for his patience during the course of this research and in the preparation of this thesis.

I would like to thank the members of my committee Dr. Sandra Houston and Dr. Claudia Zapata. It was a pleasure to be in their classes. I have learnt a lot from them. Their classes helped my gain a higher level of understanding of soil and geotechnical engineering.

Thanks to Peter Goguen for teaching me how to use the GCTS Cyclic Pneumatic Soil Triaxial System and for his assistance in setting up triaxial testing programs. I am especially thankful for his timely effort in keeping the equipment that I required, in working order and for ordering materials on time.

I want to also thank my fellow students Zbigniew 'David' Czupak, Pengbo Yuan, Mohamed Arab, and especially Elliot Bartel for their assistance throughout the course of this research.

Financial support provided by the Edward and Amelia Kavazanjian Fellowship is acknowledged.

Finally, I want to thank my wife Tafwachi L. Chamunda for her support throughout graduate school. My boys Kasumpa J. Katapa and Zanga P. Katapa were a source of inspiration that I cannot put into words.

TABLE OF CONTENTS

Page

LIST OF TABLES

Table Page

LIST OF FIGURES

Figure Page

Chapter 1

1.0 INTRODUCTION

The main objective of this work is to develop a method for recovering undisturbed samples of cohesionless soil from physical models. This work is part of a larger project to experimentally and numerically investigate the properties of resedimented cohesionless soil following earthquake induced liquefaction (Borja et al., 2008). Undisturbed samples of resedimented soil are required for laboratory stress-strain-strength tests and microstructural evaluations to achieve the project objectives.

To mitigate adverse effects of sample disturbance, cohesionless soils have to be stabilized prior to sampling. However, in order to conduct laboratory stress-strain-strength tests on the recovered samples, the stabilization method must be reversible. In this work, reversible methods of obtaining undisturbed samples of cohesionless soil are reviewed for application to the previously mentioned project. The technique selected for obtaining undisturbed samples of cohesionless soil from laboratory bench scale models for the larger project is described herein in detail. And finally, the quality of samples obtained using the selected method is evaluated using triaxial compression tests conducted on recovered samples.

1.1 Objectives

The objective of this study was to develop a method of obtaining undisturbed samples of cohesionless soil in order to evaluate their stress-strain-strength

properties and micro-structure (through post-stabilization imaging). In fulfilling this main objective, the following tasks were performed:

1. A practical method for preparing uniform soil deposits for the shake table and centrifuge tests to be conducted in the overall research program was developed.
2. A practical method of recovering intact and undisturbed samples of cohesionless soil from the physical models at the scale of models used for shake table and dynamic centrifuge experiments was developed.
3. The undisturbed nature of the intact samples recovered from physical models was investigated using triaxial compression tests.

1.2 Background

Extensive research has been performed on the process of earthquake induced liquefaction. However, the reverse process of resedimentation following liquefaction has received little attention. Earthquake induced liquefaction occurs when a soil with a well-defined soil skeleton subject to seismic loading undergoes changes and eventually behaves like a fluid. The process of resedimentation occurs when the soil particles in apparent suspension settle to once again form a well-defined soil skeleton. Much attention has been paid to studying liquefaction, as evidenced by the amount of information in the literature on the processes of liquefaction. Studies on resedimentation subsequent to liquefaction, however, are very rare.

The process of resedimentation generally involves different mechanisms from those involved in the processes of initial formation of a soil deposit, e.g. aeolian or alluvial deposition (Borja et al. 2008). Therefore, the structure of the resedimented soil is likely to be significantly different from the initial soil structure. Due to changes in structure, the resedimentation process may be expected to have profound effects on the properties of the soil. Subsequent to liquefaction, properties of the resedimented soil that may change include shear strength and stiffness. Both of these properties are expected to be related to the structure of the soil.

It is hypothesized by Borja et al. (2008) that resedimented soil has a heterogeneous structure, i.e. when a cohesionless soil liquefies, it is unlikely to settle into a homogenous structure and that this heterogeneous structure contributes to the post-liquefaction properties of the soil. The resulting heterogeneity could be of two types. The first type is due to non-uniform void ratio distribution, for example the presence of pockets of loose sand. The second type of heterogeneity is due to non-uniform particle gradation, for example, larger particles settling out faster than smaller particles.

The Borja et al. (2008) hypothesis regarding the post-liquefaction heterogeneity of soil will be investigated through an experimental program that will include shake table testing, dynamic centrifuge testing, micro-structural imaging tests, and laboratory stress-strain strength tests. Shake table and dynamic centrifuge testing will be used to liquefy soil layers. Undisturbed samples will be recovered from the liquefied soil layers. Imaging and laboratory tests will be

conducted on the post-liquefaction cohesionless samples recovered from shake table and centrifuge tests. Imaging will include X-ray computed tomography (XCT) and Bright Field Microscopy (BFM) on specimens solidified with optical grade epoxy subsequent to freezing. Laboratory tests will include triaxial compression tests on thawed specimens recovered from the physical models. Special recovery techniques will be required to preserve the structure and properties of the soil specimens recovered following liquefaction.

The techniques required to preserve the structure and properties of specimens of resedimented soil are the subject of this thesis. The quality of samples obtained from the physical models is paramount to the accuracy of the structural and stress-strain-strength evaluations performed on them. The imaging that will be conducted on recovered specimens will attempt to quantify the micro-structure of the resedimented soil. It is imperative that the sampling process does not change the microstructure from what it is subsequent to liquefaction. The study of heterogeneity of the resedimented soil cannot be performed on samples whose micro-structure in not preserved through the sampling process. The effect of disturbance on stress-strain-strength test is well documented in the literature. The disturbance effects must be minimized to obtain an accurate representation of the in situ stress-strain-strength behavior. The role of this study on the previously described larger project is to develop a reversible method of obtaining undisturbed samples from the physical centrifuge and shake table models for evaluation of stress-strain-strength properties and micro-structure.

1.3 Scope of work

Reversible stabilization methods for recovering undisturbed specimens of cohesionless soil for subsequent imaging and testing were reviewed in the initial phase of this study. Methods for preparing uniform soil deposits were also reviewed. Following the review of sample preparation methods, air pluviation was selected as the preferred technique. Following the review of methods, stabilization by freezing and sampling by coring was selected as the preferred method. Based on the previous research on sampling by freezing, a sampling method specific to this work was developed. The process developed and described in this work was designed for recovery of samples from physical models on the scale of shake table and centrifuge tests. Samples of cohesionless soil were successfully recovered from bench top models.

Following the development of specimen preparation, freezing, and sample recovery techniques, triaxial compression tests were performed on thawed specimens to demonstrate that the stress-strain-strength behavior of recovered samples was unaffected by the stabilization and sampling processes. A series of triaxial compression tests were performed on never frozen samples to provide a basis for comparison to the samples recovered using the techniques developed in this work. The test procedures and comparison results on never frozen and frozen and thawed samples are described in this work.

1.4 Organization of Thesis

This thesis is organized into the following five chapters including this introductory chapter:

Chapter 1 provides a brief background of the project to investigate the properties of cohesionless soil subsequent to liquefaction and how the project is related to the work presented in this thesis. The objectives, scope of the study and outline of the thesis are also included in this chapter.

Chapter 2 presents a review of the existing technical literature on the subject of undisturbed sampling of cohesionless soil. A review of reversible stabilization methods, including the use of sampling using biopolymers, Elmer's glue and freezing, is presented. Also presented in this chapter is a review of testing and analyses performed subsequent to stabilization and sampling to demonstrate the quality of samples obtained from the reviewed methods.

Chapter 3 presents descriptions of methods for preparation of cohesionless samples for laboratory testing. In this chapter, deposition methods for creating reconstituted samples of cohesionless soils and densification methods are described. Also presented in this chapter are the published properties of Ottawa sand.

Chapter 4 presents development of the technique to recover undisturbed samples of cohesionless soil for evaluation of mechanical properties and microstructure within the context of the larger project. Challenges encountered during the development of the technique are discussed in this chapter.

Chapter 5 presents the results of the tests performed to evaluate the quality of samples obtained using the developed sampling method. The results are analyzed and interpreted to reach reasonable conclusions.

Chapter 6 summarizes findings of the present work. Recommendations for future work in this area of research are also presented here.

Chapter 2

2.0 LITERATURE REVIEW

2.1 Introduction

Sampling of soil for laboratory testing has been a subject of interest since the early days of modern geotechnical engineering. The quality (representativeness) of laboratory test results for evaluating stress-strain-strength properties of soil, and by extension the quality of engineering evaluations based on these results, is dependent on the quality of samples obtained for these tests. Thus the objective for recovery of samples for laboratory evaluation of mechanical properties (stress-strain-strength properties) is to recover undisturbed samples. However, some level of disturbance during sampling may be inevitable due to 1) the changes in the stress state of soil that are created by removal of overburden and 2) particle reorientation from mechanical effects of sampling (pushing a sample tube in the ground). The less disturbed a sample is, the more closely the lab results reflect its in situ behavior.

According to Hvorslev (1949), "Undisturbed samples may be defined broadly as samples in which the material has been subjected to so little disturbance that it is suitable for all laboratory tests and thereby for approximate determination of strength, consolidation, and permeability characteristics and other physical properties of the material in situ".

Hvorslev (1949) suggested the following criteria for assessing the quality of relatively undisturbed samples suitable for laboratory tests:

1. No disturbance of the soil structure.

2. No change in water content or void ratio.
3. No change in constituents or chemical composition.

Mitchell (2008) has shown that freshly deposited cohesionless soil gains strength with time with no apparent disturbance to structure, void ratio change, or change in constituents, adding another dimension to the problem.

In geotechnical engineering, soils are typically divided into two broad categories: cohesive soils and cohesionless soils. Undisturbed sampling of cohesive soil is easier to achieve due to the internal cohesion of the cohesive soil (i.e. the resistance of the particles to rearrangement). Current methods for recovery of relatively undisturbed samples of cohesive soils generally employ thin walled Shelby tubes that are pushed into the soil at a slow rate or block samples obtained from test pits. The highest quality Shelby tube samples are generally recovered using 'fixed piston' types of samplers, e.g. Osterberg or Swedish foil samplers. Undisturbed samples of cohesive soils can also be obtained from large block samples cut out of the wall of test pits. However, but the depth from which such samples can be recovered is limited.

Recovery of undisturbed samples of cohesionless soils presents different problems compared to the recovery of undisturbed samples of cohesive soils due to the lack of internal cohesion to hold cohesionless soil particles together during sampling and transportation. It is difficult to recover undisturbed samples of cohesionless soil. Cohesionless soils have very little internal cohesion and thus the particles are subject to rearrangement (change in structure) during sampling.

In practice, samples of cohesionless soils are obtained using drive samplers. These samples are far from undisturbed. Their use is generally limited to laboratory index and classification tests, such as gradation and moisture content that are not sensitive to soil structure. Undisturbed sampling of cohesionless soil is not normally performed in practice. Geotechnical engineers rely on in-situ tests (such as the standard penetrometer tests) and empirical correlations to develop estimates of the undisturbed properties of cohesionless soil. A variety of methods may be used to obtain samples of cohesionless soil for classification and gradation tests. However, recovery of quality samples of cohesionless soils for micro-structure studies and stress-strain-strength determination is a difficult task. Recovery of undisturbed samples of cohesionless soil is usually attempted only for research purposes and is not typically attempted on routine geotechnical projects.

Several researchers have proposed methods to recover undisturbed samples of cohesionless soil for micro-structure studies and stress-strain-strength determination (Frost, 1982; Hvorslev, 1949; Schneider et al., 1989; Singh et al., 1982; and Yoshimi et al., 1978). The general procedure employed by most of these researchers is to first stabilize the soil, next extract the sample, and then remove (reverse) the stabilizing agent after transportation, trimming, and confining the specimen in a testing device. Reversible stabilization methods that have been investigated include biopolymers agar and agarose, Elmer's glue, and freezing. A review of each of these stabilization methods and its ability to produce undisturbed samples is presented herein.

2.2 Reversible Stabilization Methods

Reversible stabilization of cohesionless soil generally involves introduction of temporary cohesion into cohesionless soil without significant changes to its structure. The methods attempt to introduce cohesion to the soil by introducing a fluid into the pores that then solidifies in the case of agar, agarose, and Elmer's glue or that changes phase in the case of freezing. In any case, the common goal is to temporarily solidify the cohesionless soil to enable the soil to be sampled using conventional sampling methods that are used to sample cohesive soils and rocks. These stabilization methods have to be durable enough to allow handling, transportation, and trimming. The methods also have to be reversible so that the cohesionless soil can be restored to its original, or in-situ, state prior to laboratory testing for evaluation of stress-stain-strength properties.

2.2.1 Stabilization Using Agar and Agarose

Impregnation of cohesionless soils with the biopolymer agar as a method of stabilizing cohesionless soils prior to sampling was investigated by Schneider et al., (1989). Based on this initial research, Sutterer et al., (1995) investigated impregnation with agarose. Agarose is a component of agar (Araki, 1956). These stabilization media were evaluated due to their ability to form a thermo-reversible gel. Agar and agarose are liquid under higher temperatures and gel at lower temperatures, facilitating impregnation, stabilization and removal of the stabilizing gel.

In the use of both agar and agarose for undisturbed sampling, the soil pores are filled with the biopolymer solution in liquid form (at elevated

temperature). Upon cooling, the biopolymer solidifies within the pores, introducing enough rigidity to the soil that it can be sampled without particle rearrangement. The stabilized sample is then transported to the laboratory, trimmed and stored (or stored and then trimmed). During laboratory testing, the stabilized undisturbed sample is placed and confined in a testing device prior to removal of the solidified biopolymer. Then the biopolymer is removed by heating and flushing; thus restoring the soil to its original state as a cohesionless material.

Solubility in water and the relationship between consistency and biopolymer temperature is the basis for the use of agar and agarose as reversible stabilizing agents. Agar and agarose are both soluble in water. Solutions of agar and agarose in water are prepared by boiling the dry biopolymer in water, with a resulting viscosity that is dependent on biopolymer concentration. This solution stays in the liquid state until a certain temperature is reached, after which the solution turns into a rigid gel. The temperature at which the biopolymer solution turns into a gel is called the gelation temperature. The resulting gel shows temperature hysteresis, i.e. it remains stable at temperatures well above the gelation temperature. This temperature hysteresis means that agar remains in liquid form at temperatures above gelation temperature and also remains a stable gel at temperatures below the gel melting temperature. Due to temperature hysteresis, a properly constituted agar or agarose gel will not melt during transportation, trimming and handling.

Gelation and gel melting temperatures are functions of the concentration of biopolymer, the source of the biopolymer, and the extraction process (for

agarose). The variation of gelation temperature and agar concentration is shown in Figure 2.1 as determined from viscosity tests using a rotational viscosimeter (Schneider et al. 1989). Figure 2.1 also shows that the gelation temperature of agar is dependent on the source. This relationship between gelation temperature and agar source has been attributed to the fact that agar is a natural product and its properties depend upon its origin and time of harvest (Schneider et al., 1989). Similarly, the properties of agarose are a function of impurities, mixing, the source agar, and the process of separation from agar. Agarose is currently available with gelation temperatures ranging from 8°C to ≥42°C and gel-melting temperatures ranging from ≤50°C to ≥90°C (Sutterer, et al., 1995). SeaPlaque agarose, the type used by Sutterer et al. (1995), has a gelation temperature of 26-30°C at 1.5% concentration by weight in water. The gelation temperatures of agar and agarose are comparable.

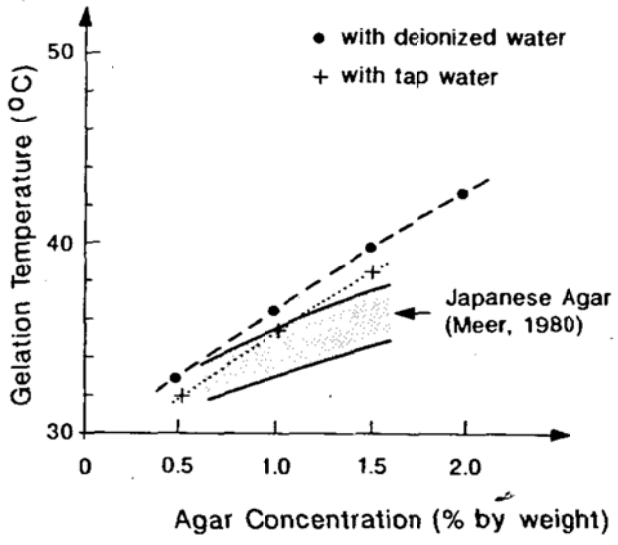

FIG. 2.1. Gelation temperature versus agar concentration (Schneider et al., 1989)

The ability of a fluid to penetrate soil pores under a low hydraulic gradient is governed by its viscosity. The relationship between agar concentration, temperature, and viscosity is shown in Figure 2.2. Schneider et al. (1989) used an agar solution of 0.5 % by weight in their work. Figure 2.2 shows that agar solutions of 0.5 % by weight have a dynamic viscosity of 2 to 4 cps over a wide range of temperature, a low enough viscosity that the biopolymer solution easily penetrated the pores in a sandy soil. The dynamic viscosity of water over approximately the same temperature range varies between 0.6 and 0.4 cps.

Sutterer et al. (1995) did not discuss the viscosity of agarose solutions that were used in their experiments. However, as mentioned above, agarose is a constituent of natural agar and the use of agar as a stabilization agent is attributed to agarose. It may be assumed that the viscosity of agarose is of the same order as that reported by Schneider et al. (1989) for agar.

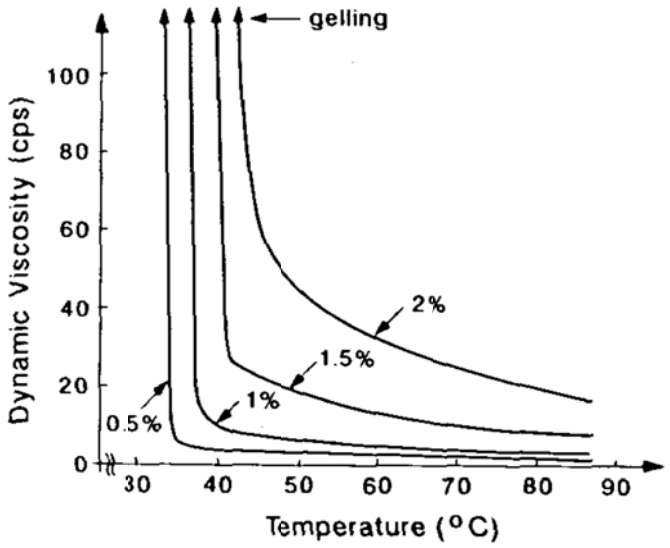

FIG. 2.2. Solution viscosity versus temperature as a function agar concentration by weight (Schneider et a., 1989)

Schneider et al. (1989) conducted unconfined compression tests on agar solutions and on mixtures of agar solutions and sand. They also examined the effects of agar concentration, sand gradation, preparation water quality, and gel aging on unconfined compression strength. The results of the unconfined compression tests conducted by Schneider et al., (1989) are shown in Figure 2.3. Based upon their testing program, Schneider et al. (1989) determined that aging had no significant effect on the strength of agar or agar/sand mixtures.

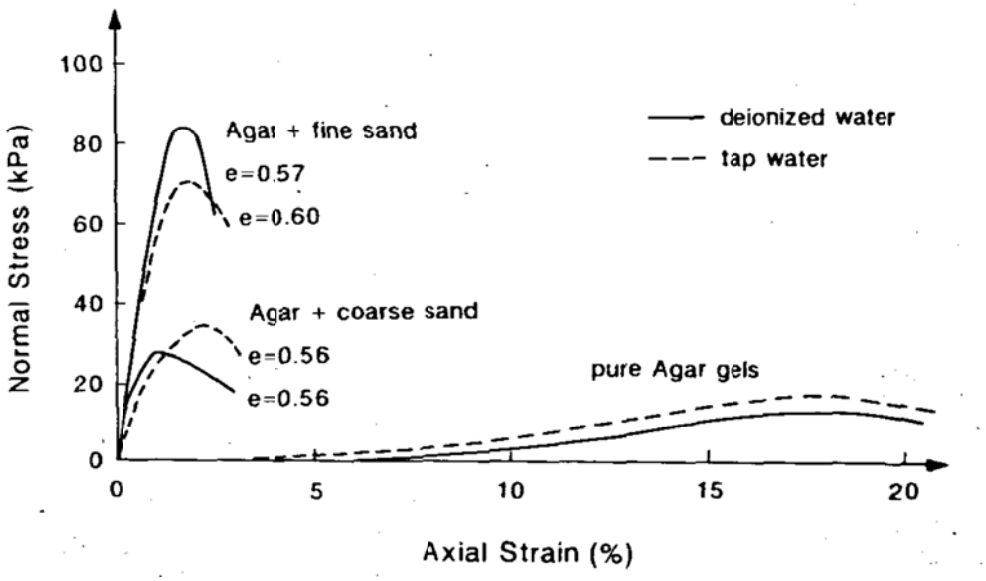

FIG. 2.3. Unconfined compression tests for an agar concentration of 1% (Schneider et al., 1989)

Schneider et al. (1989) conducted laboratory impregnation of sand with agar in a quicksand tank. The scale of the experiment and the initial conditions closely matches the conditions of the laboratory tests that will be conducted in this research program. The experimental setup used by Schneider et al. (1989) is shown in Figure 2.4. The quicksand tank was filled with Ottawa 20-30 sand. The sand was brought to a quick condition by applying an upward hydraulic gradient.

An injection tube and several small plastic tubes were inserted in the sand while it was still in the quick condition. The upward flow was stopped after the tubes were in place. It seems that this insertion procedure was employed in order to reduce the disturbance to the resedimented soil caused by the insertion of the tubes. After resedimentation, but prior to introducing the agar solution, water at 90°C was injected into the sand at a low hydraulic gradient to increase the temperature of the sand in the vicinity of the injection tube. Dyed agar solutions at 0.5% to 1.5% concentration by weight at 80°C were then injected through the injection tube at low hydraulic gradient. The agar solution was allowed to cool and solidify and then the soil was sampled. Figure 2.5 shows an excavated bulb of agar stabilized Ottawa sand.

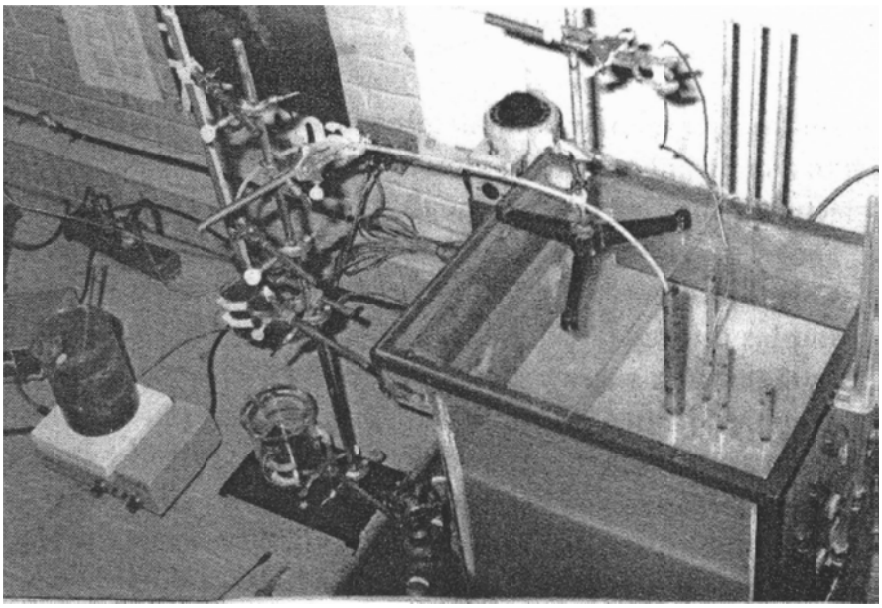

FIG. 2.4. Laboratory injection test in quicksand tank (Schneider et al., 1989)

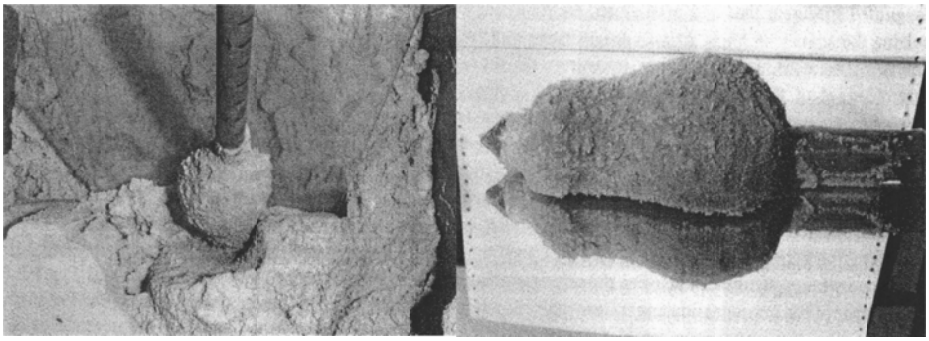

FIG. 2.5. Excavated bulb after impregnation (Schneider et al., 1989)

The following conclusions were reached from the laboratory impregnation experiment conducted by Schneider et al. (1989):

1. The agar solution effectively penetrated and displaced the pore water.
2. The solution solidified in the tank after cooling. The impregnated sand possessed enough strength and stiffness to be sampled and handled.
3. Temperature measurements demonstrated that the radius of penetration of the solution could be predicted from finite-element analyses of axis-symmetric transient heat flow condition.

A laboratory device for agar impregnation and flushing was developed by Frost (1989). This device was based on a modified triaxial test cell. A schematic of the device is shown in Figure 2.6. Sutterer et al. (1995) used a later version of the Frost (1989) system to create agarose impregnated samples in the laboratory. Sutterer et al. (1995) prepared Ottawa 20-30 and modified Ottawa F-125 sand samples by dry pluviation using a modification of the 'raining' method described by Mulilis et al. (1975). The sample preparation method involved the use of a pluviation apparatus developed by Frost (1989). The pluviation apparatus allows the creation of reproducible cylindrical samples of cohesionless soil with similar

void ratio and structure. The samples were subjected to confining pressures of 15 to 20 kPa prior to impregnation, cooling and gelation, heating and flushing the biopolymer stabilization media. The samples were then saturated using vacuum and back pressure saturation techniques until a B-value of greater than 0.95 was achieved. Cyclic mobility tests were then performed on the saturated samples. The results of this testing are presented subsequently in this thesis.

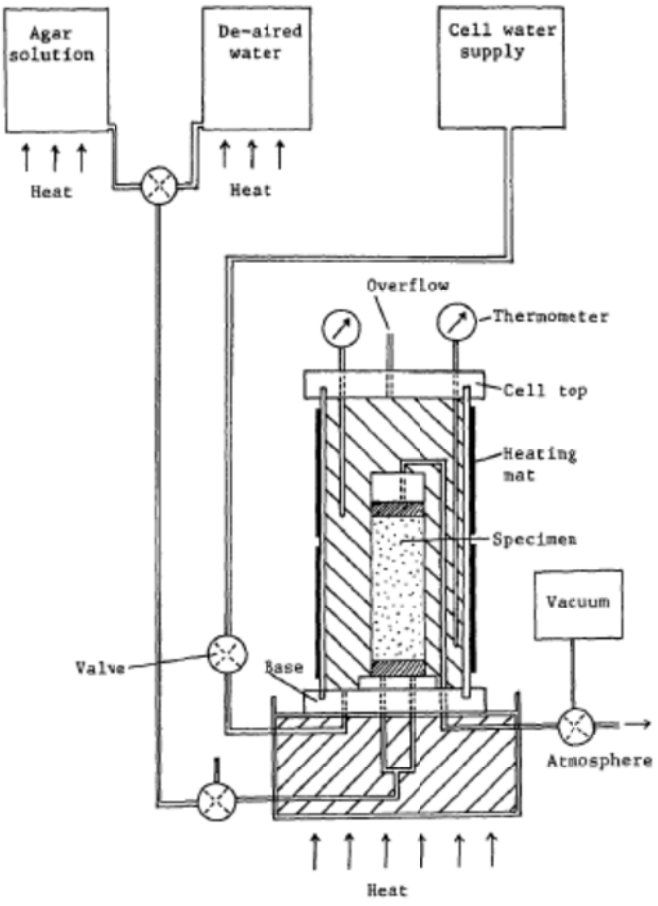

FIG. 2.6. Agar impregnation and Flushing System (Frost, 1989)

Laboratory impregnation of pluviated samples with agarose was conducted by Sutterer et al., (1995) in their laboratory agarose flushing and

impregnation system. This system is shown in Figure 2.6. The soil was heated in a hot bath to temperatures above the gelation temperature of the agarose solution. The heated agarose was then introduced into the soil sample at a differential pressure (from top to bottom) of about 10 kPa. Impregnation temperatures were on the order of 48 to 53°C (Sutterer et al. 1995). Upon cooling, the agarose gelled, resulting in enough cohesion to hold the sample together without a confining pressure. The triaxial cell was taken apart, the specimen removed, and the end platens of the cell were cleaned. The removed specimen was assumed to represent a recovered cohesionless sample impregnated with agarose. The agarose impregnated specimen was then remounted into the agar impregnation and flushing system and confined. The agarose was then flushed from the specimen for triaxial shear tests as described subsequently in this thesis.

2.2.2 Stabilization Using Elmer's Glue

Elmer's glue, also known as Carpenter's glue, has also been used to stabilize cohesionless soil for sampling. Elmer's glue is soluble in water; therefore, the stabilization process can be reversed. Yang (2002) and Evans (2005) used Elmer's glue in a two stage process for preserving the microstructure of sand specimens tested in triaxial and biaxial shear for the purpose of quantitatively studying internal soil microstructure in regions of high localized strain. Elmer's glue was used to stabilize the soil samples prior to permanently fixing them with epoxy. This two stage process was used, in part, to avoid introducing epoxy into equipment that the researcher wanted to save and reuse.

The setup used by Evans (2005) for Elmer's glue impregnation is shown in Figure 2.7. The procedure involved flushing the soil specimen with a dilute solution (7% by weight) of Elmer's glue under a small vacuum (approximately10 to 15 kPa). The solution was drawn through the specimen from bottom to top and into a waste reservoir. Once the waste reservoir contained approximately one-half to one pore volume of solution, the vacuum was released and excess glue solution was allowed to drain from the pores. After excess glue solution had drained from the specimen pores, the vacuum was reactivated and used to draw desiccated air through the pores. The relative humidity of the air leaving the top of the specimen was monitored. The relative humidity was used to indicate when the glue had cured, which also meant that the specimen had been stabilized. This curing point was reached when the relative humidity of the air leaving the specimen was below 40% (usually after 5 to 7 days) (Evans, 2005).

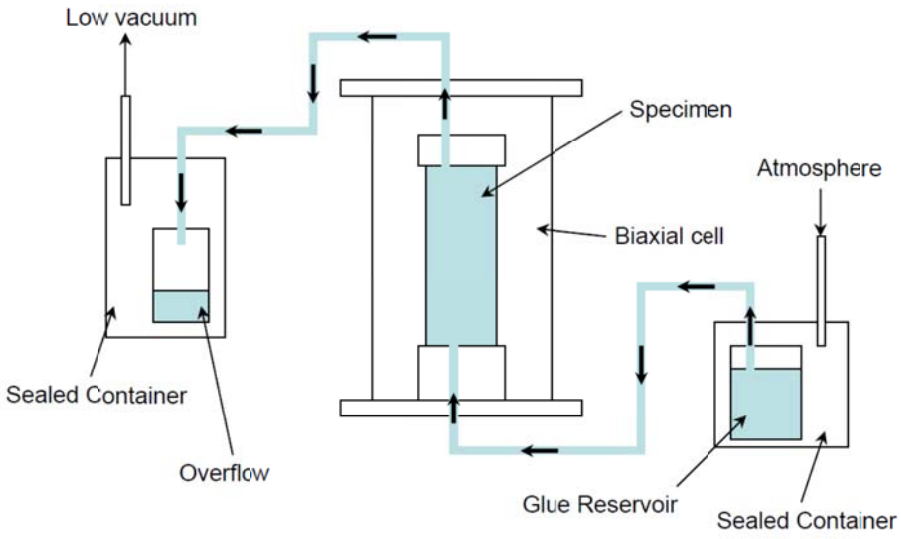

FIG. 2.7. Elmer's glue impregnation setup (Evans, 2005)

2.2.3 Stabilization Using Freezing

Sampling by freezing has long been considered a reliable means of obtaining undisturbed samples of saturated sands (Singh et al.1982). The US Army Corps of Engineers obtained intact samples of cohesionless soil using freezing at Fort Peck Dam (Hvorslev, 1949). Freezing was achieved by circulating a freezing mixture through seven pipes installed around the borehole, as shown in Figure 2.8. Samples were then obtained by coring with a 914 mm core barrel with metal teeth (Hvorslev, 1949). The core barrel is shown in Figure 2.9. According to Hvorslev (1949), based on visual inspection, the quality of the samples was 'excellent'.

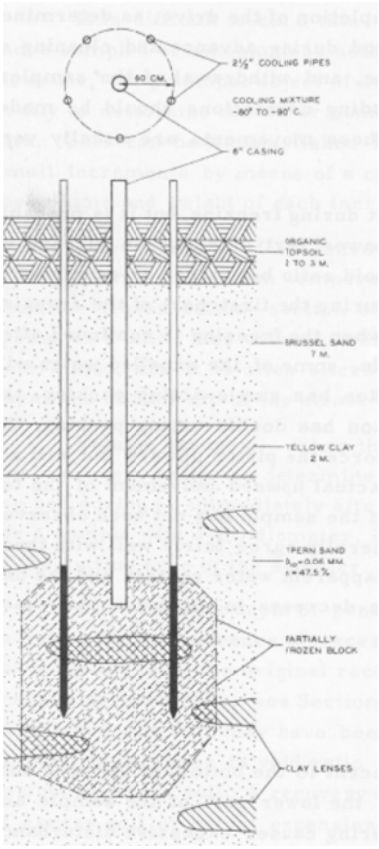

FIG. 2.8. Subsurface freezing for sampling at Fort Peck dam (Hvorslev, 1949)

Fig. 2.9. Core barrel used at Fort Peck dam (Hvorslev, 1949)

Sampling by freezing was also researched by Japanese investigators for recovery of liquefiable sands for laboratory testing (Yoshimi et al., 1978).

Yoshimi et al. (1978) proposed a field sampling procedure consisting of:

1. Inserting an open end steel tube into the ground and removing the soil from inside the tube as it penetrates (in a manner similar to installation of self-boring pressure meters).
2. After the desired depth is reached, plugging the lower end of the tube and removing water from inside the tube.
3. Inserting a smaller vinyl tube in the steel tube and feeding coolant into the tube (to freeze the surrounding soil).
4. Pulling out the steel tube with a column of frozen sand adhered to it.

Yoshimi et al. (1978) conducted laboratory experiments to investigate the effects of freezing on the properties of the sand. The setup consists of a freezing front in the form of a mixture of ethanol and dry ice applied to one end of a

saturated cohesionless soil. Field and laboratory freezing setups used by Yoshimi et al. (1978) are shown in Figure 2.10 below. The laboratory setup allows for freezing of soil in model containers of various shapes and sizes with minor adjustments to the setup shown in Figure 2.10. The Yoshimi et al. (1978) laboratory experimental setup shows a specimen in a container with a steel plate bottom that is immersed in coolant. As a result, the specimen is frozen from the bottom up. The coolant temperature used ranged from -20 to -70°C (Yoshimi et al., 1978). This range of coolant temperatures corresponded to average cooling speeds of 3 to 16 cm/hr according to Yoshimi et al. (1978).

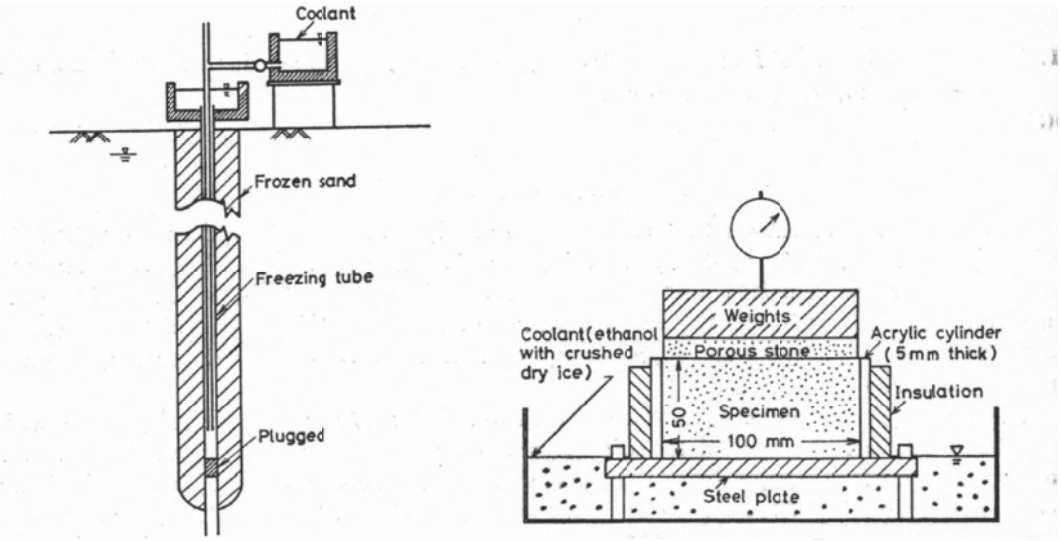

FIG. 2.10. Field and laboratory freezing setup (Yoshimi et al. 1978)

Singh et al. (1982) used a modified triaxial cell capable of testing 305 mm diameter samples for laboratory freezing experiments. The sample to be stabilized by freezing was first created within a split mold mounted in the triaxial cell using the pluviation through air methods described by Mulilis, Chan and Seed (1975). The freezing method used was very similar to the freezing method used by

Yoshimi et al. (1978) in that the coolant was ethanol with crushed dry ice, except that in this case, the coolant was placed on top of a modified triaxial cell top platen, resulting in top to bottom freezing direction. The top cap of the triaxial cell was modified to be capable of containing ethanol and crushed dry ice. Testing of the frozen specimens after thawing is described subsequently in this thesis.

2.3 Methods for Sampling Stabilized Soil

2.3.1 Sampling Agar/Agarose Stabilized Soil

The consistency of agar impregnated soil was described by Schneider et al. (1989) as similar to medium clay. This description agrees with the unconfined compression test results performed on agar impregnated sand samples. It may be assumed that agarose impregnated samples most likely have similar consistency. The results of the unconfined compressive strength tests on agar and agar impregnated soil are shown in Figure 2.3.

Schneider et al. (1989) performed field impregnation tests where they demonstrated the feasibility of recovery of agar impregnated samples in the field. In these field tests, a thin walled 127 mm diameter Osterberg sampler was used to recover samples. The Osterberg sampler is a thin wall hydraulic fixed piston sampler. A piston is attached to a thin wall sampling tube and locked in place at the head of the tube. The piston and tube are seated on the bottom of the borehole. The tube is then unlocked from the piston and is hydraulically pushed into the soil while the piston is held in place to obtain a sample. This sampling method is commonly used for undisturbed sampling of soft clays. Therefore, its use for

sampling agar impregnated soil agrees well with the medium clay consistency characterization. The field samples recovered by Schneider et al. (1989) could then be tested by extruding the specimen from the sampling tube and trimming the specimen to size.

The laboratory samples of agar impregnated soil that were recovered by Schneider et al. (1989) from the quick sand tank can be described as block samples. The samples were recovered by excavating unstabilized soil from around the agar stabilized soil. This process demonstrated that agar and perhaps agarose stabilized soil samples can also be obtained by block sampling and trimming to the required dimensions for testing provided a sufficiently large volume of soil is stabilized.

2.3.2 Sampling Elmer's Glue Stabilized Soil

Elmer's glue stabilized cohesionless soil was not sampled in the conventional sense in the work conducted by Evans (2005) and Yang (2002), as the stabilized specimens were laboratory test specimens. However, the Elmer's glue stabilized specimens were able to maintain their structure during subsequent handling after the glue cured. The samples were removed from the glue impregnation system and the confining membrane removed without the sample falling apart. The consistency of the specimens was described as 'lightly cemented' (Evans, 2005). It is conceivable that Elmer's glue stabilized soil could be sampled using block sampling, push tube methods, or even coring. However, in the absence of specific information on the consistency or unconfined

compressive strength, it is hard to tell how specimens can be properly sampled from Elmer's glue stabilized soil.

2.3.3 Sampling Soil Stabilized by Freezing

The sampling operations at Fort Peck Dam that were conducted by the US Army Corps of Engineers involved complete freezing of the soil below the bottom of the borehole (Hvorslev, 1949). Samples were recovered using the single tube 0.91 m diameter core barrel with metal teeth with a calyx shown in Figure 2.9.

Field sampling of frozen soil that was conducted by Yoshimi et al. (1978) can be best described as block sampling. The frozen sand was lifted en masse by grabbing the freeze pipe with a crane and pulling it out of the ground. This procedure produced a nearly uniform 0.4 m diameter cylindrical mass of frozen sand around the freeze pipe. Smaller samples for laboratory testing were obtained from this frozen mass by trimming from the cylindrical core.

Singh et al. (1982) did not perform any field sampling of frozen soil. However, they did obtain samples from the soil that they froze in the 300 mm diameter triaxial cell. The frozen 300 mm diameter specimen was removed from the triaxial cell and carried to a radial drill press. Using a diamond core drill, 71 mm diameter cores 18 to 25 mm long were recovered from the 300 mm diameter frozen specimen. Compressed carbon dioxide was used as the drilling fluid (Singh et al. (1982).

2.4 Removal of Stabilizing Agent

2.4.1 Removal of Agar/Agarose

Removal of agar and agarose from stabilized samples was accomplished by use of the Laboratory Agar Flushing and Impregnation system described by Frost (1989) and Sutterer et al. (1995). The version of the agar impregnation and flushing system used by Sutterer et al. (1995) is shown schematically in Figure 2.11.

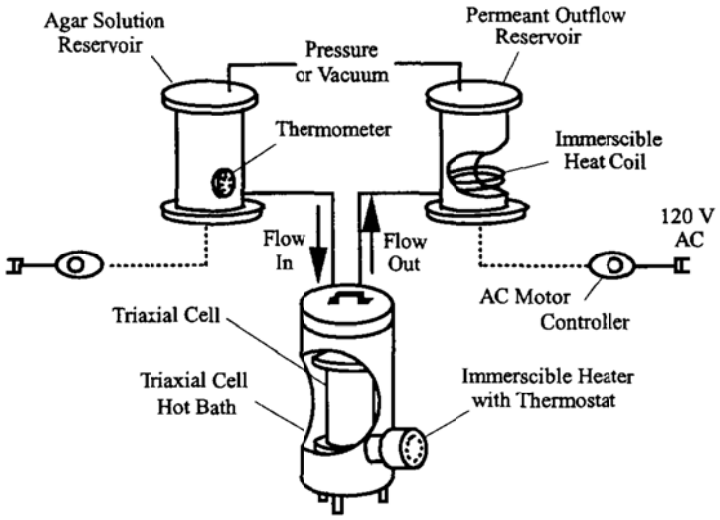

FIG. 2.11. Agarose Impregnation and Flushing System (Sutterer et al., (1995)

To remove agarose, the reservoirs shown in Figure 2.11 were filled with hot water and the confined, agarose impregnated sample was heated to the agarose gel melting temperature using a hot bath within the triaxial cell. Agarose removal temperatures were on the order of 70°C and agar removal temperatures were on the order of 90°C (Sutterer et al., 1995). The difference in removal temperature is the major advantage that agarose has over agar. The agarose removal temperature is significantly lower than the boiling point of water. When

the agarose had melted and began to flow, hot water was circulated through the sample until the agarose was flushed out. A volume of 2,500 to 4,000 ml (equal to approximately 4 to 7 pore volumes) of tap water circulated in one direction was typically required for complete removal of visible evidence of agarose. Using an earlier prototype of the system, Frost (1989) found that periods of both upward and downward flushing was necessary to remove any visual evidence of agar. Frost (1989) found that flushing in only one direction resulted in remnants of agar remaining in the specimen near the platens but Sutterer et al., (1995) reported no such problems using agarose.

2.4.2 Removal of Elmer's Glue

Elmer's glue is soluble is water. Evans (2005) relied on this property to clean his equipment following the first stage of his two-stage impregnation process. To remove the glue, he soaked Elmer's glue filled equipment in water for several days. After the glue had dissolved, the equipment was washed with water to remove any glue remnants. It can be inferred that the same process can be used to remove Elmer's glue from soil pores. The second stage of the Yang (2002) and Evans (2005) stabilization process was to impregnate the Elmer's glue cemented sample with epoxy to permanently fix the specimen. It can also be inferred from this that Elmer's glue stabilized samples had at least moderate permeability. The removal process could involve:

1. Placing specimens in a triaxial cell and applying a small confining pressure.
2. Saturating the specimen with water for a few days.

3. Flushing the specimen with water until all evidence of Elmer's glue was completely removed.

2.4.3 Restoration of Samples Stabilized by Freezing

In order to return samples stabilized by freezing to their original state, both Yoshimi et al. (1978) and Singh et al. (1982) simply allowed the soil to thaw. The samples were placed in a testing device (triaxial cell) and an effective confining pressure equal to the effective confining pressure during freezing was applied to the sample. The thawing sample was kept in contact with water during the thawing process so that water could be drawn into the sample as the pore water thawed and reduced in volume. The time required to completely thaw the sample is a function of (among other things) the ambient room temperature, the size of the sample, and the temperature of the 'free access' water.

2.5 Quality of Undisturbed Samples

Any consideration of a sampling process is incomplete without evaluating the quality of samples obtained using the undisturbed sampling technique. There is no standard method of evaluating undisturbed samples. For cohesionless soils, one can consider the Hvorslev (1949) criteria and look at void ratio changes as indication of volumetric strains and structure collapse. However, studies have shown that the specimens prepared to the same void ratio but with different preparation methods can have very different stress-strain-strength behavior (Mulilis et al. 1975). Therefore, comparison of the stress-strain-strength behavior

of recovered specimens to the in situ behavior is essential to demonstrating that the sampling method produced an undisturbed sample.

2.5.1 Quality of Agar/Agarose Stabilized Samples

The following aspects of the polymer impregnation technique for undisturbed sampling of cohesionless soil may be considered as potential sources of disturbance:

1. Volume change of the agar/agarose solution with changes in temperatures including changes in volume during gelation.
2. Volume changes in the soil and pore water during heating prior to injection of agar/agarose.
3. Disturbance from insertion of the sample tube or electrodes.
4. Effects of the agar/agarose removal process.
5. Loss of aging-induced strength gain that occurs with no discernable volume change (Mitchell, 2008).

Since the agar will replace the pore fluid, changes in the agar volume may result in changes in the soil void ratio, particularly if there is a volume increase. According to Schneider et al. (1989), a dilute agar solution above the gelation temperature exhibits the same volume change with increase in temperature as water. The results of the laboratory volume change measurements made by Schneider et al. (1989) on agar solutions are shown in Figure 2.12. Changes in agar volume during gelation were also analyzed. The agar decreased in volume upon gelation and the volume decrease of the agar during gelation was less than 2% for agar concentrations as high as 2% (Schneider et al., 1989). Gels were not

remelted to model the effects of agar removal. However, Schneider et al. (1989) state that "Observations made during the melting of cubes of agar gels indicate that the volume change effects are probably thermo reversible".

Heating generates volume and effective stress changes in saturated soil. This is due to the differential thermal expansion of the pore water and mineral particles. The volume change behavior of heated soil differs for drained heat and undrained heating. For purposes of this study, soil heating for biopolymer impregnation can be assumed to occur under drained conditions. The subject of soil temperature-volume relationships is discussed in great detail by Mitchell and Soga (2005). Under drained conditions the soil grains and the soil mass undergo the same volumetric strains. Therefore, under drained heating, pore fluid will flow out of the heated region because, for a given temperature change, the volumetric strain of water is greater than the volumetric strain of solid soil particles. Heating may also induce changes in inter particle forces if the specimen is not free to change in volume (e.g. under one dimensional conditions in the ground). Heating a soil specimen constrained from volume change can cause changes in cohesion and/or frictional resistance that may result in particle reorientation, and under extreme conditions, in particle crushing. Particle reorientation is a significant factor in soil fabric. Sutterer et al. (1995) conducted experiments using Ottawa 20-30 sand and concluded that the level of heating involved in biopolymer impregnation did not result in particle crushing.

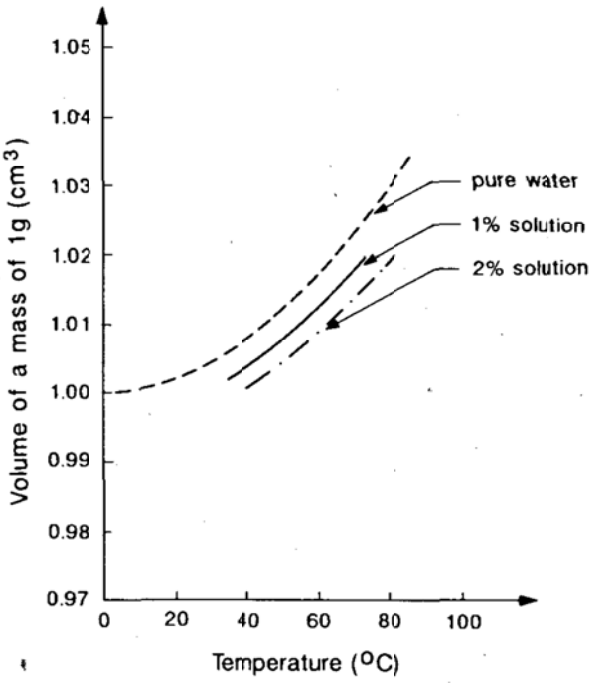

FIG. 2.12. Volume change as a function of temperature and agar concentration (Schneider et al. 1989)

The experiments of Sutterer et al. (1995) also showed that the drained heating of clean sands (germane to this study) under constant confining pressure did not result in significant volumetric strain and thus, by extension, did not result in significant void ratio changes. The volumetric strain of the soil due to heating during impregnation with agarose was estimated to be 0.1% (Sutterer et al., 1995).

In order to investigate the quality of samples obtained by agarose impregnation, Sutterer et al. (1995) conducted undrained cyclic triaxial tests under an isotropic confining stress. Undrained cyclic triaxial testing was selected as the method of comparison for the following reasons:

1. Samples are easy to prepare
2. Testing is simple to perform

3. It has been used by other researchers (Yoshimi et al. 1984, and Mulilis et al. 1975) for similar purposes.

A comparison of the cyclic triaxial test results on impregnated specimens and on control specimens is shown in Figure 2.13. Sutterer et al. (1995) developed a mathematical relationship between the Cyclic Stress Ratio (CSR) and the number of cycles to failure, N_f, presented by the equation 2.1:

$$CSR = b + ae^{\left(1-\frac{N_f}{c}\right)} \quad (2.1)$$

where b, a and c are curve fitting parameters

Based on the relationship in Equation 2.1, a comparison between impregnated samples and control samples was made. The results of the comparison showed that the variation between impregnated and control samples was within the normal range of scatter expected for this type of test. The comparison also showed that there was a slight reduction in cyclic stress resistance or cyclic mobility after agarose impregnation and flushing. This reduction was attributed to the slight expansion observed during drained heating of the soil prior to sampling and also to residual agarose in the sample. Although Sutterer et al. (1995) observed no traces of agarose in the sample after flushing with hot water, he speculated that there was still some agarose left between the particle contacts.

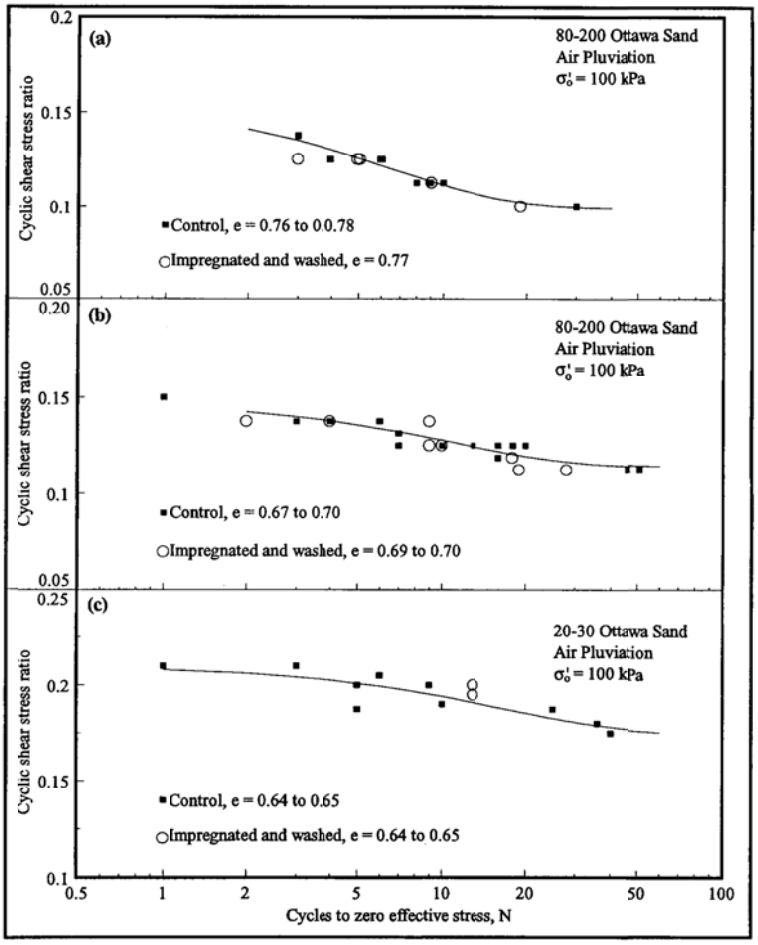

FIG. 2.13. Cyclic mobility results for impregnated versus control specimens

2.5.2 Quality of Elmer's Glue Stabilized Samples

The quality of samples stabilized by Elmer's glue was not explicitly investigated by either Yang (2002) or Evans (2005) as their work involved only study of the microstrusture of sand specimens.

2.5.3 Quality ot Freeze Stabilized Samples

Water expands approximately 9 % upon freezing. If expansion of soil pore water were allowed to occur without drainage, the soil mass would experience a concurrent increase in void ratio, loss of inter-particle contacts, and consequently

significant disturbance. The expansion of pore water during freezing is perhaps the main source of potential disturbance in the stabilization of cohesionless soil for undisturbed sampling using freezing.

The question of the expansion of water during freezing and whether this phenomenon disturbs the structure of the sand or its properties was investigated by Hvorslev (1949), Tystovich (1952), Yoshimi et al. (1978) and Singh et al. (1982). The main conclusion of all these investigations with regard to disturbance due to expansion of water upon freezing was that a unidirectional freezing front, unimpeded drainage path, and slight overburden pressure were necessary to minimize disturbance due to water expansion upon freezing. A complete review of the processes governing the volume change associated with freezing pore water is beyond the scope of this study but the essential conclusions from previous investigations are summarized below.

Hvorslev (1949) simply stated that "it is possible that the expansion of water during freezing simply will force some of the unfrozen water out of the soil and not change the void ratio or disturb the soil structure". Extensive research on the subject of freezing pore water in soil was conducted by Tystovich (1952). According to Tystovich (1952), "it was established that in water saturated sands with free drainage of water in at least one direction, water does not migrate towards the freezing point, but is squeezed out, with the result that the porosity of frozen water saturated sands remains practically the same." A more comprehensive study of the effect of freezing on cohesionless soil was conducted by Yoshimi et al. (1978) who conducted one dimensional laboratory freezing

experiments to examine the effects of the following factors on the expansion of the soil skeleton during freezing:

1. Surcharge/overburden.
2. Soil type/Fines content
3. Relative density
4. Coolant temperature.

Yoshimi et al. (1978) conducted laboratory tests to evaluate the above factors using three soils: Toyoura sand, Tonegawa sand, and Niigata sand. The gradations of the three sands are shown in Figure 2.14. The Yoshimi et al. (1978) experimental setup was shown in Figure 2.10. The specimens were frozen from the bottom by immersing the steel bottom in coolant (mixture of alcohol and crushed dry ice) and drainage was provided at the top. This setup was used to investigate the factors listed above.

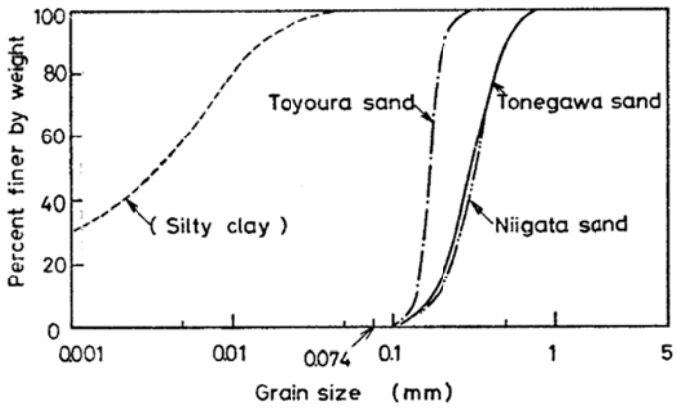

FIG. 2.14. Gradation curves (Yoshimi et al., 1978)

The Yoshimi et al. (1978) experiments showed that the two most influential factors on the amount of volumetric strains due to freezing were overburden

pressure and soil type. Yoshimi et al. (1978) found that for a given set of conditions, volumetric strains due to freezing reduced with increase in surcharge as shown in Figure 2.15. Figure 2.15 indicates that surcharge loads on the order of 0.7 to 4 kPa are sufficient to suppress volume change due to soil freezing.

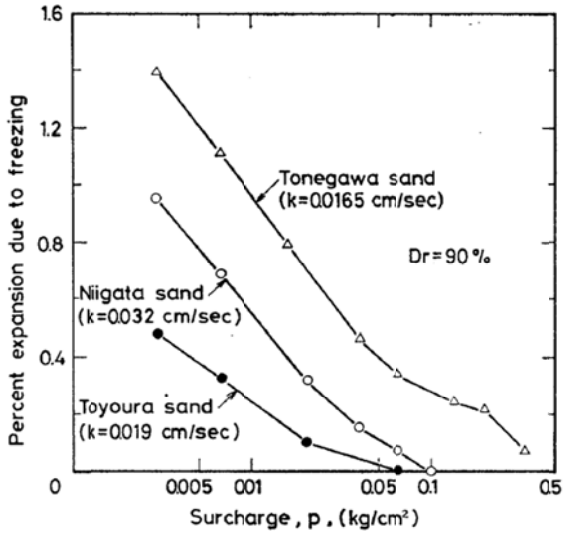

FIG. 2.15. Percent expansion versus surcharge pressure (Yoshimi et al., 1978)

It also seemed that expansion was strongly influenced by the ease with which pore water is expelled out of the pores during freezing, as the permeability of the soil also appeared to govern the volumetric strain due to freezing. It was observed that as the relative density of the soil increased, the permeability decreased and the volumetric strain due to freezing increased. The same relationship was observed with regard to fines content. Higher fines content reduced permeability and, in turn, increased volumetric strain due to freezing. The Yoshimi et al. (1978) plots of relative density versus percent expansion and percent fines versus percent expansion are shown in Figure 2.16.

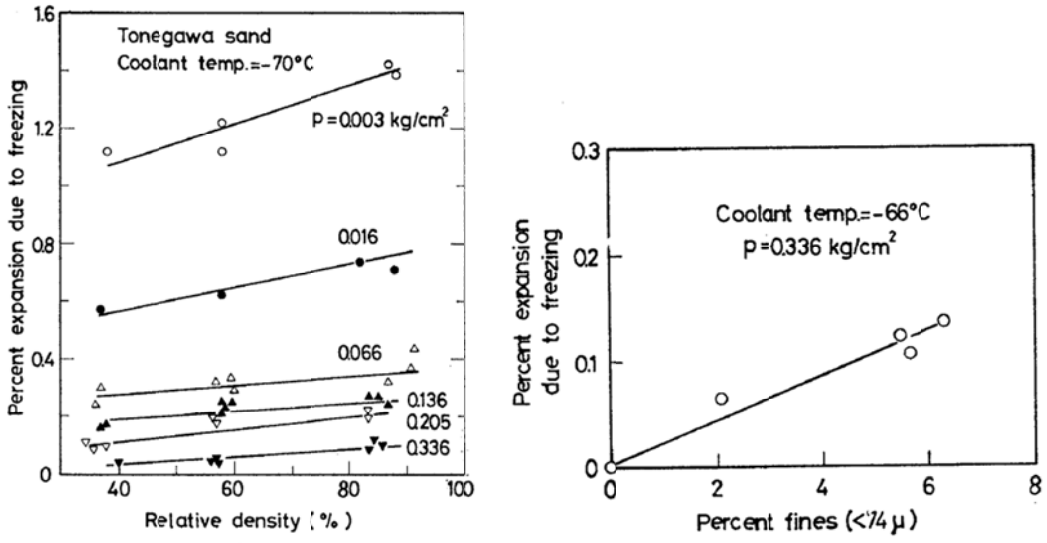

FIG. 2.16. Percent expansion versus relative density and fines content (Yoshimi et al., 1978)

To investigate the effects of freezing followed by thawing on material properties, Yoshimi et al. (1978) compared the strength and deformation characteristics of frozen and then thawed sand specimens to those of never frozen sand specimens. Drained stress/strain behavior was chosen for the comparison. Tonegawa sand and Toyoura sand were used in the drained strength and deformation behavior comparisons. The gradations of the two sands are shown in Figure 2.14.

Frozen specimens were prepared by pouring dry sand into water filled molds in several layers, tamping each layer. After the last layer was placed and tamped, a porous disc was placed on the specimen and the specimen was tapped until the desired overall density was attained. A surcharge of 9.8 kN/m^2 was placed on top of the specimen and the whole assembly was placed in a freezer. The specimens were placed in the freezer with an average temperature of -28°C for about three

hours. This freezing method does not seem to apply a unidirectional freezing front to the specimens. In fact, it is likely that the samples were frozen from all directions using this technique. Yoshimi et al. (1978) do not address this issue. The frozen specimens were placed in a triaxial cell and confining pressures of 29 to 98.1 kPa were applied. The specimens were allowed to thaw while both ends where allowed access to water. The specimens were saturated by circulating pore water through the thawed specimen for 24 hours under a maximum differential head of 300 mm.

Unfrozen specimens were prepared in the same way as the frozen specimens but without placement in the freezer. Both frozen and unfrozen specimens were prepared at a range of relative densities between 40 and 90 percent.

Drained triaxial compression tests were conducted on the two types of specimens (Frozen/Thawed and Never Frozen) at confining pressures of 3 to 10 kPa. A comparison of the two sets of tests is presented in Figure 2.17. The results presented in Figure 2.17 show that the freeze/thaw cycle has only a minor effect on the drained strength and deformation behavior of both Toyoura sand and Tonegawa sand for specimens of the same age. The comparison of friction angles for frozen and thawed specimens versus never frozen specimens, shown in Figure 2.18, indicates that the freeze thaw cycle has no significant effects on the friction angle for both sands.

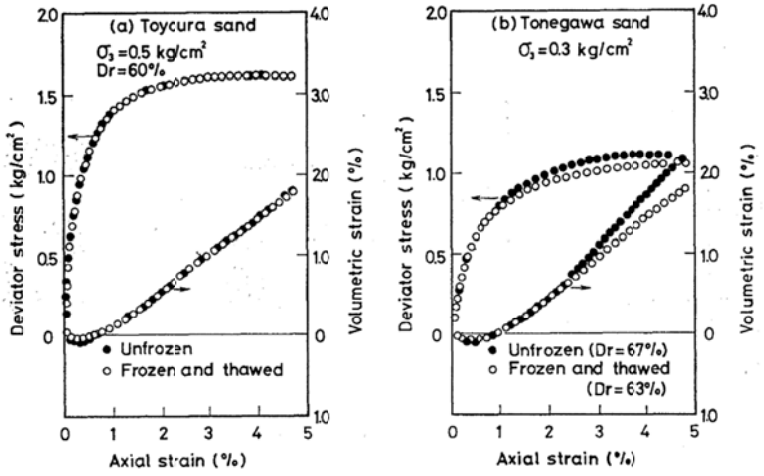

FIG. 2.17. Effect of freeze thaw cycle on strength and deformation behavior

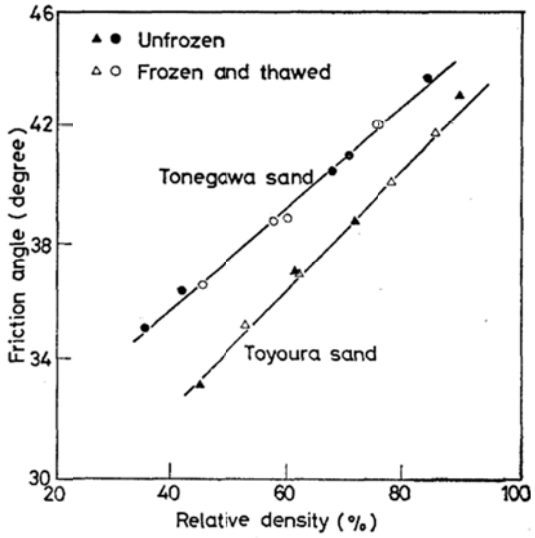

FIG. 2.18. Effect of freeze thaw cycle on friction angle

Yoshimi et al. (1978) presented an evaluation of the disturbance due to insertion of their freezing tube into saturated sand in situ. The results of the evaluation are presented in Figure 2.19. It was determined that the sand within one diameter of the tube underwent void ratio changes due to shearing of the sand during insertion of the freezing tube. The changes in the void ratio were a function of the initial density of the sand. Loose samples tended to contract,

resulting in a void ratio decrease, while dense samples tended to dilate, resulting in void a ratio increase.

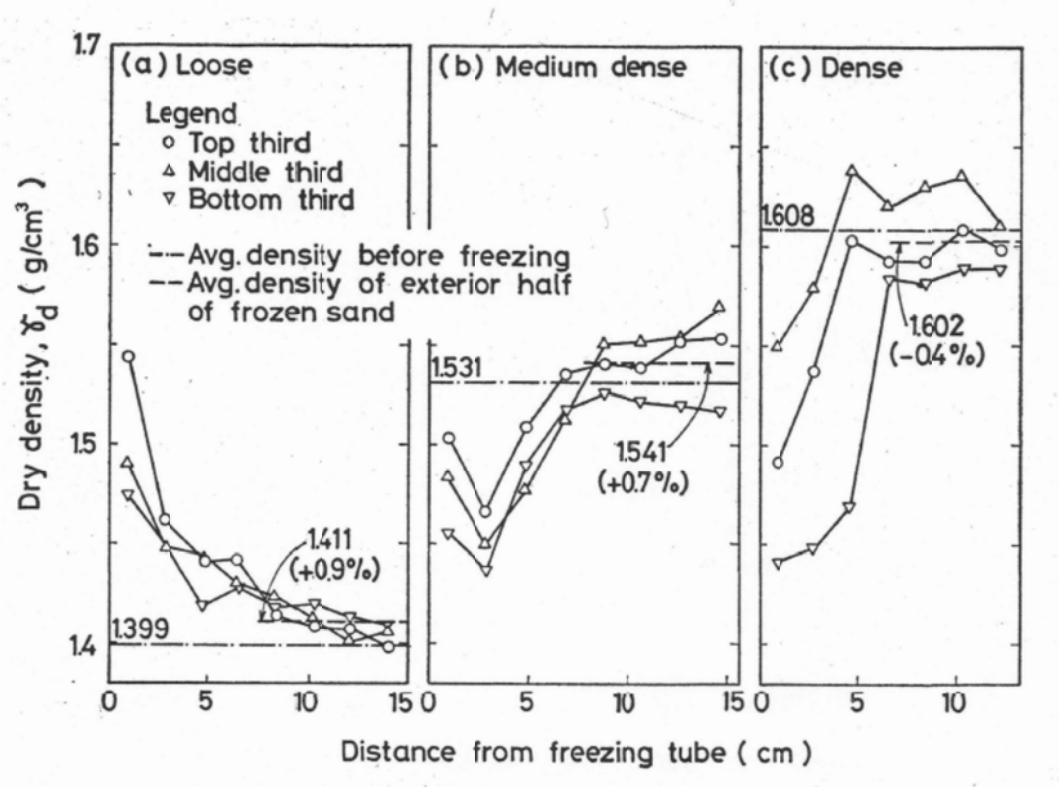

FIG. 2.19. Sample disturbance due to insertion of freeze pipe (Yoshimi et al. 1978)

Singh et al. (1982) investigated the effects of a freeze thaw cycle on the dynamic strength of sand. Test specimens were prepared by pouring and tamping according to procedure described by Mulilis et al. (1975) to a relative density of 48 percent. The specimens were then saturated and consolidated under a cell pressure of 20 kPa and a back pressure of 15 kPa. Cyclic triaxial tests were conducted on one set of specimens to establish a virgin line. A second set of

specimens was subjected to low amplitude cyclic loading prior to the cyclic triaxial tests to establish a set of specimens influenced by seismic history.

Two additional set of specimens were prepared using identical methods as the first two sets, with one set subjected to the same seismic history. The second two sets of specimens were then frozen using a unidirectional freezing front in a modified triaxial cell and subsequently thawed. Then the third and fourth sets of specimens were subjected to cyclic triaxial tests to establish their cyclic characteristic curves.

The results of the four sets of tests are shown in Figure 2.20 and Figure 2.21. Based on comparison of the cyclic triaxial test results in Figures 2.20 and 2.21, Singh et al. (1982) concluded that soil sampling by freezing and coring under conditions of unidirectional freezing and unimpeded drainage in the direction of movement of the freezing front provides an effective method of obtaining undisturbed samples of saturated sands.

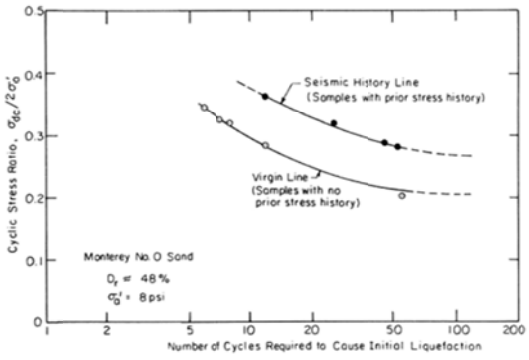

FIG. 2.20. Seismic history and virgin line for never frozen specimens

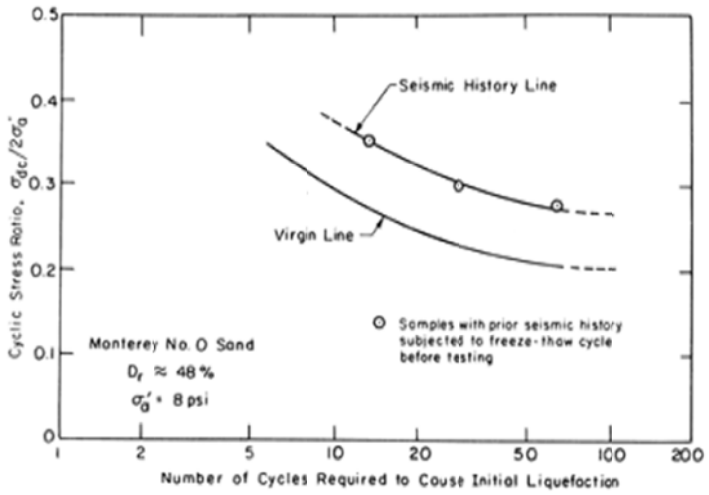

FIG. 2.21. Seismic history and virgin line for frozen/ thawed specimens

2.6 Preparation of Cohesionless Soil Samples for Laboratory Testing

For the purposes of this project, it was important to develop a method for producing samples of sand at a desired density with consistent, reproducible properties. There are numerous methods for creating reproducible samples of sand at a desired density described in the literature. However, studies have shown that both static and dynamic strength and deformational properties of sand specimens at the same density can be influenced by the method of the sample preparation (Mililis et al.1975). For purposes of this study, it was just as important to prepare the specimens with the same properties as it was to to produce samples with the same density. A summary of the most common methods of sample preparation and their various components is present in Figure 2.22. Details about each method are discussed below.

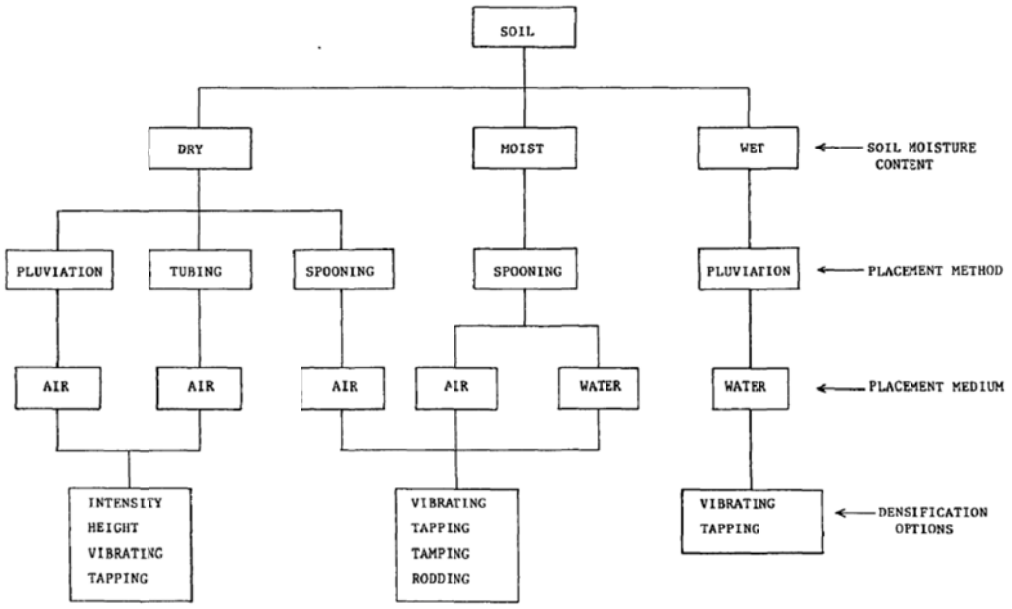

FIG. 2.22. Sample preparation methods (Frost, 1989)

2.6.1 Pluviation in Air

Pluviation in air involves pouring sand from a container into a mold through air. The variables in this method are: the number openings through which the sand in the container is poured into a mold; the size of the opening(s); and the height of fall from the opening(s) to the surface of the sand in the mold (the bottom of the container at the beginning).

Mulilis et al. (1975) used a flask filled with sand and a cork with a single opening. The flask was inverted over a mold and rotated by hand as the sand poured into the mold while maintaining a constant height. In addition to the height and size of the opening, Mulilis et al. (1975) found that the speed of rotation of the flask also influenced the density.

Miura and Toki (1982) used a conical hopper as the sand container and a series of seven sieves through which the sand cascaded. The assembly was placed over the mold as the sand was poured from the hopper while maintaining the height between the bottom sieve and the surface of the sand in the mold. The diameter of the nozzle attached to the conical hopper was varied to control the rate of discharge of the sand.

Frost (1989) used a hopper with a fall tube that contained diffuser meshes in it. This equipment was based on Miura et al. (1982) and had similar variables for controlling the density of the sample.

2.6.2 Pluviation in Water

In pluviation in water, a known amount of sand required to achieve a desired density is placed in a flask. Then deaired water is placed in the flask. The flask, containing the sand and deaired water, is boiled while a vacuum is applied to the container for approximately 15 minutes. The mold in which the sand is to be placed is then filled with deaired water. The flask containing sand and deaired water is inverted over the mold to allow the sand to be deposited into the mold completely under water. The specimen is then vibrated to compact it to the height required to achieve the desired density (Mulilis et al. (1975).

2.6.3 Dry Tubing

This method involves the use of a container shaped like the mold in which the sand is to be placed. Tube shaped containers are used to create cylindrical specimens but other shapes can also be used. The container is inserted into the

mold all the way to the bottom of the mold. This container is then filled with sand. The container is designed with holes at the bottom. The container is raised slowly allowing the sand to flow out into the mold at a very low density. The sand can then be densified using vibratory methods to achieve a desired density. A tube (container) used to create 71 mm diameter triaxial specimens by tubing is shown in Figure 2.21

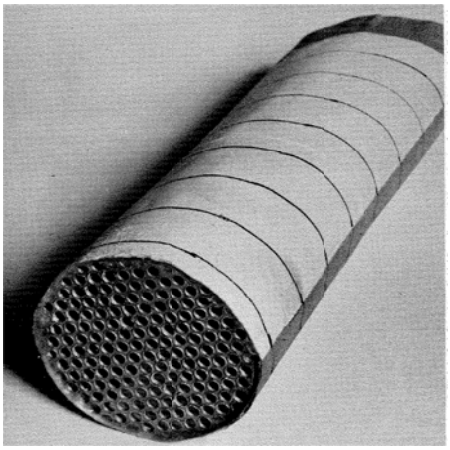

FIG. 2.23. Cylindrical tube (Mulilis et al., 1975)

2.6.4 Dry and Moist Spooning

Spooning methods involve placement of sand into a mold using a spoon. The same method is used for dry sand (dry spooning) as moist sand (wet spooning) (Frost, 1989). The sand is placed in layers and compacted using one of the densification methods discussed later in this chapter to achieve the desired density.

2.6.5 Densification Methods

Sample densification is used to 'pack' sand into a pre-determined volume in order to achieve a desired density. When densification is used in conjunction with

layered sample preparation, there is a tendency for the lower layers to be compacted more as additional layers are placed and compacted on top of them (Mulilis et al. 1975). To mitigate this problem, a procedure in which each layer is under compacted by a certain percentage of the final desired compaction may be used. The lower layer is prepared in the loosest state. The percent under compaction of a layer usually ranges from 0-20% (Mulilis et al. 1975). This under compaction procedure results in more uniform specimens but requires significant trial and error to establish the amount of under compaction for each layer.

Densification by tamping is usually used in conjunction with layered sample preparation. In this method a tamping rod is used to compact a soil layer until the height of the layers reduced enough to achieve a desired density. A picture of a tamping rod used by Mulilis et al. (1975) is shown in Figure 2.22.

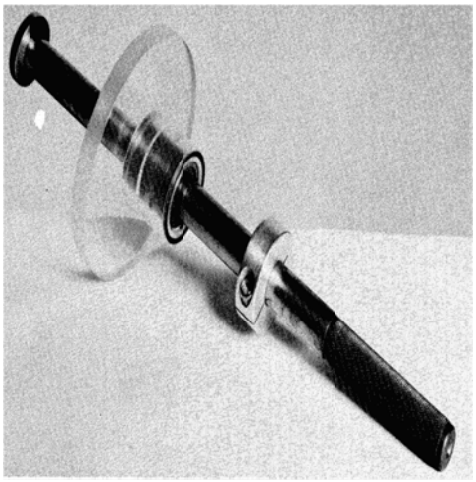

FIG. 2.24. Tamping rod (Mulilis, 1975)

Densification by tapping is achieved by tapping the specimen mold radially to reduce the height of the sand in order to achieve a desired density. The intensity

of tapping must be kept uniform throughout the specimen preparation process in order to create uniform specimens.

Rodding involve plunging a vibrating rod in and out of the specimen starting from the edges and working toward the center to achieve the desired density. The surface of the specimen is then leveled by applying a small pressure using a flat surface.

Vibrating involves vibrating the sample mold around the perimeter to densify the specimen. Vibrating a specimen allows the particles to pack in more closely and densify the specimen. Vibration can be used to densify a single layer or it can be used to densify a whole specimen by apply vibrations using a hand held vibrator at random locations along the height of the specimen.

Chapter 3

3.0 PROPERTIES OF TEST SAND AND SPECIMEN PREPARATION

Ottawa 20-30 sand (ASTM Designation C778), from U.S. Silica Company in Ottawa, Illinois was selected as the test sand for all experiments in this work. The selection was based on the fact that Ottawa 20-30 sand is readily available with near consistent properties and has been used by many researchers for experiments on cohesionless soil. Therefore, some of the properties of Ottawa 20-30 sand were available in the literature.

3.1 Properties of Ottawa 20-30 Sand

Ottawa 20-30 sand is a poorly graded sand that consists of subrounded particles and is composed primarily (99.8%) of silicon dioxide (quartz) (Evans, 2005). Numerous researchers have used Ottawa 20-30 sand for investigations involving the use of a uniform cohesionless soil (Alshibli et al. 2000, Santamarina and Cho 2001, Evans 2005, Salgado, et al. 2000).

3.1.1 Gradation

Gradation tests were performed in accordance with ASTM D6913 on Ottawa 20-30 sand obtained from U.S. Silica Company, Ottawa, Illinois for this project. The gradation of the Ottawa 20-30 sand obtained for this project is shown in Figure 3.1. The gradation results are consistent with gradations reported by other researchers for Ottawa 20-30 sand (presented in Appendix A).

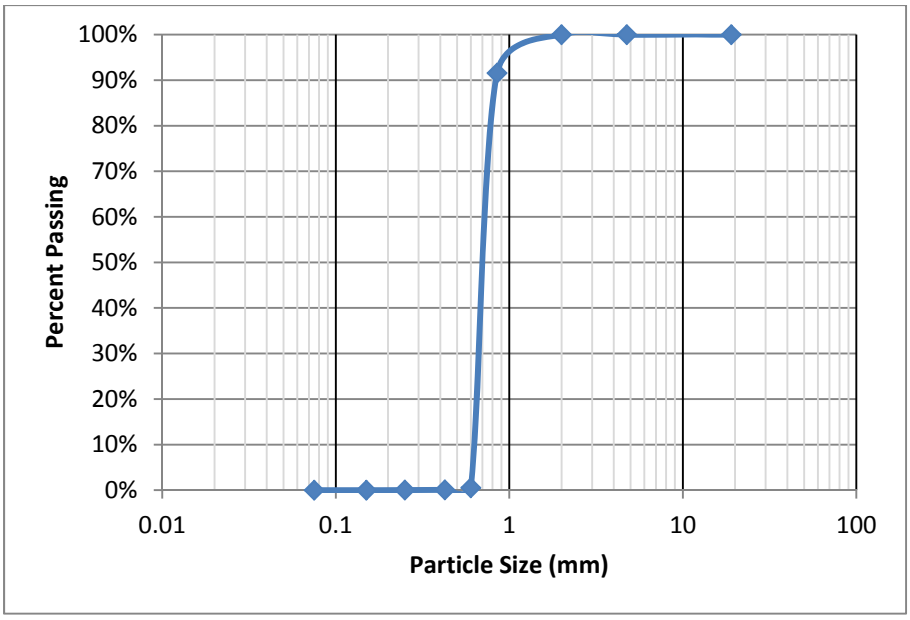

FIG. 3.1. Ottawa 20-30 Gradation

3.1.2 Maximum and Minimum Void Ratio

Maximum and minimum void ratios of Ottawa 20-30 sand published by other researchers are presented in Table 1. Void ratios published by Santamarina et al. (2001) were used calculations of minimum and maximum densities and in the determination of relative density.

Table 3-1. Ottawa 20-30 Sand Maximum and Minimum Void ratio

Maximum Void Ratio	Minimum Void Ratio	Reference
0.81	0.49	Alshibli et al. (2000)
0.742	0.502	Santamarina et al. (2001)
0.78	0.48	Salgado et al. (2000)

3.2 Specimen Preparation

3.2.1 Model Container

The development of the specimen preparation method began with the selection of a model container for use throughout this study. The size and shape of a container has a profound effect on the type of specimen preparation method that can be practically used to create a sample in that container. For example, a specimen prepared in a large container would require a relatively fast specimen preparation method so that the specimen can be prepared in a reasonable time frame. For this study, the box used on the Shaevitz centrifuge at the University of California at Davis (UC DAVIS) was used as the design basis for the specimen container. The dimensions of the Shaevitz centrifuge box are 559 mm by 279 mm by 179 mm (Fiegel, Hudson, Idriss, Kutter, & Zeng, 1994).

The model container (box) used in this work was fabricated out of aluminum except for the front face, which was made of Lexan. The fabricated box is shown in Figure 3.2. The design drawings for the box are presented in Appendix B. Key features of the box are:

1. The box was designed with five ports on the bottom for use in saturation and drainage.
2. The box was designed with a lid (shown in Figure 3.3) that locked onto the box using six latches that could hold a pressure of 10 kPa without visible deformation. At pressures higher than 10 kPa, the lexan front of the box showed visible deformation. The lid had two ports for use in the saturation procedure.

FIG. 3.2. Model container (Box)

FIG. 3.3. Box Lid

3.2.2 Air Pluviation

Based on the literature review, pluviation through air was selected as the specimen preparation method. Pluviation through air may be expected to result in a uniform void ratio and structure throughout the length of the sample. Other specimen preparation methods (Pluviation through water, Dry tubing, Dry and moist spooning) require post placement densification and/or layered specimen

preparation to achieve the desired density. Layered preparation refers to a sample preparation method that requires multiple layers that are first deposited and then compacted to achieve the desired density. Post placement densification is a process of compacting specimens (by vibration, tamping or rodding) after placement in a mold to achieve the desired density. Both layered preparation and post placement tamping require careful procedures and trial and error in order to produce uniform soil deposits. Pluviation through air does not require densification after placement or layered preparation, leading to more easily prepared uniform specimens.

The air pluviation method implemented in this work employed a modified version of the air pluviation/raining method used by Frost (1989). The sample preparation apparatus shown in Figure 3.4 was developed using a plastic funnel; a 0.3 m long, 0.08 m inside diameter PVC pipe; a 5 mm opening size screen, and a 2.5 mm opening size screen. The sample preparation apparatus was based on the pluviation apparatus fabricated by Frost (1989), and is also similar to the apparatus used at UC Davis. The two screens were securely placed at one end of the PVC pipe spaced at approximately 12 mm apart, with the coarser screen on top of the finer screen. The screens were held in place by thin wires weaved through the screens and fastened securely to the pipe through small diameter holes drilled in the pipe. The plastic funnel was attached using duct tape at the end of the pipe opposite to the screens to act as a receptacle for the sand.

FIG. 3.4. Pluviation apparatus

Specimen preparation using the pluviation apparatus was achieved by placing dry Ottawa 20-30 sand in the funnel and allowing it to fall into the specimen container to create uniform deposits of sand as illustrated in Figure 3.5. Multiple specimens were created to calibrate the pluviation apparatus. The variables that control the density of the resulting specimen are:

1. The size of the openings in the two screens that are placed at the end of the PVC pipe; and
2. The fall height of the sand from the end of the PVC pipe to the surface of the sand in the box (bottom of the box at the very beginning).

The sieves in the PVC pipe serve to disperse the sand as it falls through them, leading to uniform deposition of the sand. The intensity of sand placement (rate of discharge) is a function of the size of the openings in the sieves. The intensity is greater as the opening size increases. Higher intensities also correspond to lower densities. In this work, the openings used were 5 mm and 2.5 mm.

At a given intensity, the density of the deposited sand increases with increasing fall height. The height of fall of the sand was maintained using a nylon rope that was tied to the end of the PVC pipe. A weight was attached to the other free end of the nylon rope to keep it taut. The length of the nylon rope corresponded to the height of fall of the sand. The apparatus was maintained at a height such that the end of the rope was always at the same elevation as the sand surface in the container.

Numerous samples of Ottawa 20–30 sand were prepared using varying heights of fall and their densities were determined by the dimensions of the specimens and the weight of sand placed in a container. A plot of density versus height of fall is presented in Figure 3.6. This plot is used to determine the fall height required to desired relative density.

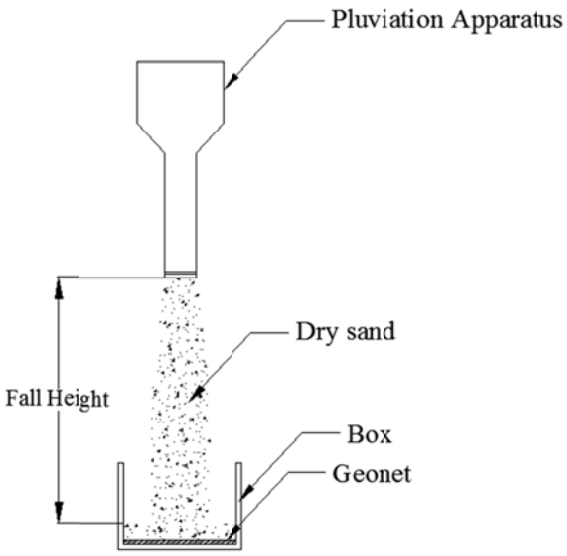

FIG. 3.5. Illustration of sample preparation procedure

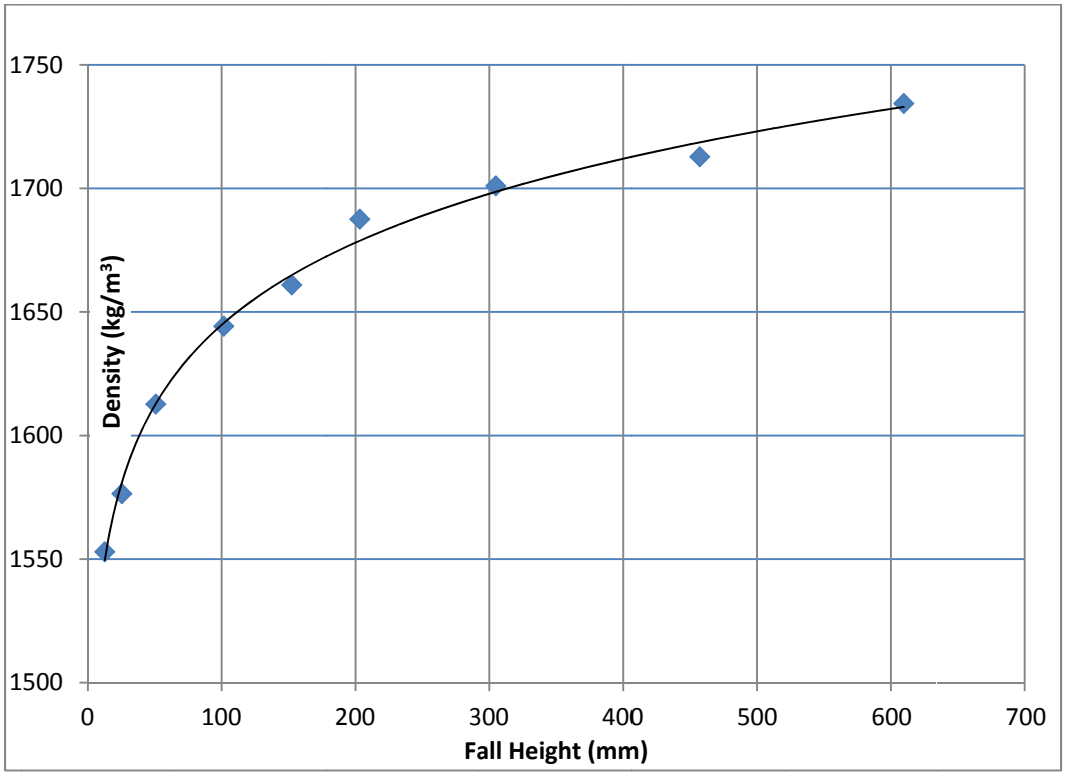

FIG. 3.6. Pluviation apparatus calibration curve

3.2.3 Preparation of Specimens in Box

The following equipment was used in preparing Ottawa 20-30 sand specimens in the specimen box:

1. The specimen box (Figure 3.2)
2. Pluviation apparatus (Figure 3.4)
3. 280 mm by 560 mm geocomposite geonet

The following steps were followed in the creation of specimens in the box:

1. The geocomposite geonet was placed on the bottom of the box. The geonet was used to distribute the water pressure evenly at the bottom of the sand during saturation procedures (described later in this chapter) and also to act as a separator to keep the sand from flowing into the drainage ports located at the bottom of the box. Figure 3.7 shows the box with geonet in place.

FIG. 3.7. Box with geonet in place

2. Using the pluviation apparatus, the specimen was created by placing sand in the funnel and letting it fall into the box. Samples were created at a fall height of 457 mm, corresponding to a density of 1,710 kg/m^3 (a dry unit weight of 16.77 kN/m^3). During pluviation, the

weight tied to the nylon rope was maintained just above the top of the sand in the model (bottom of the container at the beginning) as a way to maintain the fall height throughout the sample creation process. The pluviation apparatus was raised to maintain the height of fall while sand was continuously poured into the funnel. A picture of this sample creation step is shown in Figure 3.8. Figure 3.8 also shows the weight maintained just above the specimen surface and a completed sample. The pluviation apparatus was moved back and forth until the desired height of sand was reached.

FIG. 3.8. Pluviation in progress and a completed specimen

3.2.4 Preparation of Specimens for Triaxial Tests

The following equipment was used in the creation of 71 mm diameter specimens for triaxial testing of never frozen sand:

1. A split vacuum mold used for preparation of the 71 mm diameter specimens. The split vacuum mold was used for stretching the confining membrane to allow for pluviation of sand into the confining membrane.
2. Two 71 mm diameter porous stones.
3. One 71 mm diameter confining membrane with a thickness of 3.0×10^{-1} mm.

4. The pluviation apparatus.
5. At least two rubber O-rings
6. One source of vacuum.

The GCTS Cyclic Pneumatic Soil Triaxial System STX-050 (GCTS Testing Systems, 2005) in the Enamul and Mahmuda Hoque Geotechnical Laboratory was used for all triaxial tests. The following steps were employed in the creation of specimens for triaxial testing:

1. The top assembly of the GCTS triaxial cell was removed for easier access and to allow for pluviation of sand into the split mold. After the specimen was created, the top assembly was replaced.
2. The confining membrane was placed over the bottom pedestal of the triaxial cell and secured with at least one O-ring.
3. A porous stone was placed inside the confining membrane, on top of the bottom pedestal of the triaxial cell.
4. The vacuum split mold was placed securely on the bottom pedestal with the confining membrane inside and then the free top end of the membrane was folded over the vacuum split mold. A vacuum was applied to the split mold to hold the confining membrane taut against inside of the mold.
5. Using the pluviation apparatus, the specimen was created by placing sand in the funnel and letting it fall into the confining membrane supported by the vacuum split mold until a specimen height of at least 0.142 m was achieved. Samples were created using a fall height of 457 mm and a

corresponding density of 1,710 kg/m^3, consistent with the box model specimens.

6. The second porous stone was then placed on the top of the specimen, the top platen was placed on top of the porous stone, and the membrane was rolled over the top platen and secured with at least one O-ring.
7. A confining pressure of 10 kPa was then applied via vacuum to the specimen through the top platen drainage line of the GCTS triaxial cell. With the sample confined, the vacuum on the split vacuum mold was shut down and the split mold was removed. Steps 1 through step 4 are shown in Figure 3.9. Steps 4 through step 7 are shown in Figure 3.10.

FIG. 3.9. Triaxial test specimen preparation Steps 1- 4

FIG. 3.10. Triaxial test specimen preparation Steps 1- 7

8. The top assembly of the GCTS triaxial cell was then replaced. With the top assembly in place, the specimen preparation was complete.

3.2.5 Box Specimen Saturation Procedure

The saturation procedure used in this work was modeled after the vacuum saturation method described by Ueno (2000). The equipment used for the saturation procedure used in this work includes:

1. A source of deaired water
2. A vacuum source
3. A source of carbon dioxide (CO_2)

The sample preparation method was described in Section 3.1.3 and Section. The initial state of the specimen is dry Ottawa 20-30 sand in the model box which is capable of holding a vacuum). The saturation process employed the following procedure:

1. The lid was placed on the box and securely fastened using the six latches.
2. Air was removed from the sand specimen by applying a vacuum of 10 kPa to the box. The vacuum was applied through the top port of the box.

3. The vacuum in the box was relieved by slowly introducing carbon dioxide gas into the container using a second port on the lid of the box.
4. The carbon dioxide source was turned off and the vacuum of 10 kPa was reapplied to the container.
5. The sample was then saturated by introducing water from bottom to top. The box samples were saturated using tap water because a high level of saturation was not necessary for the sampling freezing tests. The bottom drainage ports were connected to a cooler (Igloo Quick and Cool 60 quart Model) filled with water. The cooler had a drainage port at the bottom to which a garden hose was attached. The other end of the garden hose was attached to the five drainage ports on the box via a manifold. The water level in the cooler was maintained at the same level as the top of the sand. Figure 3.11 shows the box container undergoing vacuum saturation.

FIG. 3.11. Vacuum saturation of box specimen

3.2.6 Triaxial Tests Specimen Saturation Procedure

The saturation procedure for triaxial test specimen followed the same steps as the saturation procedure for the model box specimen. The sample preparation

method was described in section 3.2.4. The saturation procedure that was used to saturate the triaxial test specimens is described below:

1. The specimen was placed inside a triaxial cell in order to change the application of the confining pressure from vacuum to cell pressure. Therefore, before the vacuum was released, a cell pressure of 10 kPa was applied to the sample using the GCTS system from the bottom drainage line of the cell (the cell was filled with water prior to application of the 10 kPa confining pressure). A confining pressure has to be applied to the specimen at all times during the sample preparation and saturation process. Otherwise, the specimen will slump over.
2. The vacuum in the specimen was relieved by slowly introducing carbon dioxide gas into the specimen through the drainage line of the bottom cap.
3. The carbon dioxide source was turned off and the vacuum of 10 kPa was reapplied to the sample using the top cap drainage line.
4. The sample was then hydrated, under vacuum from bottom to top using deaired water. The vacuum and deaired water were turned off when the sample was fully hydrated as indicated by the appearance of water in the vacuum line.
5. Saturation was then achieved using back pressure procedure described subsequently.

Chapter 4

4.0 SAMPLING PROCEDURE

4.1 Selection of Sampling Method

Based on the project constraints, the following criteria were established for the required sampling method:

1. The method should be able to recover samples in a manner that retains their micro structure and stress-strain behavior.
2. Since the project is a collaborative effort between three different universities, it was important that the method be simple enough to be reproducible by different research groups with little difficulty.
3. The method also needed to be adaptable to different model containers, including the types used at the University of California at Davis (UC Davis) centrifuge and State University of New York at Buffalo shake table.
4. Sampling should be able to be performed in a relatively short time so as not to tie up any equipment for extended periods of time.
5. The sampling method should be non-destructive to the model container.

After establishing the criteria for the required sampling method, a systematic evaluation of the sampling methods reviewed in the literature was conducted. The three sampling methods were evaluated on the basis of the above mentioned criteria.

4.1.1 Biopolymers Agar and Agarose

The agar and agarose processes are similar in implementation. For the purposes of technology evaluation, the agar and agarose processes were considered under the same title of biopolymer. The following challenges were identified with the biopolymer process:

1. From the literature review, Schneider et al. (1989)'s laboratory experiments match closely with this study's initial condition of the soil. Schneider et al. (1995) used tubes inserted in the cohesionless soil for installation of: electrodes for heating the soil; thermometers for temperature monitoring; and an injection tube for injection of biopolymer. All these tubes are necessary for successful impregnation with biopolymer. Experiments performed by Yoshimi et al. (1978) show the extent of disturbance that results from pushing a tube into cohesionless soil. Yoshimi et al. (1978) showed that a placement of a tube in cohesionless sand results in disturbance over a distance approximately equal to the diameter of the tube. This study may require sampling from small containers with limited exposed surface area. Cohesionless samples would have to be obtained at distances sufficiently far enough from all tubes to be free of disturbance. The placement of the required tubes would effectively reduce the number of samples that can be obtained from a physical model.
2. The biopolymer process requires heating the soil to a certain minimum temperature prior to impregnation. Temperature monitoring is required in order to keep the soil temperature above the gelation temperature of the biopolymer and below the boiling temperature of water. The process of

heating the soil also presents an opportunity for disturbance. The possibility of boiling the pore water is a problem that we wished to avoid. Mitchell et al. (2005) suggests that drained heating would not result in significant volume change and by extension, significant disturbance. However, it is a possibility that some undrained heating might occur during heating the soil for purposes of impregnation with biopolymer, This was also identified as a potential source of disturbance.

3. Schneider (1989) and Sutterer et al. (1995) used the agarose impregnation and flushing devise to remove the biopolymer from samples prior to testing. There is not information on other biopolymer removal processes that do not rely on the use of the impregnation and flushing device. The biopolymer impregnation and flushing device was specifically designed for triaxial test specimens. This did not suit the selection criteria because it requires fabrication of a special device for biopolymer removal. Triaxial compression tests are planned for the recovered undisturbed samples. The use of a special fabricated device to remove biopolymer from triaxial specimens meant that additional devices would be needed for subsequent tests.
4. Complete removal of the biopolymer is difficult to achieve.

For the reasons outlined above, the biopolymer process was judged not to be simple enough to be seamlessly transferable and reproducible at different universities. The biopolymer process also provided multiple opportunities for introducing disturbance in the samples.

4.1.2 Elmer's Glue

The use of Elmer's glue presented similar challenges as the agar as far as impregnation and complete removal. These challenges and other problems specific to the use of Elmer's glue are discussed below.

1. Evans (2005) used the glue on dry samples of sand. The sand that will be used in this work will be water saturated. This presented a problem because Elmer's glue is soluble in water. Maintaining the concentration of the glue during impregnation would be difficult unless the soil is drained prior to impregnation with Elmer's glue. Draining the soil could introduce disturbance to the specimen due to hydraulic gradients and changes in effective stress.
2. The glue impregnation process required specialized equipment. The humidity of the air coming from the glue impregnated sand was monitored to determine when the glue had cured. When the relative humidity was below 40 %, the glue had cured (Evans 2005). If this method was used, impregnation and curing equipment with the capability to measure relative humidity would be required. The need for specialized equipment made the Elmer's glue method less than ideal for this work's application.
3. Elmer's glue took 5-7 days to cure (Evans, 2005). This curing period was expected to be longer for water saturated cohesionless soil. The time required to cure Elmer's glue stabilized samples was judged to be impractical for this work's application.
4. Complete removal of Elmer's glue from the soil pores without significantly disturbing the soil structure may not be possible.

5. Evans (2005) did not perform any tests to assess the quality of samples obtained using Elmer's glue. It was not clear from the literature if Elmer's glue stabilized samples were undisturbed.

Based on the discussion above stabilization and sampling by use of Elmer's glue was determined to be impractical for our application.

4.1.3 Freezing

Stabilization and sampling using freezing was selected from the methods reviewed as the preferred way to obtain undisturbed samples of cohesionless soil. This method fit the criteria that were developed for selection of a sampling method very well.

The freezing method should be able to recover samples in a manner that retains their micro-structure and stress-strain behavior. The literature review shows that different investigators have looked at the void ratio changes associated with the freezing and thawing of cohesionless soil. If a unidirectional freezing front is applied, a minimal overburden stress applied, and at least a single drainage path is maintained in the direction of freezing, the void ratio changes in a cohesionless soil during freezing have been found to be insignificant. Yoshimi et al. (1978) compared the drained stress-strain behavior of frozen and then thawed soil with never frozen soil and found that there was no significant difference between the two. The results of the stress-strain behavior comparison of Yoshimi et al. (1978) are presented in Figure 2.16.

The laboratory freezing process used by Yoshimi et al. (1978) to investigate the volume changes due to freezing (shown in Figure 2.10) appeared simple enough to be easily replicated and is therefore the basis of the freezing process that was developed for this study. Since the project is a collaborative effort between three different universities, it was important that the method be simple enough to be reproducible by different researchers with little difficulty. The freezing process does not require insertion of anything into the soil. The soil is frozen by application of a cold front at the surface of the model. Yoshimi et al. (1978) applied the freezing surface at the bottom of the soil.

Freezing is adaptable to different model containers. Since the freezing front is applied at the surface of the container, the freezing application contact area can be increased or reduced to suit the size of model container and thus, is adaptable to different size containers. This adaptability is important because the freezing method will be used at both the University of California at Davis (UC Davis) centrifuge and State University of New York at Buffalo shake table in this research program.

4.2 Development of Freezing Procedure

Following the selection of freezing as the stabilization method, a plan for development of a freezing method was initiated. The objective of the plan was to develop a method to freeze uniform specimens of sand by applying a unidirectional freezing front while maintaining at least one drainage path in the direction of freezing front propagation.

4.2.1 Freezing Procedure

As mentioned above, the objective of the work described herein was to develop a method for undisturbed sampling of cohesionless soil within the laboratory environment. The freezing procedure was developed for the box model container that was described earlier. The freezing procedure was modeled after the bottom up laboratory procedure that was used by Yoshimi et al., (1978). The following equipment/materials were required for freezing and sampling the soil in the model box:

1. A metal pan with a flat bottom. A baking pan 254 mm by 508 mm by 25.4 mm was used in our freezing tests.
2. Ethanol. Koptec 200 proof ethanol was used in all freezing tests
3. Dry ice

The freezing procedure consisted of the following steps:

1. The initial state of the specimen to be frozen was the saturated sand in the box connected to a cooler full of water with no head difference between the cooler and the box. The first step was to establish a drainage path for water expelled from the box. This was achieved by making sure that the connection between the box and cooler was open.
2. Dry ice was placed into the pan, the pan containing dry ice was then carefully placed on top of the saturated sand in intimate contact with the sand, and the alcohol was slowly poured into the pan using a funnel.

3. The dry ice was replenished as it was used up while monitoring the progress of the freezing. Freezing progress was monitored through the lexan panel that formed one side of the box.
4. When the required thickness of sand was frozen, the freezing process was stopped by removing the pan filled with the mixture of alcohol and dry ice from the specimen. The pan had a tendency to stick to the surface of the sand. A little tapping was required to free the pan from the frozen sand. The time it takes to freeze the sample is a function of, among other things, the quantity of sand to be frozen, the ambient temperature, and the material to be frozen. Freezing the entire mass of sand caused the sand to stick to the geonet and interfere with the sample recovery. To avoid this, the sand was only frozen to approximately 25 mm from the bottom, as observed through the lexan side of the box. It took approximately 2.5 to 3.5 hours to freeze the sand in the box to a depth of approximately 150 mm.

4.2.2 Numerical Modeling of Freezing Front Propagation

The literature review indicated that during freezing of water saturated sand, pore water migrates in the liquid phase to accommodate the expansion of the pore water as it freezes. A uni-directional freezing front is desired such that no liquid water is trapped due to impeded drainage by either frozen sand or an impermeable surface. If other freezing fronts developed at the bottom or sides of the box, e.g. due to potential freezing temperatures along the metal sides of the container, then the freezing front would not be uni directional. Multiple freezing fronts in the box

might trap liquid water leading to disturbance of the soil structure. Therefore, a two dimensional finite element numerical analysis of heat flow were conducted to establish that a unidirectional freezing front was induced in the model during the freezing setup.

The finite element program SVHeat (Soil Vision, 2010) was used to model the freezing method. A two-dimensional steady state analysis was conducted in the short (279 mm (11 inches)) dimension of the box, as the short dimension was logically, the critical cross section with respect to heat flow (or cold) transfer along the metal sides of the box. A sketch of the SVHeat model is shown in Figure 4.1. The numerical model shows the aluminum box bounded by layers of air on both sides and finally, coolant to top consistent with the described freezing method.

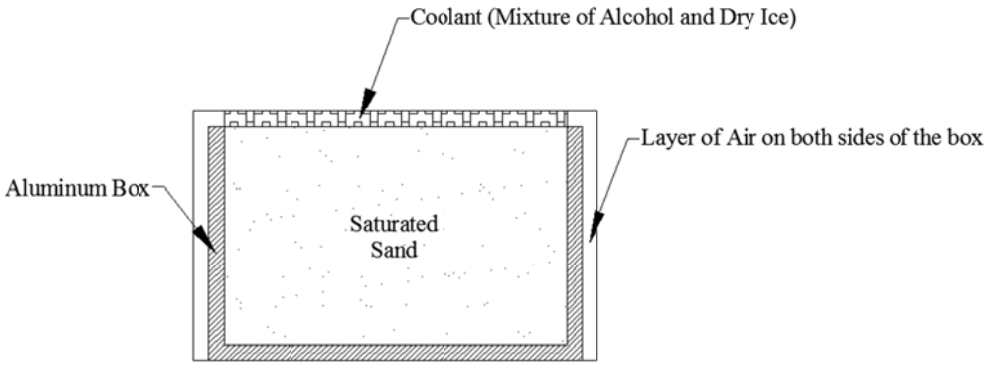

FIG. 4.1. Sketch of numerical model

The box was conservatively modeled to be made entirely of aluminum (the front is made of lexan). The geometry of the box was as built, 13 mm thick aluminum with inside dimensions of 280 mm by 180 mm. Layers of air were

defined around the aluminum box to simulate laboratory boundary conditions. The outside boundaries of the air layers had a constant temperature of 80°F (room temperature). We measured the temperature of the alcohol and dry ice mixture to be -68°C. This is similar to the temperature reported by Yoshimi et al (1978). The bottom of the model was modeled as constant flux boundary.

The result of the finite element investigation showed that freezing front would propagate from the coolant surface down to the bottom of the box without creating secondary freezing fronts from the sides of the box. Figure 4.2 shows the results of the numerical modeling.

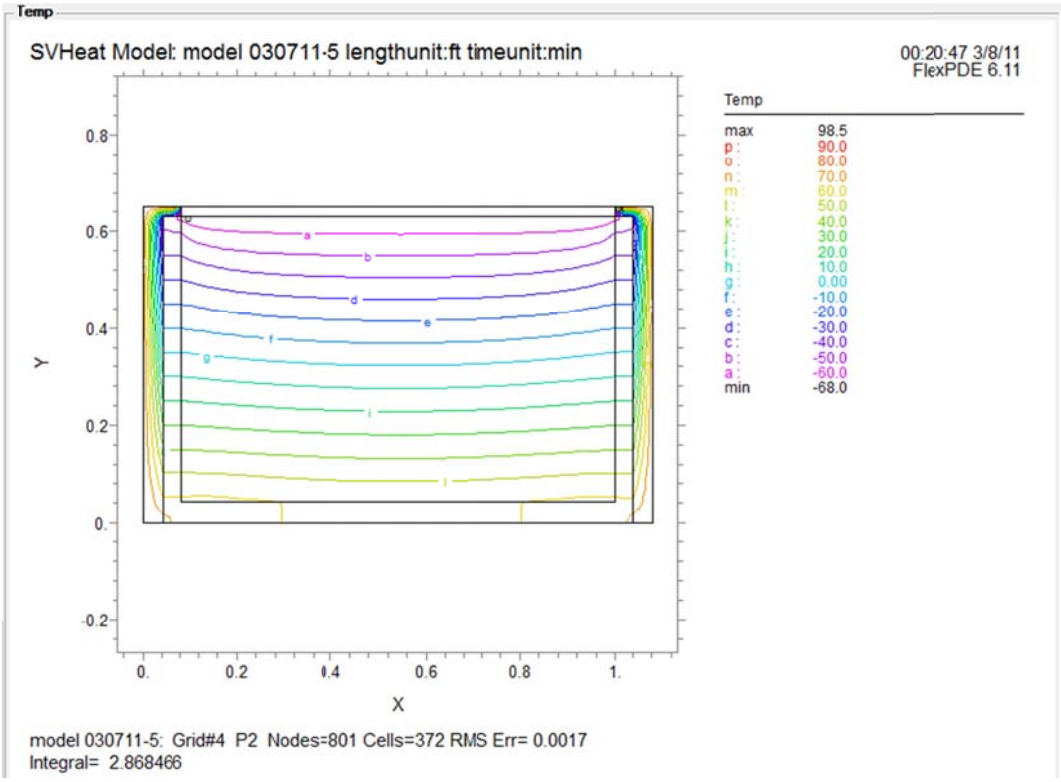

FIG. 4.2. Numerical Modeling of Freezing Front Propagation

4.2.3 Experimental Investigation of Freezing Front Propagation

Laboratory experiments were also conducted to investigate the propagation of the freezing front. Freezing experiments were setup by placing sand in the model box as described above except that eight thermocouples were placed in the model at predetermined different locations prior to placement of sand by pluviation. The thermocouples were placed in the model using a wooden form that was fabricated for this experiment to securely hold the thermocouples in place during pluviation. Sketches of the form and the locations of the thermocouples are shown in Figure 4.3. Only the short dimension (280 mm) was investigated because, as noted before, it is the most critical dimension. The thermocouples were placed in only half of the cross section because the freezing was expected to be symmetrical about the middle plane of the box. The thermocouples were numbered as shown in Figure 4.3.

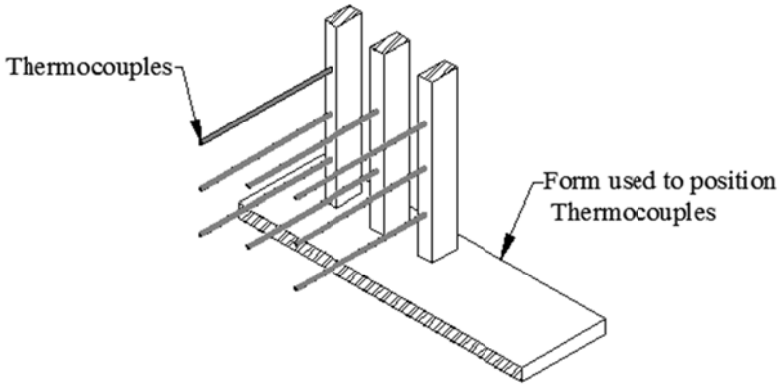

(a)

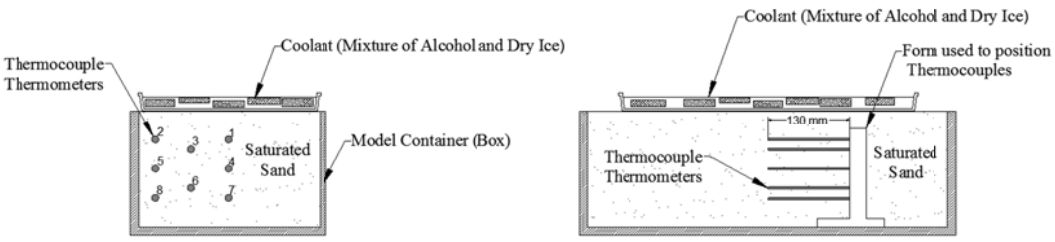

(b)

FIG. 4.3. Freezing front investigation experimental setup

After saturation, freezing was initiated by placing the metal pan containing the coolant on top of the saturated sand. The thermocouples were monitored to record the temperature of the sand at the locations shown in Figure 4.3 with time. The trend of temperature drop was noted and the onset of freezing was assumed to coincide with the thermometers recording a temperature of 0° C.

The results of the experiments showed that the freezing front propagated uni-directionally to the same configuration as predicted by the numerical analyses. Thermocouple 1 was the first to freeze and thermocouple 8 was last to record a freezing temperature. Thermocouple 4 recorded a freezing temperature before Thermocouple 5. If a secondary freezing front developed along the sides of the container, thermocouples 2, 5 and 8 would have frozen much sooner than they did. Following completion of the freezing front propagation investigation, the frozen soil was excavated to inspect the shape of the frozen soil. The shape of the bulb of the frozen soil also confirmed the numerical analysis result. The excavated frozen bulb is shown in Figure 4.4.

FIG. 4.4. Form with thermometers and frozen bulb of sand

The thermocouple experiment showed that the freezing method described in section 4.2.1 induced a unidirectional freezing front to the saturated soil. The shape of the frozen soil excavated after the experimental investigation was consistent with the conclusions reached from the temperature measurement data steady state numerical analysis.

4.2.4 Expansion of Saturated Soil during Freezing

Yoshimi et al. (1978) concluded that a unidirectional freezing front, drainage path, and surcharge were necessary to limit the disturbance of the cohesionless due to freezing of pore water. Ottawa 20-30 sand specimens in the box were frozen multiple times in order to investigate the expansion due to freezing soil under the conditions described in Section 4.2.1.

As discussed in the previous section, it was confirmed that the freezing technique described in section 3.3 resulted in a unidirectional freezing front from top to bottom. The drainage path was also kept open throughout the freezing process. Based on observations made during multiple freezing trials, it was

concluded that the surcharge due to the weight of the pan filled with coolant (0.8 kPa) was adequate to limit expansion to negligible levels. Significant expansion of the frozen soil would result in heaving of the soil surface or deformation of the box to accommodate the expansion. Water in liquid phase was observed flowing out over the edge of the model box, during freezing experiments, consistent with the theory that water is expelled in front of the freezing front to accommodate the nine percent expansion of water when it changes phase from liquid to solid. Figure 4.5 shows water flowing over the edge of the model box as the freezing front propagated.

FIG. 4.5. Water flowing out of box during freezing

4.3 Development of Coring Technique

Following the development of a freezing technique, a method to recover frozen samples was also developed. Most triaxial testing systems are capable of testing 35mm diameter and 71 mm diameter test samples without requiring specialized platens. Samples required for microstructure studies are on the scale of 35 mm diameter samples. For these reasons, it was decided initially that 35mm diameter samples were going to be recovered for testing.

4.3.1 Coring Equipment

A Milwaukee 6.35 mm Magnum Drill was used in conjunction with a 37.5mm (inside) diameter diamond core drill bit to drill through the frozen soil and recovered cores of soil samples. Maintaining the drill and core barrel assembly in vertical position during coring was a problem during the first few drilling trials. A drill guide was designed and fabricated to be fitted over the box and hold the drill in vertical position during drilling. Design drawings of the drill guide are presented in Appendix B. With practice, it was possible to drill without the drill guide, making it possible to recover more samples than can be recovered using the drill guide. Figure 4.6 shows the equipment used to recover 35 mm diameter cores, including the drill, 37.5 mm diamond core drill bit, and the drill guide.

FIG. 4.6. Milwaukee drill, 35 mm diameter core barrel and drill guide

4.3.2 Coring Procedure for 35.6 mm Diameter Core Samples

The state of the box and specimen after freezing and prior to coring is shown in Figure 4.7. To recover samples, the drill guide was fitted on the box and then the diamond core dill bit was placed through the tubular part of the drill guide to

start drilling. Drilling was performed by one person and did not require an excessive amount of force. After drilling through the frozen material, the drill bit was removed and the frozen cores simply fell out of the drill bit. Figure 3.18 shows sample recovery in progress. A typical sample recovered using this technique is shown in Figure 4.8. The sample shown in Figure 4.8 was approximately 35 mm in diameter and 162.5 mm in length. Note that although a 37.5 mm core barrel was used, the recovered core was melty around the perimeter. The samples were stored in a freezer soon after recovery to avoid premature thawing. Figure 4.9 shows the frozen mass of soil after samples have been recovered from it.

FIG. 4.7. Box after freezing

FIG. 4.8. Coring in progress and recovered 35 mm diameter core

FIG. 4.9. Box and sand after coring

After samples were recovered, they were placed in a confining membrane and stored in a freezer for later retrieval and testing.

4.3.3 Coring Procedure for 71 mm Diameter core Samples

For reasons discussed in Chapter 5, it was decided that 71 mm diameter core samples were required for triaxial testing. The following equipment was used to recover 71 mm diameter core samples:

1. 71 mm internal diameter steel pipe (Shown in Figure 4.10)
2. Shelby tube drill adaptor (Shown in Figure 4.11). The design drawing of the Shelby tube drill adaptor is presented in Appendix A
3. A Milwaukee 6.35 mm Magnum Drill (see Figure 4.6)
4. Husqvarna DR 150 Core Drill Rig (Shown in Figure 4.12)
5. Core Drill Rig Adaptor (Shown in Figure 4.12)

FIG. 4.10. Steel pipe used for 71 mm cores

FIG. 4.11. Shelby tube drill adapter

FIG. 4.12. Husqvarna DR 150 core drill rig

FIG. 4.13. Core drill rig adaptor

Project collaborators from Bucknell University reported that they had success coring frozen sand using a nominal 75 mm diameter Shelby tube. The adapter shown in Figure 4.11 was fabricated for use with the Milwaukee 6.35 mm Magnum drill and a Shelby tube. The initial attempt to drill with a Shelby tube did

not work because the Shelby tube wobbled and deformed the adaptor on the first try. The decision was made to use a machined steel pipe which was more rigid, nearly circular and did not wobble as much as the Shelby tube during drilling. The pipe was also strong enough to be ground to create cutting teeth on the pipe.

It was significantly harder to start coring with the 71 mm steel pipe than with the 37.5 mm core barrel. The cutting teeth created prior to coring helped a lot in this regard but also wore out as the coring progressed. The pipe was nearly perfectly round and, it wobbled slightly during coring but not as much as the Shelby tube wobbled. The procedure used to advance the core was to hold the spinning pipe on the surface of the sand as steady as possible until enough penetration was achieve to hold the pipe in place. Considerable effort was required to initiate and continue drilling to depth. Coring with the 71 mm diameter pipe is shown in Figure 4.14.

FIG. 4.14. Coring with 71 mm diameter steel pipe

Samples were readily obtained after coring without much difficulty. Occasionally, the cores got stuck in the pipe and a sample extruder was used to

recover the sample. The 71 mm diameter sample and the model box after samples have been recovered from it are shown in Figure 4.15.

FIG. 4.15. Large 71 mm diameter samples and specimen after sample recovery

The samples recovered using the Milwaukee 6.35 mm Magnum Drill and Shelby tube were generally acceptable except that they were often not long enough for triaxial testing. Due to the difficulty in keeping the Shelby tube in one place and vertical at the beginning of coring, the top 10 to 30 mm portion of the sample was usually tapered. For triaxial testing of 71 mm diameter samples, samples are required to be at least 142 mm in height. The thickness of the frozen sand in the box container specimens ranged from approximately 150 mm to 165 mm. The tapered portion of the recovered samples had to be trimmed in order to achieve a uniform cross section of the triaxial test sample. In certain cases, the combination of the recovered sample height and the length of the tapered section resulted in trimmed samples that were too short for triaxial testing.

Initial coring trials with the Husqvarna DR 150 core drill rig were conducted with a steel tube without any cutting teeth. A steel tube, with a thinner wall than the tube that was used with the Milwaukee 6.35 mm Magnum Drill was fabricated

for use with the core drill rig. The steel tube cored through the frozen sand with minimal effort (weight of the assembly). Significant melting of the sample was observed from the initial trials. The samples recovered, were less than 71 mm in diameter and in certain trials, were tapered at the top. Increasing the speed of coring by application of pressure reduced the amount of melting and tapering but did not eliminate the problem out right. The thin walled steel tube was ground to create cutting teeth in manner similar to the cutting teeth created on the 71 mm internal diameter pipe that was used with the Milwaukee 6.35 Magnum Drill. The use of a pipe with cutting teeth eliminated the melting and tapering problem. Coring with the coring rig is shown in Figure 4.16 and samples obtained using the coring rig are shown in Figure 4.17

FIG. 4.16. Coring with coring rig

FIG. 4.17. Sample Recovered Using Coring Rig

Following recovery, the 71 mm diameter samples were wrapped in 'house hold plastic wrap" wrap and aluminum foil and then stored in a freezer.

4.3.4 Coring Challenges

The following challenges were encountered in the development of the sampling technique:

1. Keeping the 37.5 mm diamond core drill bit vertical during drilling was a challenge. The drill guide was designed to solve this problem and it worked well. However, when more samples are required and there is a need to drill in the middle of the box, the drill guide cannot be used. With practice the challenge of keeping the core drill vertical without the drill guide was overcome; a second person was used to help orient and correct the inclination of the drill bit during drilling.

2. When the specimen in the box is frozen all the way to the bottom, the samples tended to stick to the filter fabric at the bottom of the box. When this happened, the sample stayed within the hole when the diamond core drill bit was withdrawn. Recovery of the sample without damage was difficult to achieve in this instance.
3. During drilling, it was important to drill nonstop. When drilling was stopped while the diamond core drill bit was still in the hole, the material around the diamond core bit froze making it very difficult to restart the drill. There were times when the specimen had to be abandoned because sampling could not be restarted after the diamond core bit got stuck.
4. Cohesion between the inside of the diamond core drill bit and the sample sometime kept the sample trapped in the core barrel. When sample for stuck in the core barrel, it was removed by pouring cold tap water around the outside of the diamond core drill bit. The relatively warm tap water melted the surface of the sample, freeing it from the diamond core drill bit. This method of freeing the sample came at a risk of reducing the diameter of the recovered sample by melting too much of the surface.
5. The samples were stored in a cold freezer right after recovery to mitigate premature thawing. An easily accessible storage facility or container capable of maintaining freezing temperatures was required.
6. Coring 71 mm samples using the Milwaukee drill and the steel pipe was very difficult because the steel pipe used as a core barrel was not perfectly round and tended to wobble during drilling. In the absence of a

drill guide, it was difficult to start coring through the sand, so the top of the recovered samples were significantly tapered. As a result, recovery of samples that were 71 mm in diameter and at least 142 mm long (as required for triaxial testing) was rare. As a solution to this problem, a Husqvarna DR 150 core drill rig and machined pipe were used to recover 71 mm diameter samples.

7. The coring process crushed sand particles during sampling. Repeated use of the sand led to changes in particle angularity and gradation. As a solution to this problem, the Ottawa sand was used only once and then discarded.

Chapter 5

5.0 TESTING OF NEVER FROZEN SAND SPECIMENS AND RECOVERED SAMPLES

The GCTS Cyclic Pneumatic Soil Triaxial System STX-050 (triaxial system) discussed in Chapter 4 was used to perform the monotonic triaxial compression tests for the work described herein. The test sand was Ottawa 20-30 sand (ASTM Designation C778) supplied by U.S. Silica Company, Ottawa, Illinois. A total of 116 tests were performed. The purpose of these tests included:

1. Training on the data acquisition and experimental control components of the triaxial system.
2. Drained and undrained tests to establish the baseline stress-strain-strength response of never frozen Ottawa sand specimens prepared using the pluviation technique described in Chapter 3.
3. Drained and undrained tests performed on samples of Ottawa sand recovered using the freezing and coring techniques described in Chapter 3 and then thawed in order to assess the quality of the samples after thawing.

Comparisons of the stress-strain-strength and pore pressure-strain plots of never frozen sand and the frozen and then thawed samples were used to assess the quality of the samples obtained using the procedures present in this work.

5.1 Test Parameters

5.1.1 Initial Density

All tests specimens were prepared using the pluviation apparatus described in Chapter 3. The fall height was maintained at 457 mm. The density of the samples prepared at this fall height was approximately 1,710 kg/m^3. Maximum and minimum densities of Ottawa 20-30 sand were calculated as 1,764 kg/m^3 and 1,521 kg/m^3, respectively, using values of minimum and maximum void ratio published by Santamatina et al. (2001), assuming zero percent saturation. Based on the calculated maximum and minimum densities, the relative density of the resulting specimens was 80%.

The density of each specimen prepared for this testing program was verified using direct measurements on the prepared specimens. One method to determine how much sand is in a specimen is to start with a known mass of sand and then weigh the remaining sand after the sample has been created. However, pluviation results in significant loss of sand due to scatter. Therefore, to verify the density of the pluviated specimens, the sand in the specimen was collected after completion of the triaxial compression tests, oven dried, and weighed.

The density of the specimen created in the box was also confirmed by measuring the density of six cores recovered from the frozen box sample using methods described in Chapter 4. These samples were used for density tests only, no triaxial tests were performed on these samples. The density was determined by measuring the volume of the frozen cores, oven drying the cores, and then

measuring the mass of the dry sand. The results of the density tests are presented in Table 5-1.

Table 5-1. Density Confirmation Test Results

Core #	1	2	3	4	5	6
Density (kg/m^3)	1699	1688	1709	1696	1697	1689

5.1.2 Confining Pressure

The triaxial compression tests were conducted at an effective confining pressure of 60 kPa. This confining pressure was chosen to be consistent with the confining pressures employed by Bucknell University, one of our collaborating partners on the larger project.

5.1.3 Specimen Saturation

Following vacuum hydration of the sample as described in Chapter 3, back pressure techniques were used to saturate the specimen. Based on the relationship between Skempton's B-value (the ratio of the change in pore pressure to the change in isotropic confining pressure under undrained conditions) and the degree of saturation, a B-value of at least 0.90 was chosen as the indicator of saturation, i.e. of the point at which the triaxial tests could be performed. As illustrated in Figure 5.1, the level of saturation for Ottawa sand is nearly 100 percent when the B-value (pore pressure parameter, B) is 0.9. This standard was applied to both drained and undrained tests.

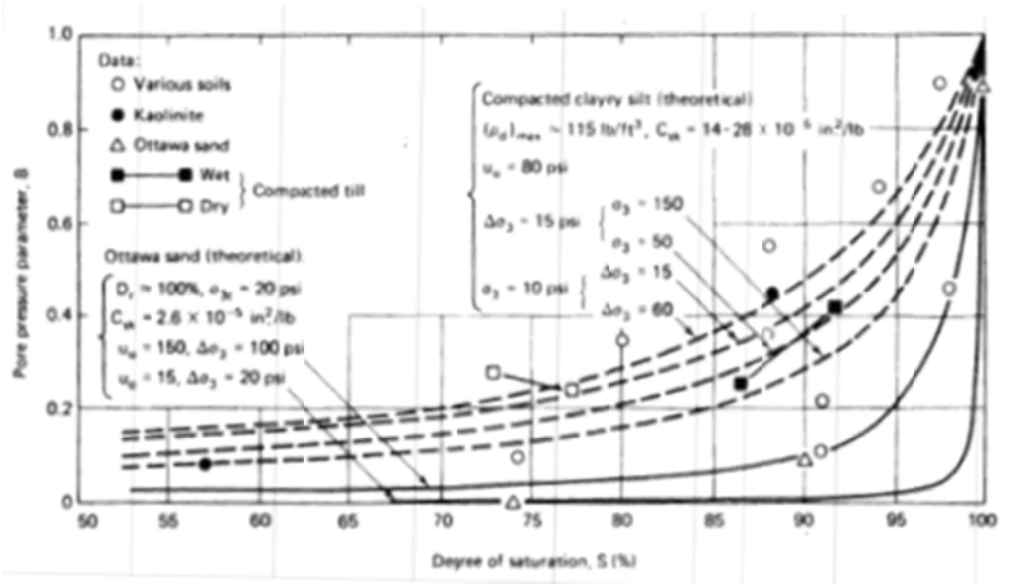

FIG. 5.1. B-value as a function of degree of saturation (Holtz & Kovacs 1981)

For the initial step in back pressure saturation, the sample was hydrated and confined under an effective pressure of 20 kPa. The triaxial cell was then placed under the load cell and a nominal seating load was applied to stabilize the sample. The B-value was determined by increasing the confining pressure by 10 kPa with the drainage lines closed and recording the resulting change in pore water pressure. The drainage lines were reopened after the B-value test. If the calculated B-value was less than 0.9, the back pressure was increased by 10 kPa and the confining pressure was also increased by 10 kPa to maintain the effective confining pressure of 20 kPa. A new B-value was then determined at the new back pressure by repeating the above procedure. This procedure was repeated until a B-value greater than 0.9 was achieved. B-values of 0.9 were typically achieved at back pressures on the order of 150 kPa.

5.1.4 Strain Rate

Samples were loaded in triaxial compression at a strain rate of 0.625 % per minute. A sensitivity analysis was performed to investigate the effect of strain rate on triaxial testing under previously mentioned test conditions. The sensitivity analysis revealed that decreasing the strain rate from the 0.625 % per minute to as low as 0.125% per minute in undrained loading did not change the stress-strain-strength behavior of the specimen.

5.2 Test Procedures and Data Acquisition

5.2.1 Tests on Never Frozen Sand Specimens

Specimens of never frozen Ottawa sand were created as described in Chapter 4 and tested on the same day they were created. The never frozen Ottawa sand specimens were tested under drained and undrained conditions. Following back pressure saturation and consolidation, the triaxial compression test was initiated. Except for the drainage conditions, the rest of the test parameters were the same in both drained and undrained tests.

5.2.2 Tests on Recovered Frozen Cores

Frozen core samples were recovered from the model box as described previously. Four to nine frozen core samples were recovered from each model prepared in the box. Due to the need to thaw the specimens, samples could not be tested on the day that they were recovered. Therefore, cores were wrapped in plastic wrap and aluminum foil and stored in a freezer for later retrieval and testing. The samples were typically stored for one to five days before testing.

The following steps were followed in preparing frozen samples for both drained and undrained triaxial testing:

1. Upon retrieval from storage, the frozen samples were trimmed to a height of approximately twice their diameter. In the case of the 35 mm diameter samples, the height was at least 71 mm and in the case of the 71 mm diameter samples the height was at least 142 mm. A conventional hacksaw with a bi-metal blade was used to trim the frozen sample. A frozen sample retrieved from storage for testing is shown in Figure 5.2. A trimmed sample is shown in Figure 5.3.
2. After trimming, the frozen sample was mounted in the triaxial cell, confined in a latex membrane using two O-rings on each end (i.e. on both the top and bottom platen), and subject to an effective confining pressure of approximately 10 kPa applied to the sample through the top platen drainage line using a vacuum. It was important to complete steps 1 and 2 as fast as possible to avoid thawing of the sample prior to confinement. The samples were handled with oven mitts to avoid thawing due to heat transfer from the hands to the sample.
3. The chamber was then placed upon the triaxial cell in order to change the confining pressure from vacuum to chamber pressure. Prior to releasing the vacuum, the chamber was filled with water and a cell pressure of 10 kPa was applied to the sample using the GCTS system from the bottom drainage line of the chamber.

4. After releasing the vacuum, the sample was allowed access to deaired water through both the top and bottom platen drainage lines and allowed to thaw. Since water is expelled from the sand during freezing, water will be drawn into the sample during thawing. The samples typically thawed within four to six hours. However, samples were not tested until at least 12 hours had passed.

Steps 1 through Step 3 are illustrated in Figure 5.3. Following completion of these steps, the back pressure saturation technique described above was used to saturate the samples.

FIG. 5.2. 71 mm diameter frozen core sample wrapped in aluminum foil

(a) (b) (c)

FIG. 5.3. 71 mm diameter sample preparation for testing: (a) Frozen sample after trimming; (b) Frozen sample mounted on triaxial cell and confined in latex membrane with vacuum confining pressure applied; (c) Frozen sample with cell chamber in place**.**

5.2.3 Triaxial Tests and Data Acquisition

The GCTS system is equipped with a computer and digital signal control device. Following back pressure saturation, triaxial testing was conducted using an internal GCTS system program that specifies, among other things, the type of test (drained or undrained), type of loading, data acquisition rate, strain at the end of the test, and strain rate. The strain rate was presented in Section 5.1. Data was collected every second during the test. The end of test was specified as 15% strain but tests were regularly terminated a few percent strain after the peak deviator stress was observed to have occurred, i.e. after the deviator stress began to decrease.

5.2.4 Problems Encountered During Testing

Initially, 35 mm diameter frozen core samples were recovered from the model box. However, the results of the triaxial compression tests on the 35 mm-diameter specimens were inconsistent with the tests performed on 71 mm diameter, never frozen specimens. Furthermore, results of the tests on the 35 mm diameter specimens were very hard to reproduce. There was wide variability in the results from the 35 mm-diameter specimens. This variability was attributed to the size of the sample. In order to reduce the variability, it was decided to recover 71 mm diameter samples from the model box for all triaxial testing.

Soil microstructure studies performed on the 35 mm samples obtained using the methods described in this work did not show variability in microstructure commensurate with the variability that was observed in the triaxial tests (Czupak, 2011). Therefore, for purposes of the microstructure studies, recovery of 35 mm-diameter samples continued throughout the course of this work.

5.3 Drained Tests Results

5.3.1 Never Frozen Sand Tests Results

The results of five consolidated drained triaxial tests conducted on never frozen specimens of Ottawa 20-30 sand prepared by air pluviation are presented in this section. The initial densities of the tests are presented in Table 5-2. The drained stress-strain-strength characteristics of these never frozen Ottawa 20-30 sand specimens are presented in Figure 5.4. The volume change-strain behavior during these tests is presented in Figure 5.5.

Table 5-2. Initial Properties of Never Frozen Sand Test Specimens

Test #	Sample Height (mm)	Mass of Sand (g)	Initial Density (kg/m^3)	Relative Density (%)
1	150	1019	1710	80
2	150	1022	1715	82
3	150	1018	1708	79
4	148	1007	1713	81
5	150	1019	1710	80

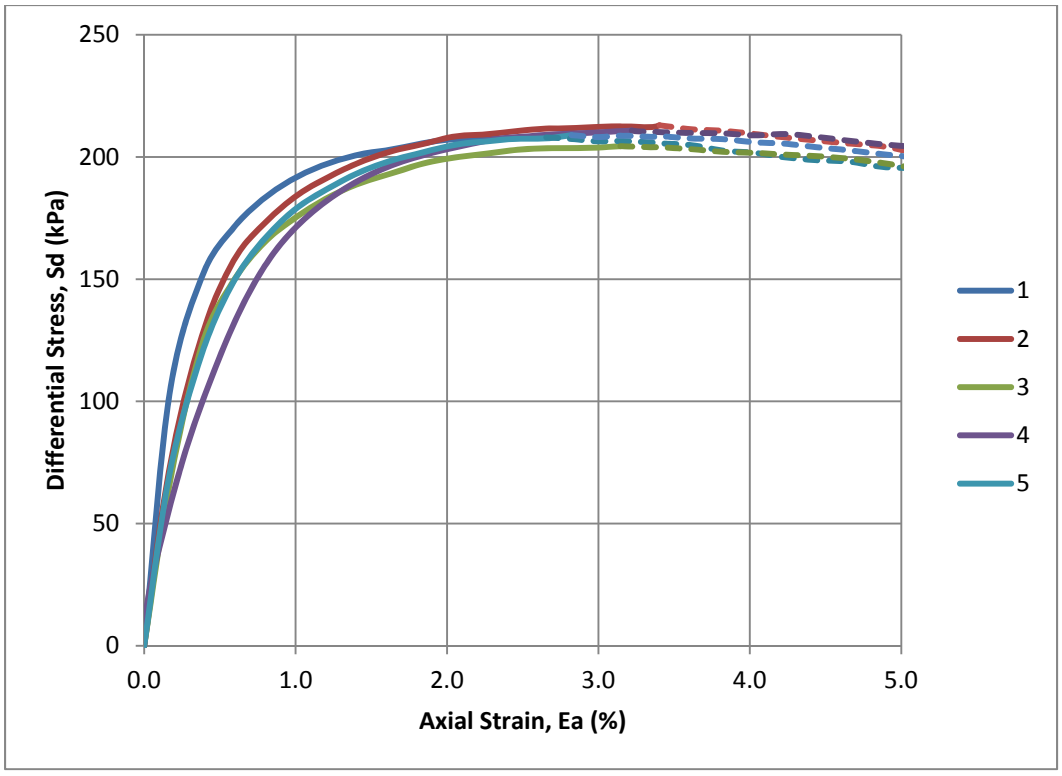

FIG. 5.4. Never frozen Ottawa 20-30 sand drained stress-strength-strain results

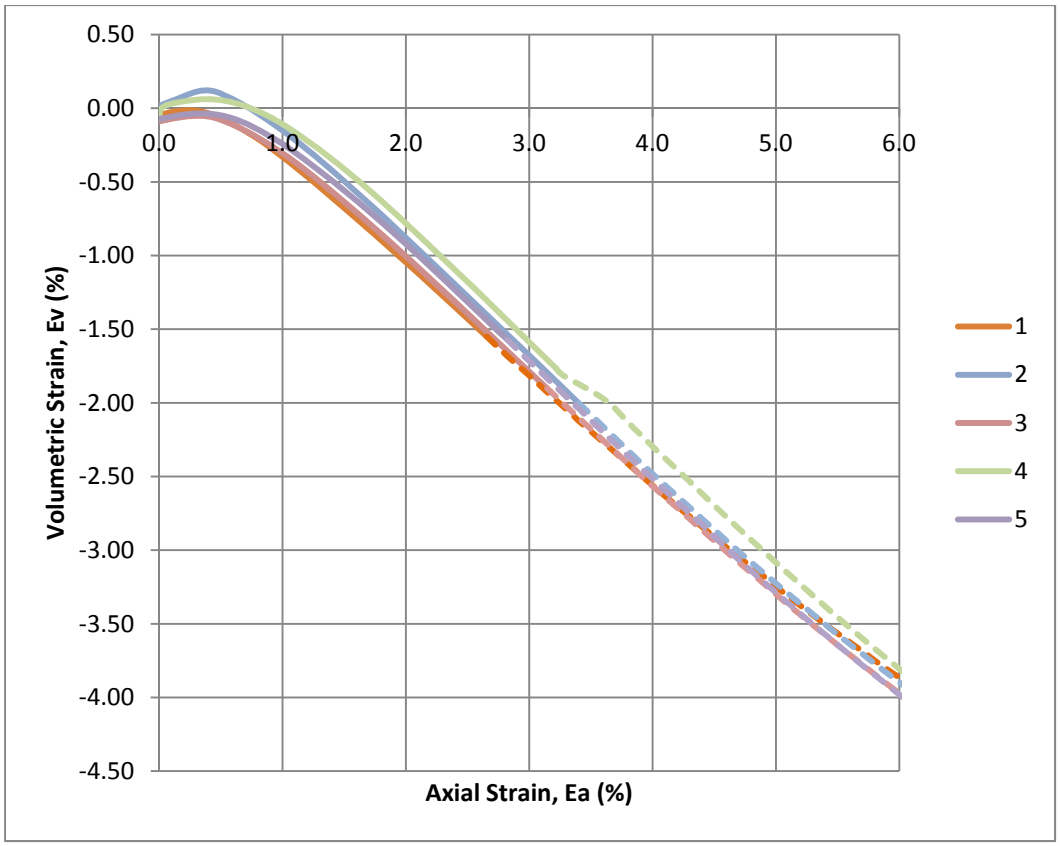

FIG. 5.5. Never frozen sand volume strain-axial strain results

5.3.2 Frozen and Thawed Test Results

Four recovered cores were tested to develop stress-strain-strength behavior of frozen and thawed sand. The initial densities of the recovered samples that were determined by weighing oven dried sand after testing are shown in Table 5-3. The stress-strain-strength behavior in drained triaxial compression tests conducted on four recovered frozen cores of Ottawa 20-30 sand after thawing is presented in Figure 5.6. The volume change-strain behavior during these tests is presented in Figure 5.7.

Table 5-3. Initial Properties of Frozen Core Test Specimens

Test #	Sample Height (mm)	Mass of Sand (g)	Initial Density (kg/m^3)	Relative Density (%)
1	144	977	1705	78
2	145	983	1707	79
3	144	977	1708	79
4	148	1005	1710	80

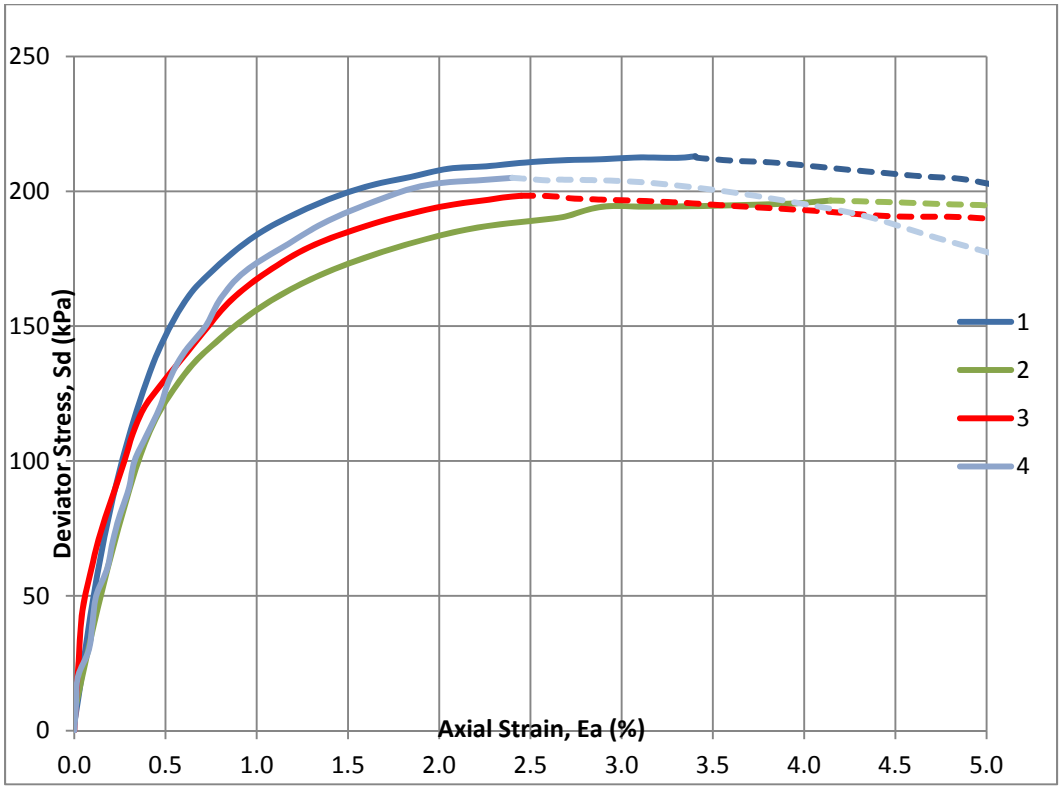

FIG. 5.6. Results of drained triaxial compression tests on recovered frozen cores of Ottawa 20-30 sand samples

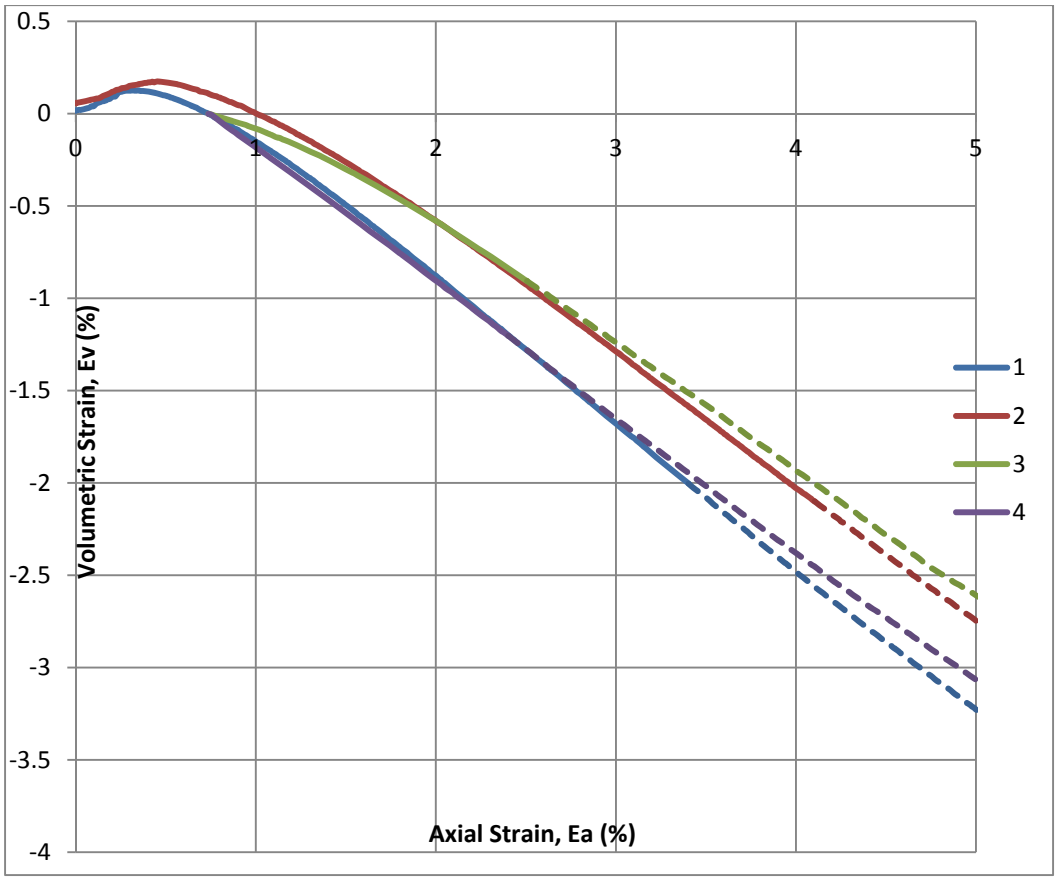

FIG. 5.7. Drained volume change-Strain results

5.3.3 Comparison of the Drained Triaxial Compression Test Results

The results of the triaxial compression tests conducted on never frozen sand and on the recovered frozen samples after thawing were compared, to determine whether the frozen and then thawed sand retains its drained deformation characteristics. The results of this comparison serve as an indication of the level of disturbance due to the sampling techniques developed in this work.

Mean stress-strain-strength and volume curves were developed from the two groups of curves (never frozen, and frozen and then thawed) from the drained triaxial testing. The two median stress-strain-strength curves are shown in Figure

5.8. Median volume change-strain curves for the never frozen sand and for the frozen and thawed cores are presented in Figure 5.9. Comparison of the median stress-strain-strength and volume change-strain curves indicate that the sampling process has at worst minor effects on the drained deformation characteristics of Ottawa 20-30 sand.

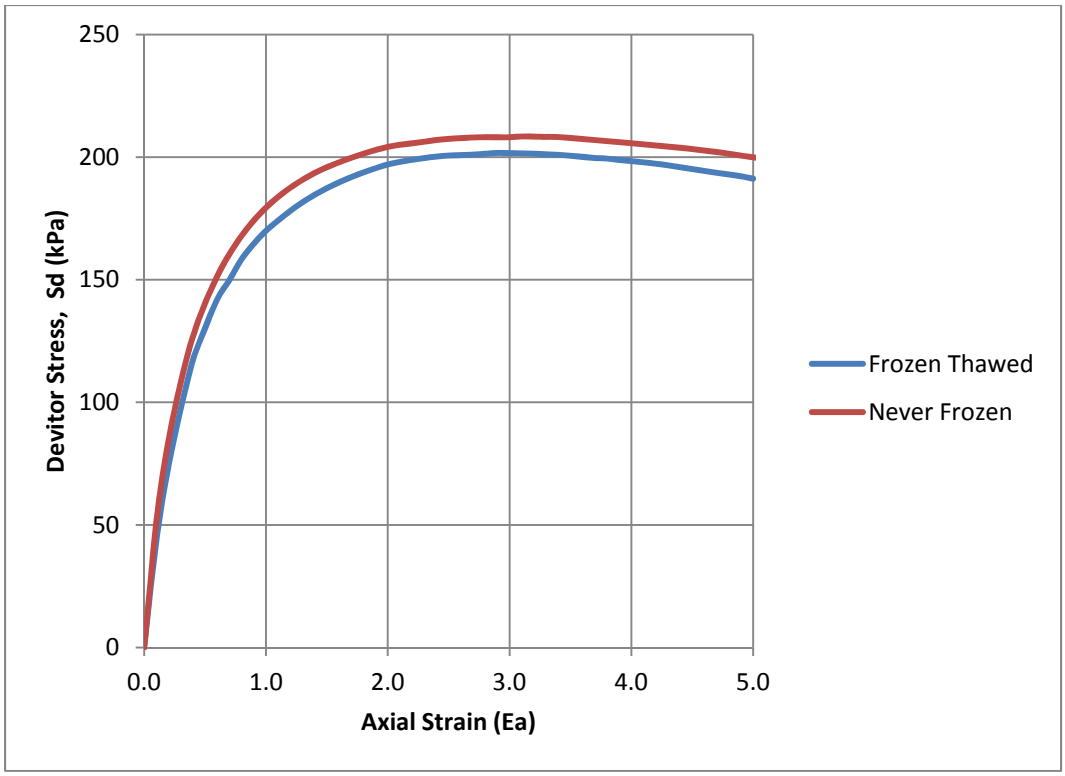

FIG. 5.8. Median stress-strain-strength curves

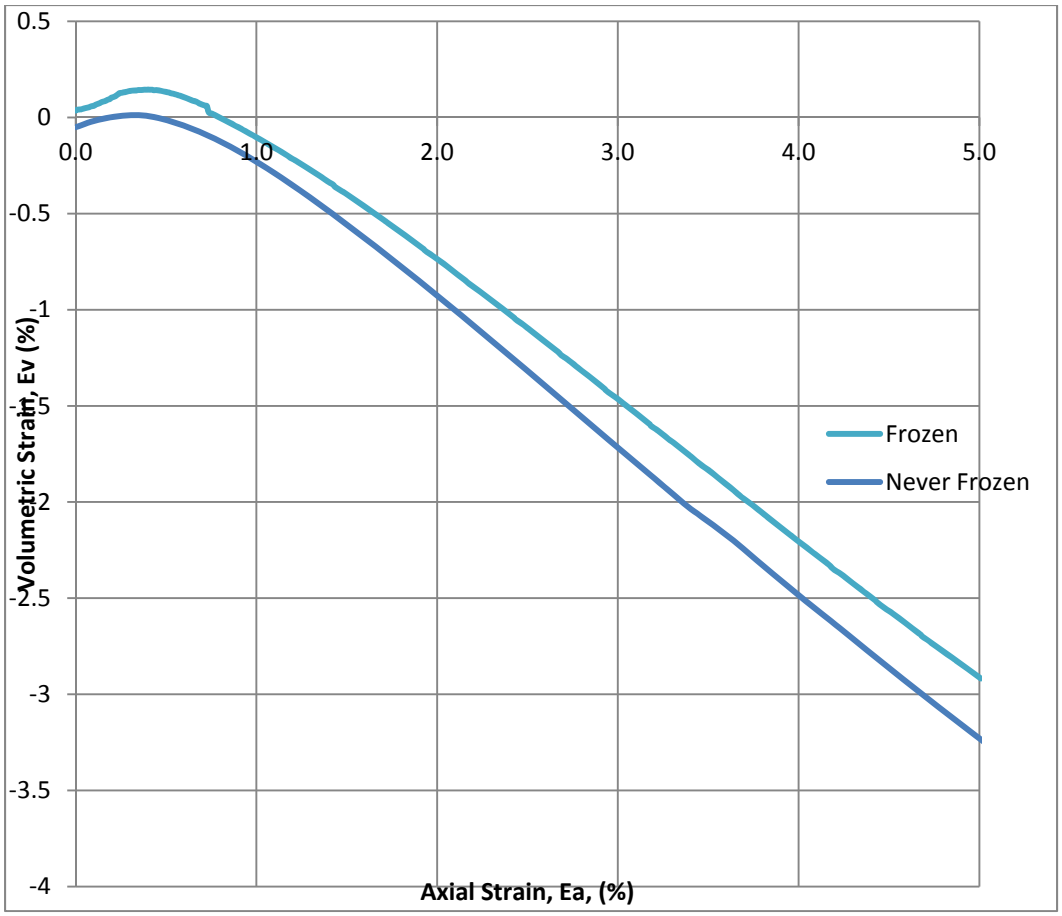

FIG. 5.9. Median strain-volume change curves

In order to conduct a statistical comparison of the two groups of curves, the stress-strain-strength curves were approximated by a hyperbola using procedures described by Duncan et al. (1980). This hyperbola can be represented by the equation:

$$(\sigma_1 - \sigma_3) = \frac{\varepsilon}{\frac{1}{E_i} + \frac{\varepsilon}{(\sigma_1 - \sigma_3)_{ult}}} \quad (5.1)$$

where:

$(\sigma_1-\sigma_3)$ = the stress difference (deviator stress),

ε = axial strain

E_i = the initial tangent modulus, and

$(\sigma_1-\sigma_3)_{ult}$ = the asymptotic value of stress difference for the fitted hyperbola.

The value of $(\sigma_1-\sigma_3)_{ult}$ is usually greater than the strength mobilized in a triaxial test, $(\sigma_1-\sigma_3)_f$. Therefore, Duncan et al. (1980) defined a third parameter R_f to analytically describe a stress-strain curve, where R_f was defined as the ratio of the mobilized strength to $(\sigma_1-\sigma_3)_{ult}$:

$$R_f = (\sigma_1-\sigma_3)_f/(\sigma_1-\sigma_3)_{ult} \quad (5.2)$$

As described by Duncan et al. (1980), two points (typically, points corresponding to 70% and 95% of the strength mobilized in the test) from each stress-strain curve were used to derive the two variables (E_i and $(\sigma_1-\sigma_3)_{ult}$) that describe the hyperbola.

In order to compare the volume change curves, three parameters were abitrarily chosen for comparison. The volume change at 70 %, 95 % and at 100% of the strength mobilized in the test were the chosen parameters. Therefore, in total, six parameters derived from the drained triaxial compression tests were employed to compare test results: three parameters describing the volume change-strain characteristics and three parameters decribing the stress-strain-strength characteristics.

A statistical comparison of the six parameters was conducted for the two groups of drained triaxial test results. The statistical analyses used a t-distribution

for two variables. A statistical hypothesis, two-population test (H0: $\mu_1=\mu_2$ {Null Hypothesis} and $\mu_1\neq\mu_2$ {Alternative Hypothesis}) was conducted. The critical assumptions of the analysis were that the mean values of the two samples were unknown and that they were equal. The results of the statistical analyses of the curves shown in Figures 5.4 through Figure 5.7 are presented in Table 5-4.

Table 5-4. Statistical Comparison of Drained Test Results

Parameter	Tests on Unfrozen Sand[a]	Tests on Frozen Cores[a]	Acceptance	Confidence
E_{li}	727 %/kPa	578 %/kPa	Yes	90 %
$(\sigma_1-\sigma_3)_{ult}$	243 kPa	240 kPa	Yes	90 %
F_{ry}	0.86	0.85	Yes	90%
e_{ve} at 70% $(\sigma_1-\sigma_3)_{max}$	0.17 %	0.39 %	Yes	90 %
e_{ve} at 95% $(\sigma_1-\sigma_3)_{max}$	-0.67 %	-0.56 %	Yes	90 %
e_{ve} at 100% $(\sigma_1-\sigma_3)_{max}$	-1.14 %	-1.35 %	Yes	90%

[a] Arithmetic mean values for each parameter are presented in this table. However, values for each test were used for statistical comparison.

Although widely accepted laboratory testing procedures were used in this work, a bias statement on drained triaxial testing of cohesionless soil was not found. The sample size was chosen based on other criteria unrelated to the variability of the tests used. The drained tests on unfrozen soil were both reproducible and consistent. Therefore, drained testing on never frozen samples was stopped at five samples. The results of drained testing on frozen and thawed cores presented here are the results of tests performed on samples recovered using

the Husqvarna DR 150 core drill rig. The statistical comparison of this limited sample size shows that the two groups of tests are the same at a confidence of 90%. It can be concluded from the results that the sampling process produces undisturbed samples that retain their drained deformation characteristics.

5.4 Undrained Test Results

5.4.1 Never Frozen Sand Test Results

The results of five consolidated undrained triaxial tests conducted on never frozen specimens of Ottawa 20-30 sand prepared by air pluviation to a relative density of approximately 80% are presented in this section. The initial densities of the tests are presented in Table 5-5. The undrained stress-strain-strength behavior of never frozen Ottawa 20-30 sand specimens tested in triaxial compression are presented in Figure 5.10. The excess pore pressure-strain results during the undrained triaxial tests are presented in Figure 5.11.

Table 5-5. Initial Properties of Undrained Baseline Tests Specimens

Test #	Sample Height (mm)	Mass of Sand (g)	Initial Density (kg/m^3)	Relative Density (%)
1	150	1019	1710	80
2	149	1013	1712	81
3	150	1012	1714	82
4	150	1019	1710	80
5	149	1012	1710	80

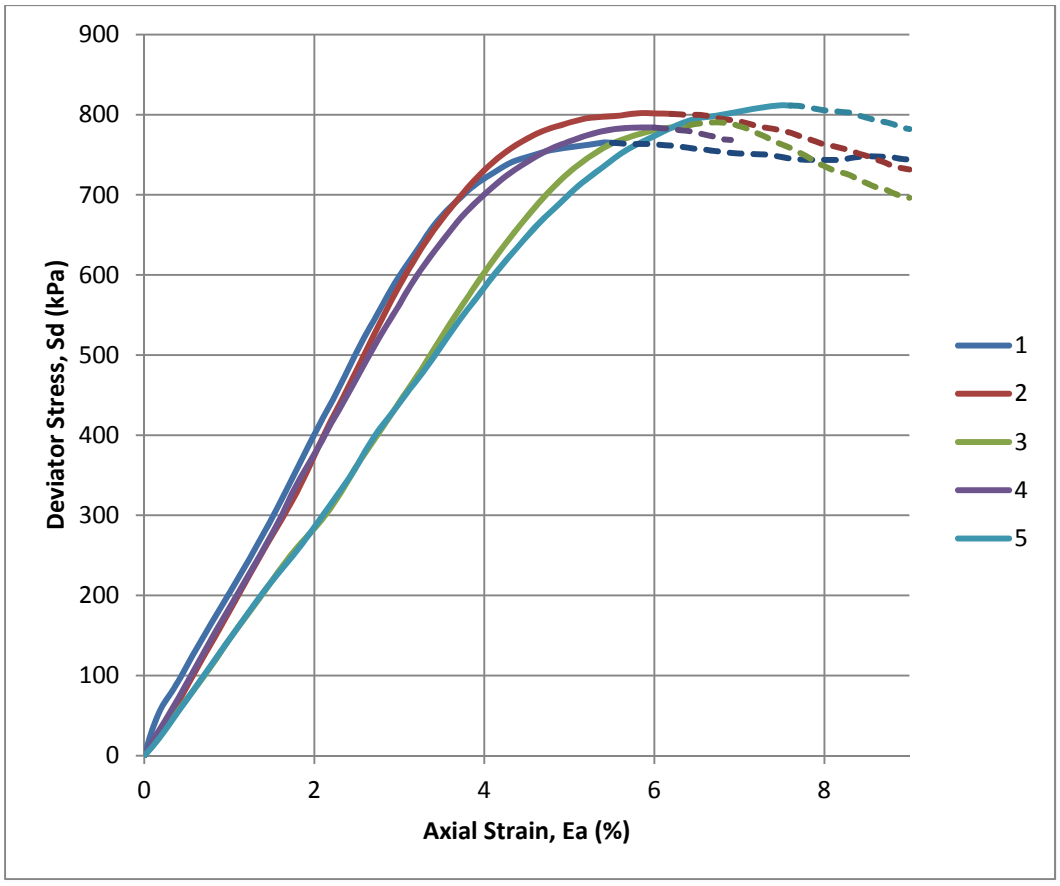

FIG. 5.10 Never frozen Ottawa 20-30 sand undrained stress-strength-strength results

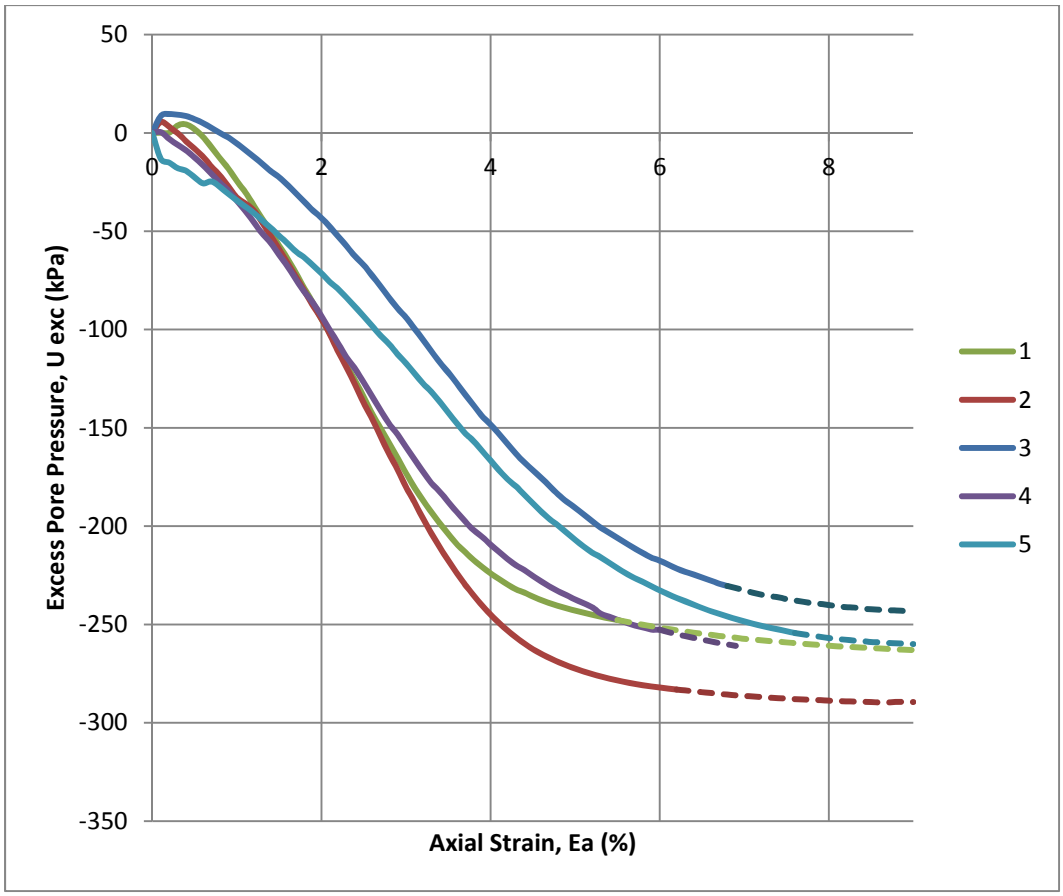

FIG. 5.11. Never frozen sand pore pressure change-strain results

Three consolidated undrained triaxial compression tests were conducted on the recovered frozen and then thawed cores of Ottawa sand. The initial properties of the specimens are presented in Table 5-5. The results of the three consolidated undrained triaxial compression tests conducted on recovered frozen and then thawed cores of Ottawa 20-30 sand are presented in Figures 5.12 and 5.13. Figure 5.12 presents the stress-strain-strength results from these tests and the volume change-strain results from these tests are presented in Figure 5.13.

Table 5-6. Initial Properties of Frozen Core Test Specimens

Test #	Sample Height (mm)	Mass of Sand (g)	Initial Density (kg/m^3)	Relative Density (%)
1	150	1020	1711	80
2	145	985	1708	79
3	144	979	1710	80

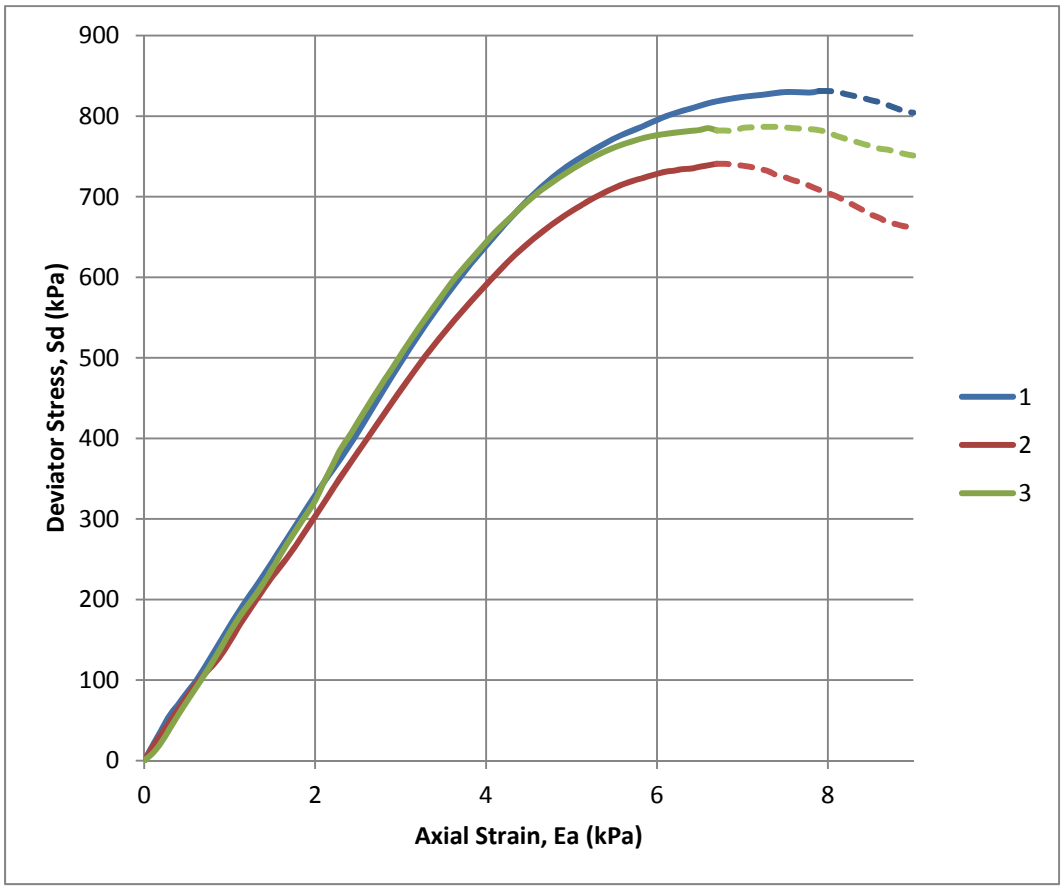

FIG. 5.12. Results of undrained triaxial compression tests on recovered frozen cores of Ottawa 20-30 sand samples.

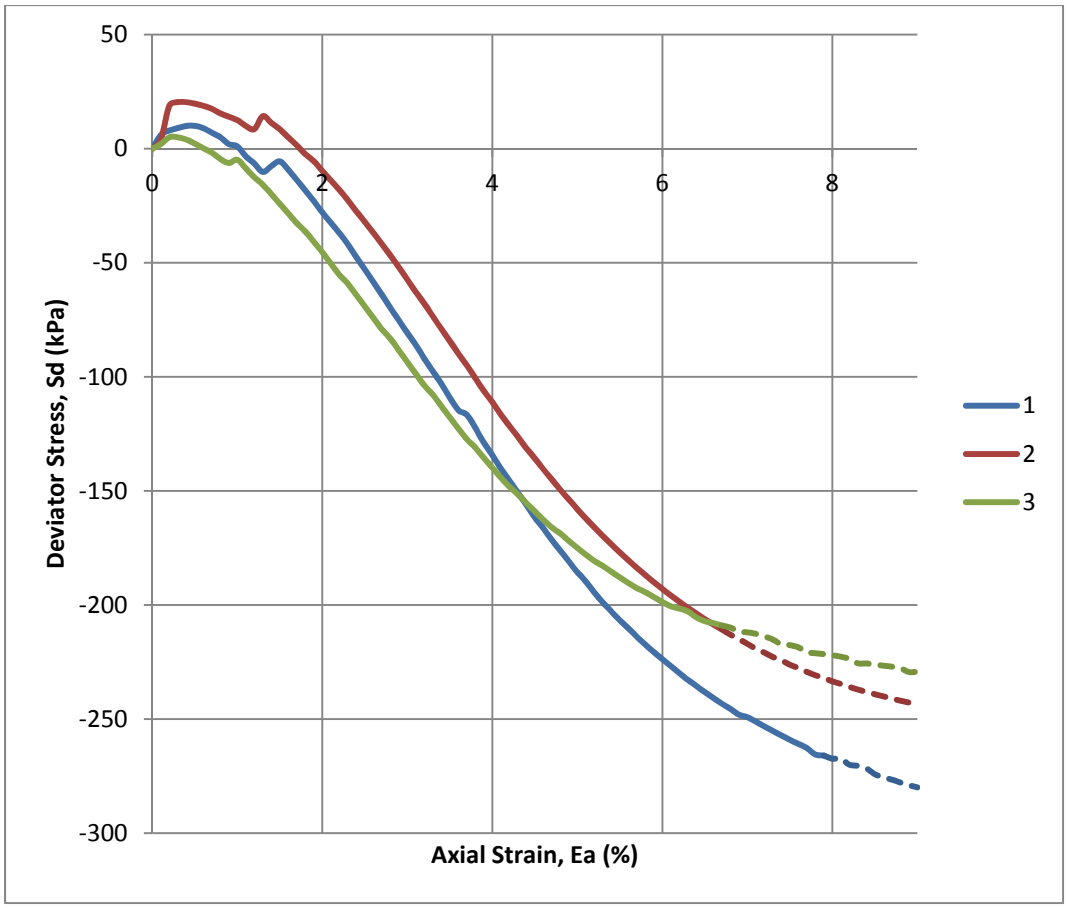

FIG. 5.13. Pore pressure change-axial strain results

5.4.2 Comparison of the Undrained Triaxial Compression Test Results

The results of the undrained triaxial compression tests conducted on never frozen sand and on the recovered frozen and then thawed samples were compared to determine whether the sampled sand retains its undrained deformation characteristics.

The Duncan et al. (1980) stress-strain curve fitting equation was not used for statistical comparison of undrained triaxial test results. The curve fitting equation was developed from drained tests. An attempt to use this curve fitting method on undrained tests was made. The curve fitting method produced unrealistic numbers

e.g. R_f of 0.37, when the typical range for sands is 0.5 to 0.9. For this reason, it was decided not to use the Duncan et al. curve fitting method on undrained tests results.

An alternative comparison method was used for undrained test results. The mean undrained stress-strain-strength curve was developed from the baseline undrained triaxial compression tests performed on never frozen sand. Standard deviations of the deviator stress at discrete strain levels were calculated from the five baseline tests. A confidence interval was developed that was bound at the top by the mean plus two standard deviations and at the bottom by the mean minus two standard deviations. The frozen/thawed tests results were plotted on the confidence interval plot to demonstrate how well the results on the recovered samples compared with the baseline results. The stress-strain-strength comparison figure is presented in Figure 5.14. The excess pore pressure-strain results were compared using methods used to compare stress-strain-strength behavior (described previously). The results of the comparison are presented in Figure 5.15.

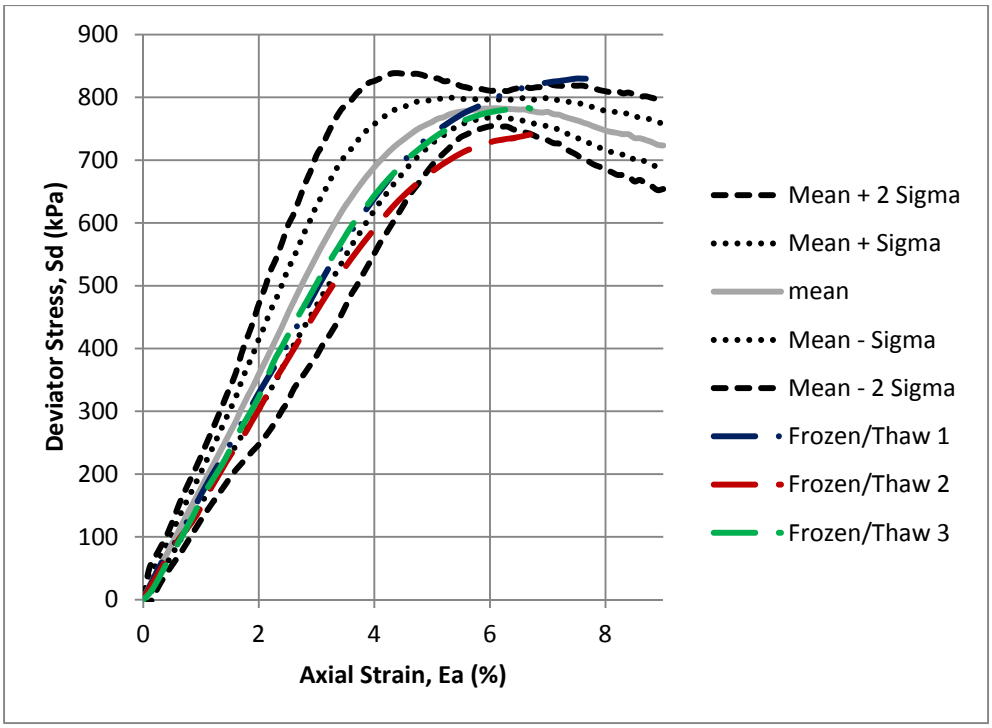

FIG. 5.14. Undrained stress-strain-strength results plotted on confidence interval developed from baseline undrained triaxial tests.

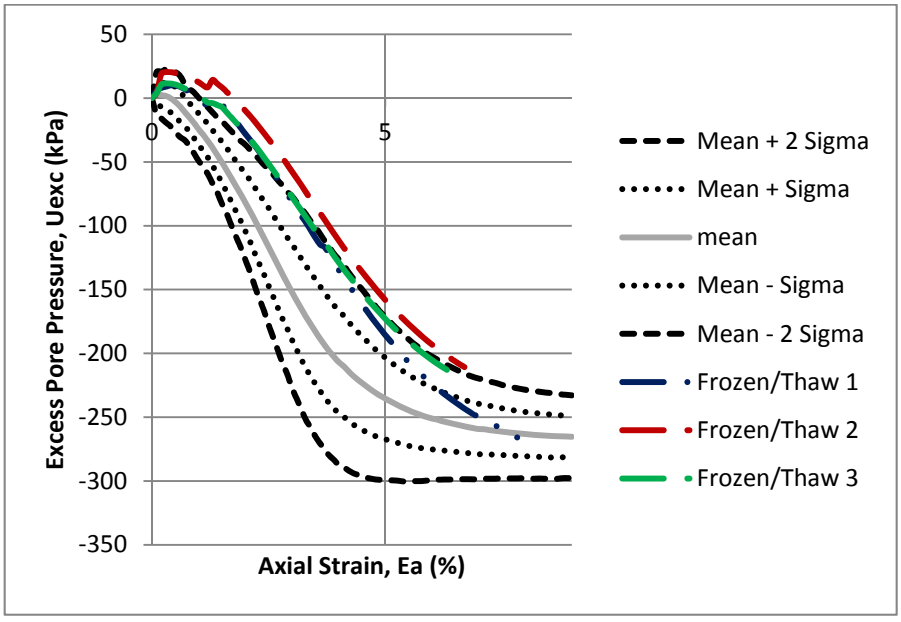

FIG. 5.15. Median excess pore pressure-axial strain curves

The results of the undrained tests conducted on never frozen sand and on recovered cores were also analyzed by comparing the stress and excess pore water pressure at three strain levels: at one percent, three percent, and five percent strain. The three strain levels were chosen arbitrarily. The three strain levels were assumed to represent the stress-strain-strength, and the excess pore pressure-strain relationship developed from the consolidated undrained test results data.

A statistical comparison of the parameters was conducted for the two groups of undrained triaxial test results. The statistical analyses used a t-distribution for two variables. A statistical hypothesis, two-population test (H0: $\mu_1=\mu_2$ {Null Hypothesis} and $\mu_1\neq\mu_2$ {Alternative Hypothesis}) was conducted. The critical assumptions of the analysis were that the mean values of the two samples were unknown and that they were equal. The results of the statistical analyses of the curves shown in Figures 5.10 through Figure 5.13 are presented in Table 5.7 and Table 5-8.

Table 5-7. Statistical Comparison of Deviator Stress – Strain Results

Parameter	Tests on Unfrozen Sand[a]	Tests on frozen Sand[a]	Acceptance at 90% confidence
S_d at 1%	171 kPa	158 kPa	Yes
S_d at 3%	526 kPa	486 kPa	Yes
S_d at 5%	749 kPa	719 kPa	Yes

[a] Arithmetic mean values for each parameter are presented in this table. However, values for each test were used for statistical comparison.

Table 5-8. Statistical Comparison of Excess Pore Water Pressure - Strain Results

Parameter	Tests on Unfrozen Sand[a]	Tests on frozen Sand[a]	Acceptance at 90% confidence	Acceptance at 95% confidence
U_{exc} at 1%	-26 kPa	3 kPa	No	No
U_{exc} at 3%	-145 kPa	-77 kPa	No	Yes
U_{exc} at 5%	-230 kPa	-173 kPa	Yes	Yes

[a] Arithmetic mean values for each parameter are presented in this table. However, values for each test were used for statistical comparison.

The undrained tests on both never frozen sand and on recovered cores showed a lot of variability and were very difficult to reproduce. The stress-strain-strength behavior and excess pore water pressure developed during undrained triaxial loading is dependent on the level of saturation, the pore fluid stiffness, and the void ratio at the beginning of the tests. According to William Houston, undrained shear strength of saturated or nearly saturated sand is generally elusive and hard to reproduce (Personal communication, June 3, 2011). This variability and difficulty to reproduce the shear strength is attributable to the difficulty to produce specimens of sand that have identical B-values, identical degrees of saturation and, identical pore fluid stiffness in the laboratory (W. Houston, Personal communication, June 3, 2011).

The results of the tests conducted on recovered cores compare favorably with the baseline deformation behavior in undrained triaxial loading that was established from the five undrained tests conducted on never frozen Ottawa 20-30 sand. The differences observed between the two sets of tests (tests of unfrozen sand and tests on recovered cores) are well within the variability in the test results

observed during testing and also within the results, that can be expected from undrained triaxial testing of saturated sand. It can be concluded from the results that the sampling process has at most only minimal effects on the undrained deformation characteristics of saturated Ottawa sand. The sampling procedure described in this work produces undisturbed samples that retain their undrained deformational characteristics.

Chapter 6

6.0 CONCLUSIONS AND RECOMMENDATIONS

6.1 Conclusions

The main objective of this work was to develop a method for recovering undisturbed samples of cohesionless soil from physical models. This work is part of a larger project to experimentally and numerically investigate the properties of resedimented cohesionless soil following earthquake induced liquefaction. The work presented in this thesis resulted in the development of a practical method for preparing uniform soil deposits in laboratory bench scale and centrifuge models and the development of a practical method of recovering intact and essentially undisturbed samples of cohesionless soil from these physical models.

The technique for preparation of uniform sand specimens was developed based on methods used by Frost (1989) and also by UC Davis. The technique is based on air pluviation. A pluviation apparatus was developed that allows for creation of samples of Ottawa 20-30 sand samples at target densities by varying the height of fall of the sand. The apparatus is simple, can be created from easily obtainable parts, and does not require specialized fabrication. A calibration curve for the pluviation apparatus was developed relating fall height to the post-placement density of Ottawa 20-30 sand. Using this technique, specimens of Ottawa 20-30 sand can be created in containers of varying sizes at densities ranging from 1,550 kg/m^3 to 1,730 kg/m^3 (96 lb/ft^3 to 108 lb/ft^3).

A method for recovering undisturbed samples of cohesionless soil from laboratory bench scale models was developed. The technique can also be used on centrifuge- and shaking table-scale models. The sampling method involved stabilization of cohesionless soil by freezing and recovery of samples by coring. A freezing method was developed that used crushed dry ice and ethanol placed in a metal pan as a coolant. The temperature of the mixture of dry ice and ethanol was measured to be -68°C. The pan filled with coolant was placed on top of the saturated model specimen, from which samples were to be recovered, inducing a top-down freezing front.

The propagation of the freezing front that was induced by the chosen freezing method was experimentally and numerically investigated. A unidirectional freezing front, a surcharge, and a drainage path in the direction of the freezing front are requirements for the freezing of cohesionless soil with minimal volume change. The results of the experimental and numerical investigations showed that these requirements were met by the technique employed herein. The freezing front propagated from top to bottom without the development of any secondary freezing fronts with the potential to trap water between impermeable (or very low permeability) surfaces. The drainage path was maintained through the bottom of the model container and through the sides between the walls of the container and the frozen portion of the specimen during the freezing process. Water was observed flowing from the container over the sides as the specimen froze. The weight of the pan and coolant appeared to provide adequate surcharge pressure on the specimen to limit expansion during freezing. Significant expansion of the

cohesionless soil models was not observed during numerous freezing experiments conducted in this work.

Equipment for coring 35 mm diameter and 71 mm diameter samples of frozen cohesionless soil was developed. Using this equipment, numerous samples were successfully recovered from the physical models. The sampling methods are simple and can be replicated at different locations without requiring sophisticated fabrication effort.

The undisturbed nature of the samples was investigated using triaxial compression tests. Drained and undrained triaxial compression tests were performed on never frozen Ottawa 20-30 sand pluviated to create a specimen with a relative density of 80% to establish baseline deformation characteristics. Recovered frozen cores were confined in a triaxial cell and allowed to thaw. The same tests that were performed on never frozen Ottawa 20-30 sand specimens were then performed on the thawed cores. The results of the tests on never frozen and frozen and then thawed specimens were compared to assess the undisturbed nature of the samples obtained using the sampling techniques developed in this work.

Based on the experiment results and analyses reported in this thesis, it can be concluded that the samples recovered using the sampling techniques developed in this work retain their original drained and undrained deformation characteristics. The freezing and thawing process has only minimal effects on the deformation characteristics of the Ottawa 20-30 cohesionless soil. The differences between deformational characteristic of never frozen sand and frozen and thawed sand

appear to be within the normal variation that can be expected from testing different samples of the same soil.

6.2 Recommendations

The specimen creation and sampling techniques presented in this work are suitable for use in the larger project and projects of similar scope and size. Based on the testing conducted in this work, the samples obtained using methods described in this thesis can reasonably be expected to maintain their structure and deformational characteristics. However, there are a number of other factors that were not addressed in this work that might have bearing on the quality of samples obtained using methods described herein.

The effect of the moisture content of the dry sand on the pluviation technique was not addressed in this work. Although, samples with consistent density were produced using the pluviation method, the moisture content of the sand was not considered during sample creation. Future testing could be performed using oven dried sand in order to maintain constant moisture content during sample preparation.

The ASTM standard for consolidated drained triaxial compression tests (CD tests) does not have a bias or variability statement. Data on the bias and variability of the CD test was not found in the literature. The number of tests performed on never frozen sand in this study was relatively small. Although the test results were fairly consistent and easily reproducible, the number of tests was too small to confidently establish bias and variability of the CD test. Future studies could

perform more tests to develop a better estimate of the bias and variability of the test.

A test standard for the consolidated undrained triaxial compression tests (CU test) was not found in the literature. The results of the testing conducted in this research showed that the CU test results showed greater variability than the CD test results. It seems the CU test is more sensitive to small variability in initial specimen density and saturation level (B-value). This variability made the CU test a difficult method to use for purposes of investigating the deformation characteristics of sampled cohesionless soil. The number of samples tested in this study is relatively small. Future study could focus on conducting a statistically significant number of CU tests in order to develop an estimate of the bias and variability for the test itself. The CU test bias and variability, could lead to better comparisons of deformation characteristics of never frozen sand and frozen sand. The CU test bias and variability could also be applied in other cases where CU test on cohesionless soil may be required.

This research was interested in investigating the large strain behavior, consistent with the focus of the larger project (post liquefaction properties of cohesionless soil). Future research could investigate the effects of freezing and thawing on small strain behavior e.g. by measuring shear wave velocity in never frozen specimens and also in frozen and then thawed specimens.

Poorly graded Ottawa 20-30 sand was used in this work. The sand has uniform sub-rounded particles. Future research could perform the tests conducted in this work using graded sand with sub-rounded particles, and also using sand

with angular particles. This research could investigate the effect of changing the test soil on expansion due to freezing, deformation characteristics of frozen and thawed soil, and creation of uniform deposits of sand using the pluviation techniques described in this work.

Another area of additional study is the effect of the sampling techniques on the 'aging effect' of sands described by Mitchell (2008). Future research could investigate whether cohesionless soil sampled using freezing loses strength gained through aging. This research could provide insight to whether samples obtained from an aged deposit of sand would retain its aged strength gain, i.e. whether freezing followed by thawing erases aging effects.

7.0 REFERENCES

Alshibli, K. A., Sture, S., Costes, N. C., Frank, M. L., Lankton, M. R., Batiste, S. N., et al. (2000, September). Assessment of Localized Deformations in Sand Using X-Ray Computed Tomography. *Geotechnical Testing Journal, 23*(3), 274-299.

Araki, C. (1956). Structure of agarose, a main polysaccharide of agar-agar. *memoirs of the faculty of industrial arts*, 21-25.

Borja, R. I., Kavazanjian, E., & Evans, J. C. (2008). *Properties of Cohesionless Soil Subsequent Liquefaction and Resedimentation.* Proposal.

Czupak, Z. D. (2011). *"Stabilization and Imaging of Cohesionless Soil Samples".* Tempe: Arizona State University.

Czupak, Z. D. (2011). *Stabilization and Imaging of Cohesionless Soil Samples.* Tempe: Arizona State University.

Duncan, J. M., Byrne, P., Wong, K. S., & Mabry, P. (1980). *Strength, Stress-Strain and Bulk Modulus Parameters for Finite Element Analyses of Stresses and Movements in Soil Masses.* Berkeley: University of California at Berkeley.

Evans, M. T. (2005). *Microscale Physical and Numerical Investigations of Shear Banding in Granular Soils.* Atlanta: Georigia Institute of Technology.

Fiegel, G. L., Hudson, M., Idriss, I. M., Kutter, L. B., & Zeng, X. (1994). Effect of model containers on dynamic soil response. In Leung, Lee, & Tan (Ed.), *Centrifuge 94* (pp. 145-150). Rotterdam: Balkema.

Frost, J. D. (1989). *Studies on the Monotonic and Cyclic Behavior of Sands.* West Lafayette: Purdue University.

GCTS Testing Systems. (2005). *CATS Advanced and Universal 1.89.* Tempe: GCTS Testing Systems.

Holtz, R. D., & Kovacs, W. D. (1981). *"An Introduction to Geotechnical Engineering".* Englewood Cliffs: Prentice Hass.

Holtz, R. D., & Kovacs, W. D. (1981). *An Introduction to Geotechnical Engineering.* Englewood Cliffs: Prentice Hass.

Hvorslev, J. M. (1949). *Subsurface Exploration and Sampling of Soils for Civil Engineering Purposes.* Vicksburg: Waterways Experiment Station.

Mitchell, J. K. (2008). Aging of Sand - A Continuing Enigma? *6th International Conference on Case Histories in Geotechnical Engineering* (pp. 1-21). Arlington: Virginia Tech.

Mitchell, J. K., & Soga, K. (2005). *Fundamentals of Soil Behavior* (3rd ed.). Hoboken, New Jersey: John Wiley & Sons, Inc.

Miura, S., & Toki, S. (1982). A Sample Preparation Method and its Effect on Static and Cyclic Deformation Strength Properties of Sand. *Soils and Foundation*, 61-77.

Mulilis, P. J., Chan, C. K., & Seed, B. H. (1975). *The Effects of Method of Sample Preparation on the Cyclic Stress-Strain Behavior of Sands.* Berkeley: University of California, Barkeley.

Salgado, R., Bandini, P., & Karim, A. (2000). Shear Strength and Stiffness of Silty Sand. *Journal of Geotechincal and Geoenvironmental Engineering*, 451-462.

Santamarina, C. J., & Cho, C. G. (2001, June). Determination of Critical State Parameters in Sandy Soils - Simple Procedure. *Geotechnical Testing Journal, 24*(2), 185-192.

Schneider, H. R., Chameau, J.-L., & Leonards, G. A. (1989). Chemical Impreganation of Cohesionless Soils. *Geotechnical Testing Journal, 12*(3), 204-210.

Singh, S., Seed, B. H., & Chan, C. K. (1982). Undisturbed Sampling of Saturated Sands by Freezing. *Journal of Geotechnical Engineering*, 247-264.

Soil Vision. (2010). *SVHeat User's Manual.* Saskatoon: Soil Vision Systems Limited.

Sutterer, K. G., Frost, D. J., & Chameau, J.-L. A. (1995). Polymer Impregnation to Assist Undistrurbed Sampling of Cohesionless Soils. *Journal of Geotechnical Engineering*, 209-215.

Tystovich, N. (1952). *Principles of the Mechanics of Frozen Soils.* Academy of Sciences, U.S.S.R.

Ueno, K. (2000). "Methods for Preparation of Sand Samples". In Kusakabe, & Takemura (Ed.), *Centrifuge 98* (pp. 1047-1055). Tokyo: Balkema.

Yang, C.-T. (2002). *Boundary Condition and Inherent Stratigraphic Effects on Microsctructure Evolution in Sand Specimen.* Georgia Institute of Technology. Atlanta: Georigia Institute of Technology.

Yoshimi, Y., Hatanaka, M., & Oh-Oka, H. (1978). Undisturbed Sampling of Saturated Sands by Freezing. *Soils and Foundation*, 59-73.

APPENDIX A

DESIGN DRAWINGS FOR THE BOX USED IN FREEZING AND SAMPLING EXPERIMENTS, AND OTHER FABRICATED EQUIPMENT

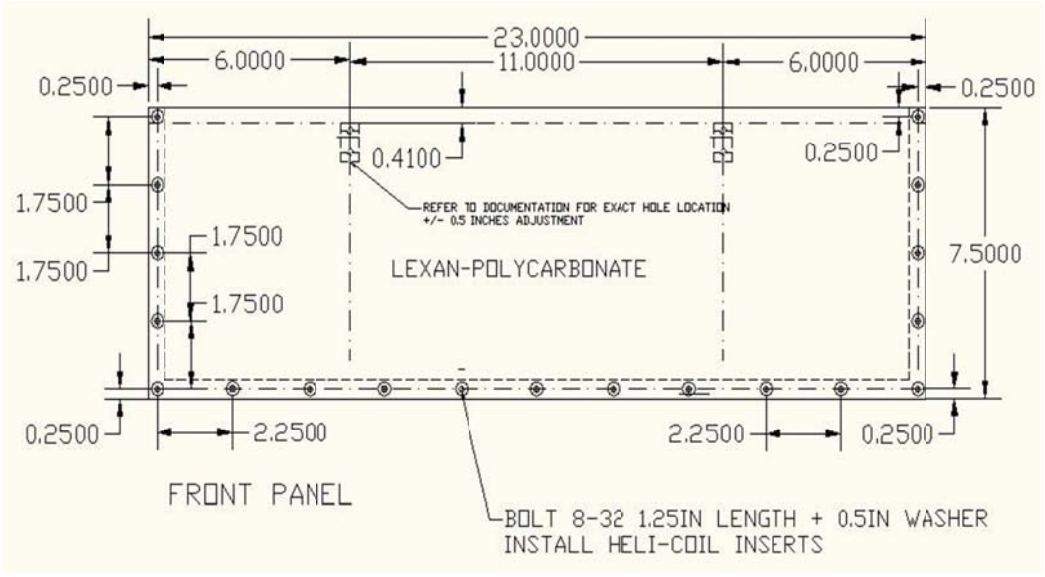
23.0000
6.0000
11.0000
6.0000
0.2500
0.2500
0.4100
0.2500
REFER TO DOCUMENTATION FOR EXACT HOLE LOCATION
+/- 0.5 INCHES ADJUSTMENT
1.7500
1.7500
1.7500
1.7500
LEXAN-POLYCARBONATE
7.5000
0.2500
2.2500
2.2500
0.2500
FRONT PANEL
BOLT 8-32 1.25IN LENGTH + 0.5IN WASHER
INSTALL HELI-COIL INSERTS

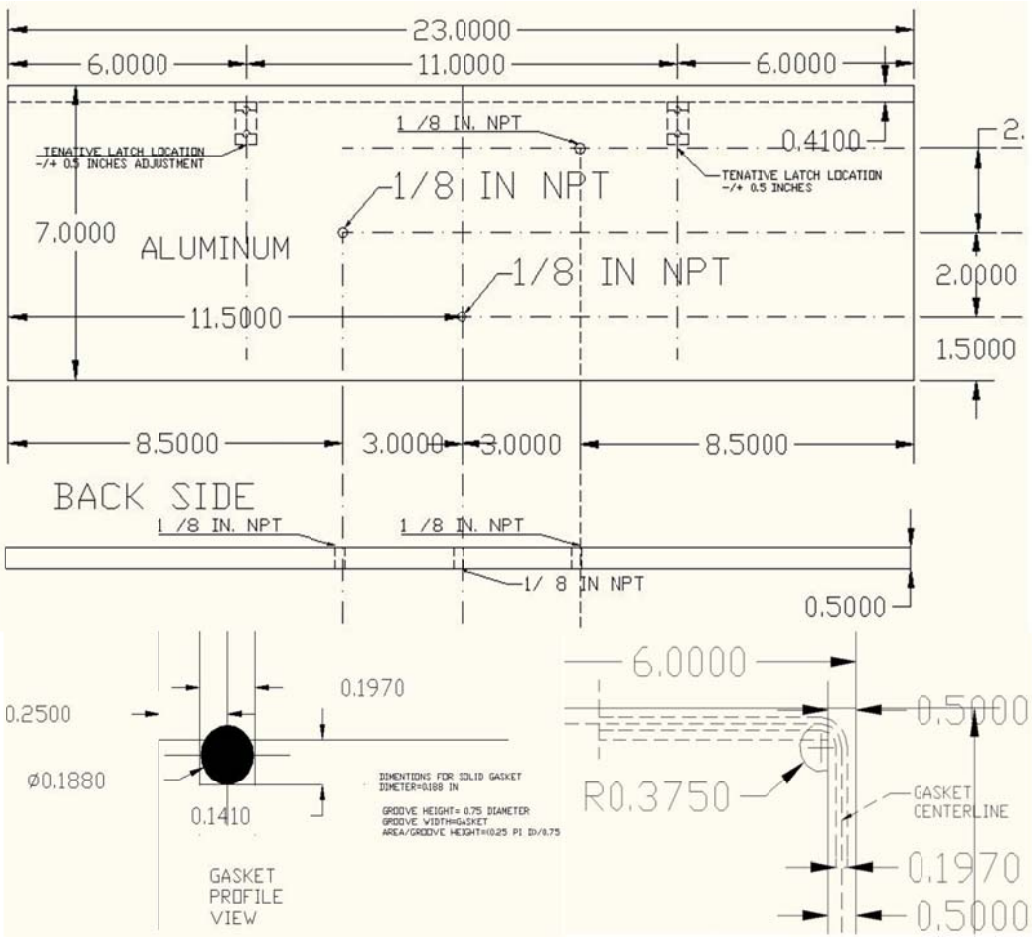
23.0000
6.0000
11.0000
6.0000
TENATIVE LATCH LOCATION
-/+ 0.5 INCHES ADJUSTMENT
1 /8 IN. NPT
0.4100
TENATIVE LATCH LOCATION
-/+ 0.5 INCHES
1/8 IN NPT
7.0000
ALUMINUM
1/8 IN NPT
2.0000
11.5000
1.5000
8.5000
3.0000
3.0000
8.5000
BACK SIDE
1 /8 IN. NPT
1 /8 IN. NPT
1/ 8 IN NPT
0.5000
0.2500
0.1970
Ø0.1880
0.1410
DIMENTIONS FOR SOLID GASKET
DIMETER=0188 IN
GROOVE HEIGHT= 0.75 DIAMETER
GROOVE WIDTH=GASKET
AREA/GROOVE HEIGHT=(0.25 PI ID/0.75
GASKET
PROFILE
VIEW
6.0000
0.5000
R0.3750
GASKET
CENTERLINE
0.1970
0.5000

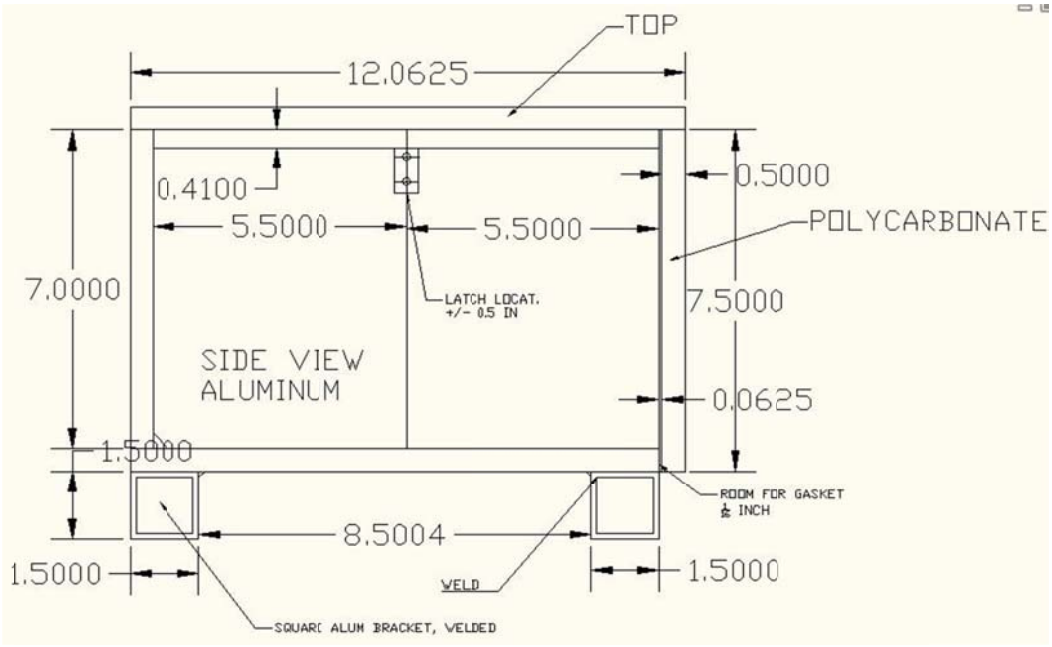
TOP
12.0625
0.4100
5.5000
5.5000
0.5000
POLYCARBONATE
7.0000
LATCH LOCAT.
+/- 0.5 IN
7.5000
SIDE VIEW
ALUMINUM
0.0625
1.5000
ROOM FOR GASKET
1/8 INCH
8.5004
1.5000
WELD
1.5000
SQUARE ALUM BRACKET, WELDED

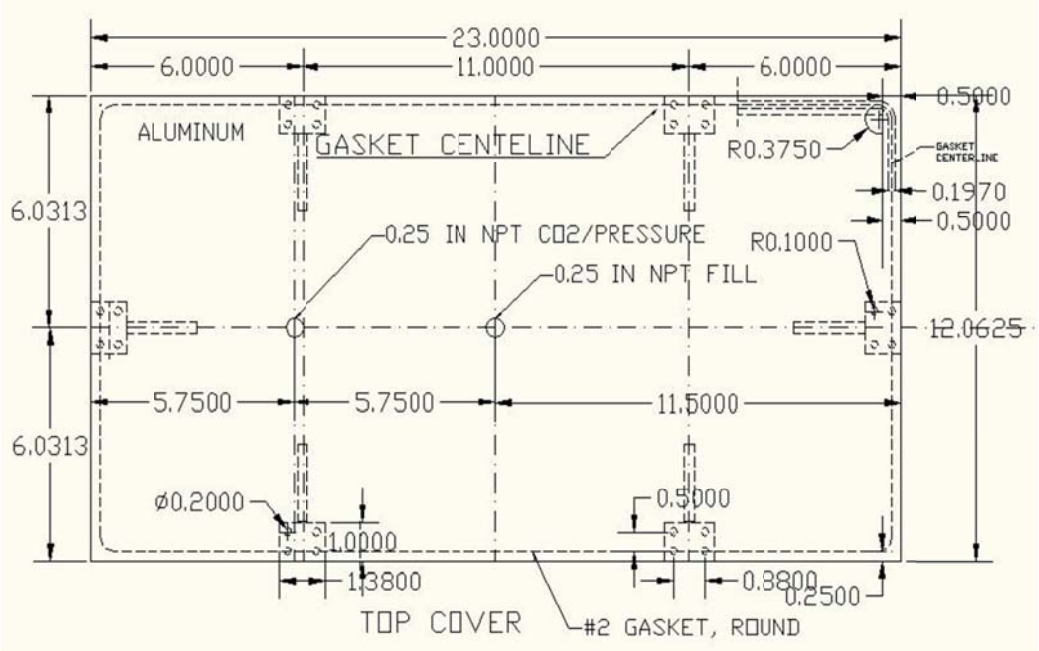
23.0000
6.0000
11.0000
6.0000
0.5000
ALUMINUM
GASKET CENTELINE
R0.3750
GASKET
CENTERLINE
0.1970
0.5000
6.0313
0.25 IN NPT CO2/PRESSURE
R0.1000
0.25 IN NPT FILL
12.0625
5.7500
5.7500
11.5000
6.0313
ø0.2000
0.5000
1.0000
1.3800
0.3800
0.2500
TOP COVER
#2 GASKET, ROUND

TC-334

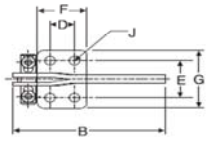

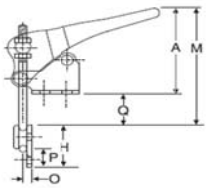

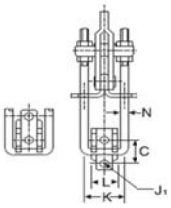

Latch plate included with all clamps listed below **except TC-374**. Furnished with a thumb control lever.

Discount *29* applies.

Cat. No.	A	B	C	D	E	F	G	H	Drawing Movement	J	J1	K	L	M	N	O	P	Q	Thread Size	Holding Capacity (Lbs)	Price Each 1-49
Steel																					
TC-324	2.00	3.35	.56	.50	.88	1.00	1.38	1.00	1.53	.20	.17	.81	.53	2.69	.14	.19	.63	.91	M4	500	**17.43**
TC-334	2.44	4.25	.81	.75	1.00	1.11	1.56	1.50	2.00	.28	.22	1.13	.68	3.69	.25	.35	.69	1.35	M6	1,000	**21.63**

1. DRILL GUIDE – All Dimensions are in inches.

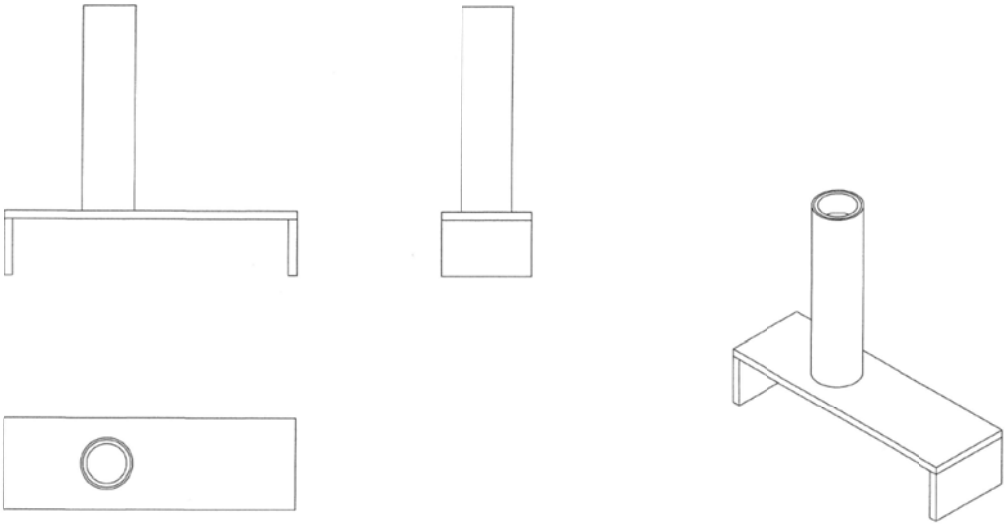

Assembly

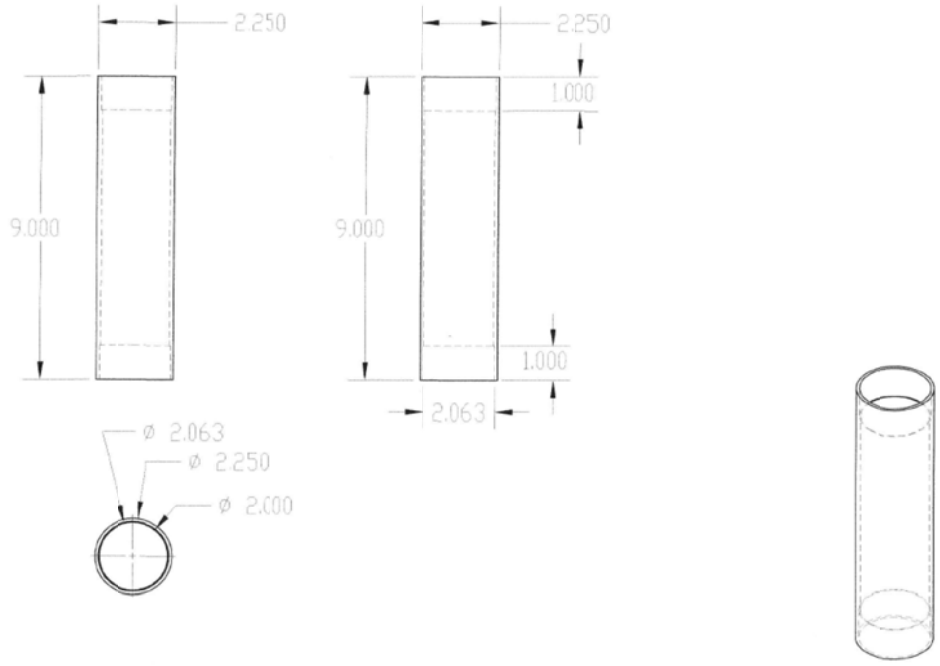

Part 1 – Made out of Aluminum

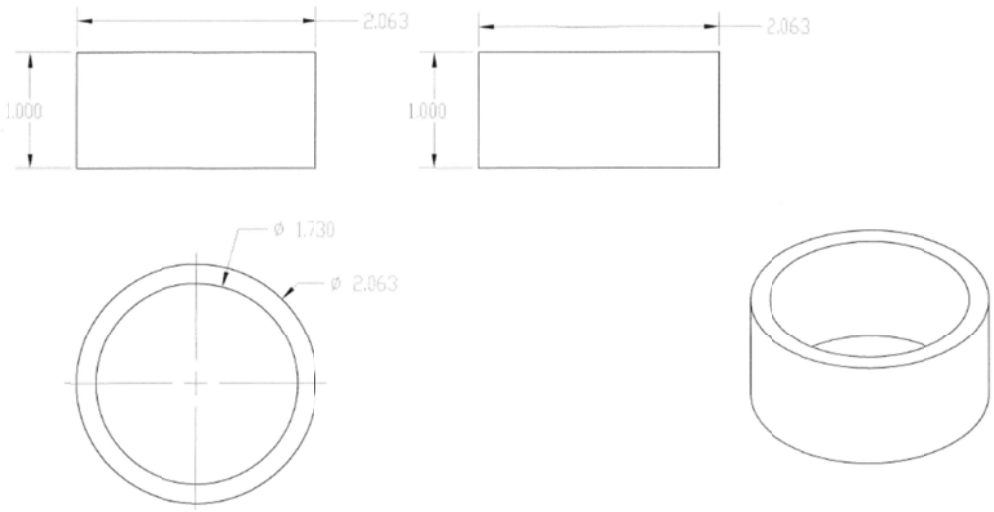

Part 2 – Made out of Delrin

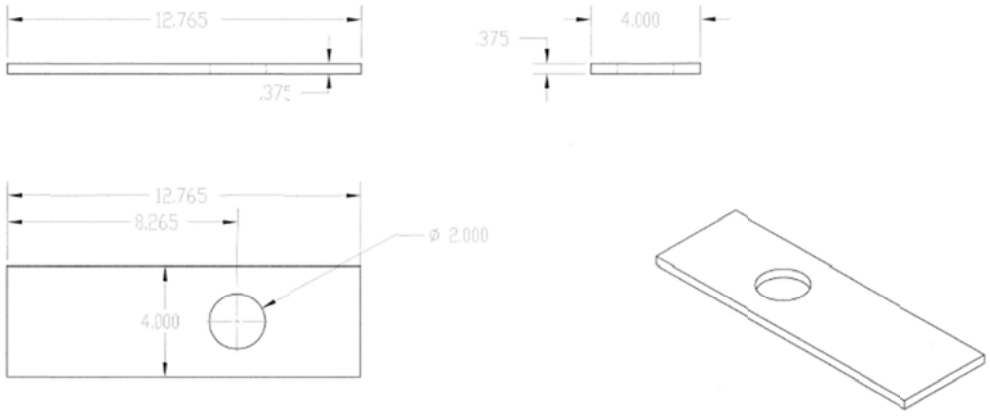

Part 3 – Made out of Aluminum

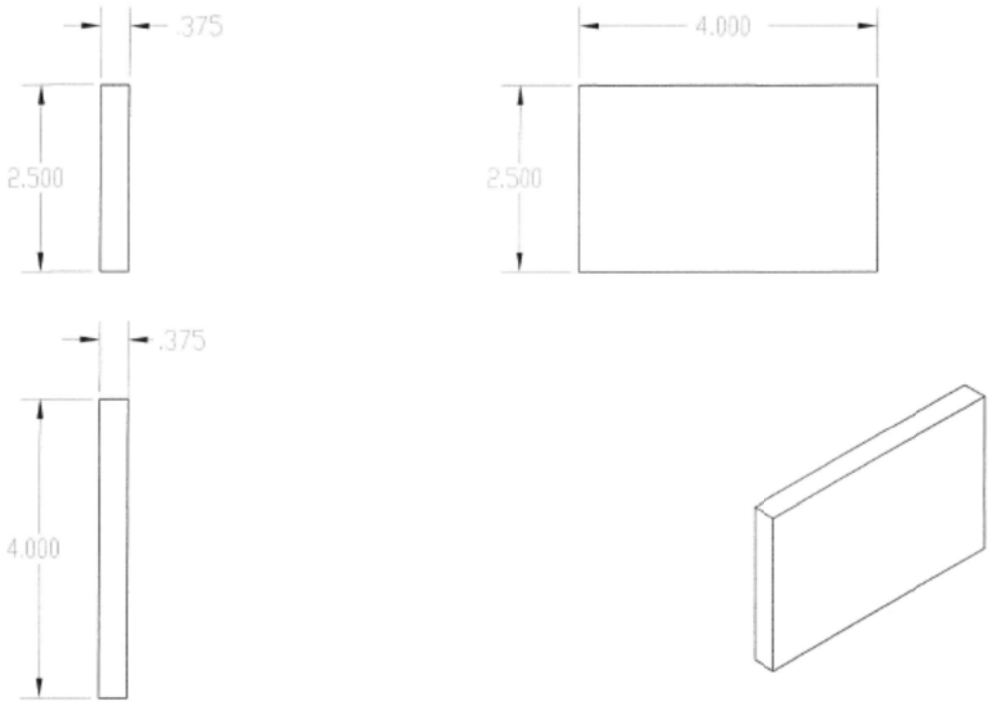

Part 4 – Made out of Aluminum

APPENDIX B

TRIAXIAL TESTS RESULTS AND EVALUATIONS

Initial Properties of Never Frozen Sand Test Specimens

Test #	Sample Height (mm)	Mass of Sand (g)	Initial Density (kg/m^3)	Relative Density (%)	B-Value
1	150	1019	1710	80	0.95
2	150	1022	1715	82	0.97
3	150	1018	1708	79	0.95
4	148	1007	1713	81	0.96
5	150	1019	1710	80	0.94

Never frozen Sand Tests Data

1			2			3			4			5			Mean		
Ea	S_d	Ev	Ea	S_d	Ev	Ea	S_d	Ev	Ea	S_d	Ev	Ea	S_d	Ev	Ea	Sd	Ev
0.0	0	-0.05	0.0	0	0.0	0.0	0	-0.1	0.0	0	-0.1	0.0	0	-0.1	0.0	0	-0.1
0.2	103	-0.02	0.2	73	0.1	0.2	68	-0.1	0.0	23	0.0	0.2	71	0.0	0.1	67	0.0
0.4	151	-0.03	0.4	127	0.1	0.4	123	-0.1	0.2	75	0.1	0.4	120	0.0	0.4	119	0.0
0.6	171	-0.11	0.6	158	0.1	0.6	149	-0.1	0.5	112	0.1	0.6	149	-0.1	0.6	148	0.0
0.8	184	-0.21	0.8	173	0.0	0.8	165	-0.2	0.7	141	0.0	0.8	167	-0.1	0.8	166	-0.1
1.0	192	-0.34	1.0	184	-0.2	1.0	176	-0.3	0.9	162	0.0	1.0	179	-0.2	1.0	179	-0.2
1.2	197	-0.48	1.2	192	-0.3	1.2	183	-0.4	1.1	176	-0.2	1.2	187	-0.4	1.2	187	-0.3
1.4	201	-0.62	1.4	198	-0.4	1.4	189	-0.6	1.3	186	-0.3	1.4	194	-0.5	1.4	194	-0.5
1.6	203	-0.77	1.6	202	-0.6	1.6	193	-0.7	1.5	193	-0.4	1.6	199	-0.7	1.6	198	-0.6
1.8	206	-0.93	1.8	205	-0.8	1.8	197	-0.9	1.7	198	-0.6	1.8	202	-0.8	1.8	202	-0.8
2.1	207	-1.09	2.1	208	-0.9	2.1	200	-1.0	1.9	202	-0.7	2.1	205	-1.0	2.0	204	-0.9
2.3	207	-1.24	2.3	209	-1.1	2.3	201	-1.2	2.1	205	-0.9	2.3	206	-1.1	2.2	206	-1.1
2.5	208	-1.40	2.5	211	-1.3	2.5	203	-1.4	2.3	207	-1.0	2.5	207	-1.3	2.4	207	-1.3
2.7	208	-1.55	2.7	212	-1.4	2.7	204	-1.5	2.5	208	-1.2	2.7	208	-1.4	2.6	208	-1.4
2.8	207	-1.68	2.8	212	-1.5	2.8	204	-1.6	2.7	209	-1.3	2.8	209	-1.6	2.8	208	-1.6
3.0	206	-1.81	3.0	212	-1.7	3.0	204	-1.8	2.9	210	-1.5	3.0	208	-1.7	3.0	208	-1.7
3.1	207	-1.93	3.1	213	-1.8	3.1	204	-1.9	3.0	210	-1.6	3.1	209	-1.8	3.1	208	-1.8
3.4	206	-2.08	3.4	212	-2.0	3.4	204	-2.1	3.2	211	-1.8	3.4	208	-2.0	3.3	208	-2.0
3.4	206	-2.13	3.4	213	-2.0	3.4	204	-2.1	3.3	210	-1.8	3.4	209	-2.0	3.4	208	-2.0
3.6	205	-2.28	3.6	211	-2.2	3.6	203	-2.3	3.6	210	-2.0	3.6	208	-2.2	3.6	207	-2.2
3.8	203	-2.43	3.8	211	-2.3	3.8	202	-2.4	3.8	210	-2.1	3.8	207	-2.4	3.8	206	-2.3
4.0	202	-2.58	4.0	209	-2.5	4.0	202	-2.6	4.0	209	-2.3	4.0	206	-2.5	4.0	206	-2.5
4.2	200	-2.72	4.2	208	-2.7	4.2	201	-2.7	4.2	209	-2.5	4.2	205	-2.7	4.2	205	-2.7
4.4	199	-2.87	4.4	207	-2.8	4.4	200	-2.9	4.4	208	-2.6	4.4	204	-2.9	4.4	204	-2.8
4.7	198	-3.02	4.7	206	-3.0	4.7	199	-3.1	4.7	207	-2.8	4.7	203	-3.0	4.7	202	-3.0
4.9	196	-3.16	4.9	204	-3.1	4.9	198	-3.2	4.9	205	-3.0	4.9	201	-3.2	4.9	201	-3.1
5.1	195	-3.30	5.1	202	-3.3	5.1	196	-3.4	5.1	204	-3.1	5.1	200	-3.3	5.1	199	-3.3
5.2	195	-3.41	5.2	201	-3.4	5.2	194	-3.5	5.2	203	-3.3	5.2	199	-3.5	5.2	198	-3.4
5.5	193	-3.55	5.5	199	-3.6	5.5	193	-3.6	5.5	201	-3.4	5.5	197	-3.6	5.5	197	-3.6
5.7	192	-3.67	5.7	197	-3.7	5.7	191	-3.8	5.7	200	-3.6	5.7	196	-3.8	5.7	195	-3.7
5.9	190	-3.78	5.9	195	-3.8	5.9	191	-3.9	5.9	198	-3.7	5.9	194	-3.9	5.9	194	-3.8
6.1	189	-3.89	6.0	193	-3.9	6.1	188	-4.0	6.1	196	-3.8	6.0	193	-4.0	6.0	192	-3.9

Duncan and Chang (1970) fitting

		S_d max	Ea	Ea/sd
83 (Test 1)	0.7	146	0.4	0.002
	0.95	198	1.4	0.007
84 (Test 2)	0.7	149	0.5	0.004
	0.95	202	1.6	0.008
86 (Test 3)	0.7	143	0.5	0.004
	0.95	194	1.7	0.009
87 (Test 4)	0.7	148	0.7	0.005
	0.95	200	1.8	0.009
88 (Test 5)	0.7	146	0.6	0.004
	0.95	198	1.6	0.008

	Ei	Sd ult	R_f	Ev @ 0.7 S_d	Ev at 0.95 S_d	Ev at S_d ma
83	1153	224	0.93	-0.0367	-0.5	1.5504
84	714	245	0.87	1	-0.5	-2.0039
86	681	234	0.87	-0.05	-0.95	-1.901
87	456	264	0.80	0	-0.63	-1.7681
88	630	247	0.85	-0.05	-0.78	-1.5712
Mean	**727**	**243**	**0.86**	**0.17**	**-0.67**	**-1.14**
STDEV	**231**	**13**	**0.04**	**0.41**	**0.17**	**1.35**

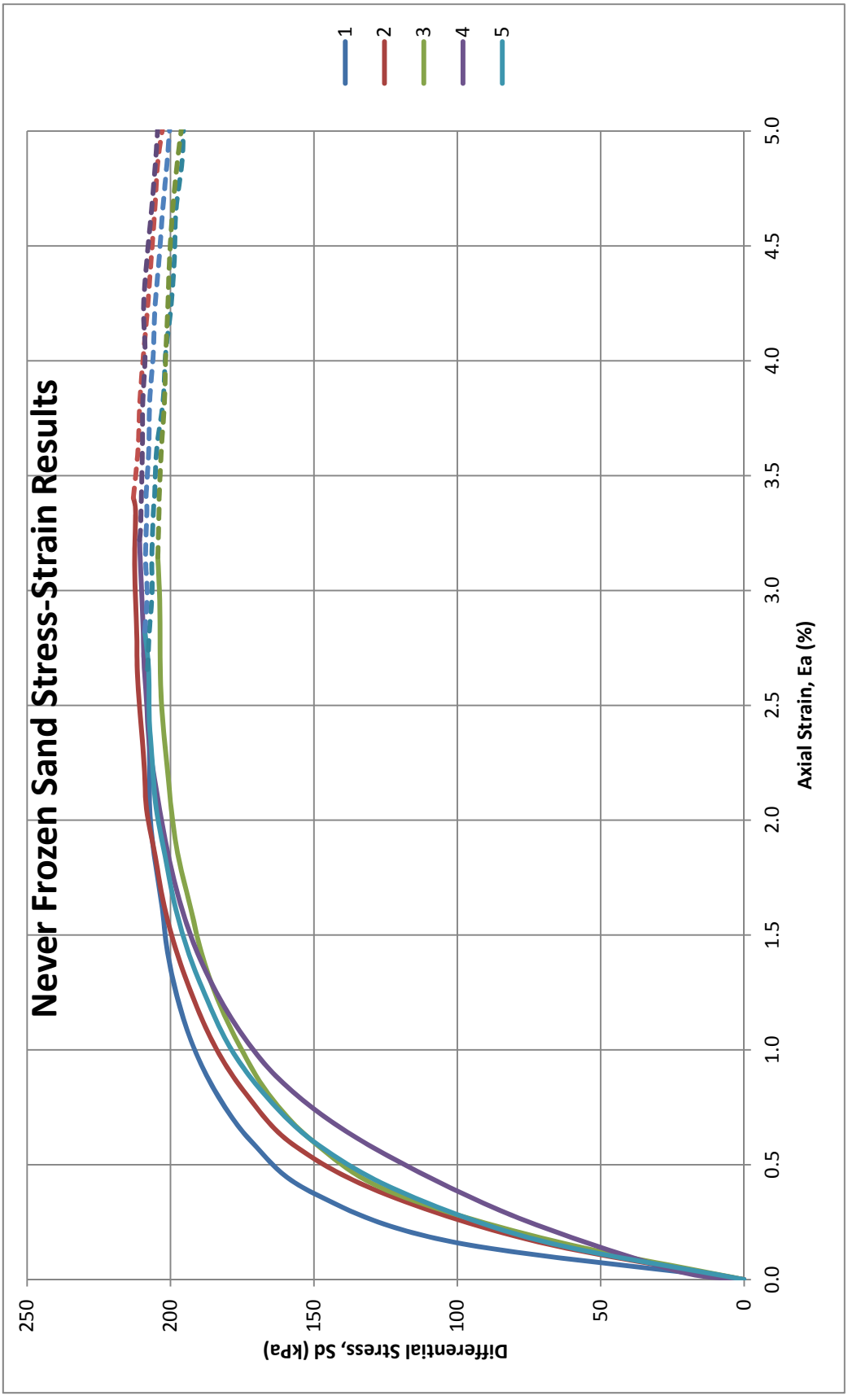
Never Frozen Sand Stress-Strain Results
Differential Stress, Sd (kPa)
Axial Strain, Ea (%)
0
50
100
150
200
250
0.0
0.5
1.0
1.5
2.0
2.5
3.0
3.5
4.0
4.5
5.0
1
2
3
4
5

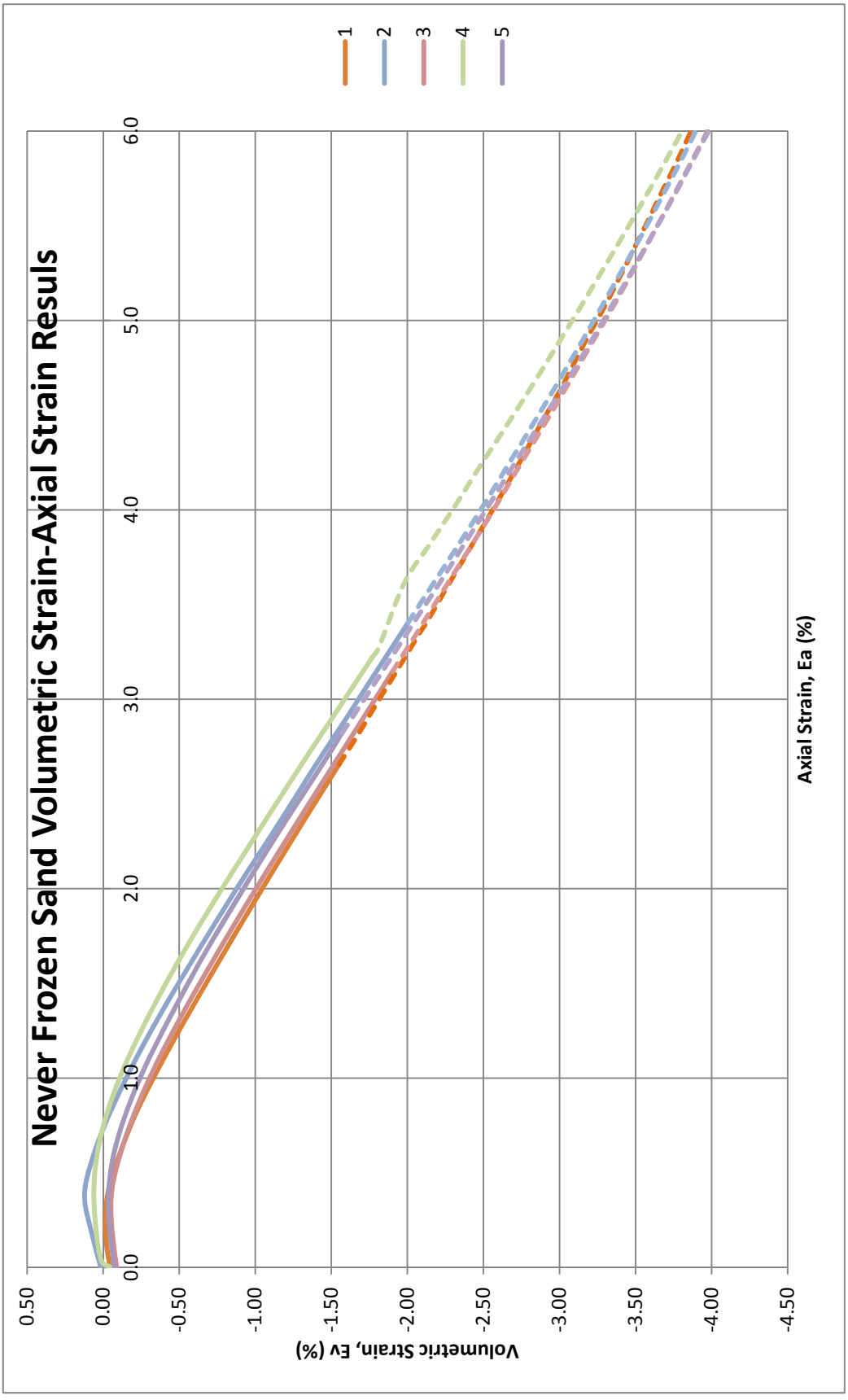
Never Frozen Sand Volumetric Strain-Axial Strain Resuls
1
2
3
4
5
0.0
1.0
2.0
3.0
4.0
5.0
6.0
Axial Strain, Ea (%)
0.50
0.00
-0.50
-1.00
-1.50
-2.00
-2.50
-3.00
-3.50
-4.00
-4.50
Volumetric Strain, Ev (%)

Initial Properties of Frozen Core Test Specimens

Test #	Sample Height (mm)	Mass of Sand (g)	Initial Density (kg/m^3)	Relative Density (%)	B-Value
1	144	977	1705	78	0.93
2	145	983	1707	79	0.94
3	144	977	1708	79	0.93
4	148	1005	1710	80	0.93

Frozen/Thawed Test Data

	1		2		3		4		Mean	
Ea	Sd	Ev	Sd	Ev	Sd	Ev	Sd	Ev	Sd	Ev
0.0	0	0.00	0	0.00	0		0		0	0.00
0.1	45	0.07	36	0.09	54		40		44	0.08
0.2	81	0.12	64	0.13	85		67		74	0.13
0.3	106	0.13	87	0.16	106		90		97	0.14
0.4	130	0.11	108	0.17	121		110		117	0.14
0.5	144	0.08	120	0.16	130		126		130	0.12
0.6	158	0.04	132	0.14	139		140		142	0.09
0.7	166	-0.01	139	0.11	147	0.00	148	0.00	150	0.02
0.8	173	-0.06	145	0.07	155	-0.03	160	-0.07	158	-0.02
0.9	178	-0.12	151	0.03	162	-0.06	168	-0.15	165	-0.07
1.0	184	-0.17	156	-0.02	167	-0.10	173	-0.22	170	-0.13
1.1	188	-0.24	160	-0.07	172	-0.13	177	-0.27	174	-0.18
1.2	191	-0.31	164	-0.12	176	-0.17	182	-0.35	178	-0.24
1.3	194	-0.38	167	-0.17	180	-0.22	185	-0.42	182	-0.30
1.4	197	-0.45	170	-0.23	182	-0.27	189	-0.50	185	-0.36
1.5	199	-0.53	173	-0.29	185	-0.33	192	-0.57	187	-0.43
1.6	202	-0.60	175	-0.35	187	-0.37	195	-0.63	190	-0.49
1.7	203	-0.68	178	-0.42	189	-0.43	197	-0.71	192	-0.56
1.8	205	-0.75	180	-0.48	191	-0.49	200	-0.79	194	-0.63
1.9	206	-0.84	182	-0.55	193	-0.55	202	-0.86	195	-0.70
2.0	208	-0.91	183	-0.61	194	-0.61	203	-0.94	197	-0.77
2.1	209	-0.99	185	-0.68	195	-0.67	204	-1.00	198	-0.83
2.2	209	-1.08	186	-0.75	196	-0.73	204	-1.08	199	-0.91
2.3	210	-1.15	187	-0.81	197	-0.80	205	-1.16	200	-0.98
2.4	210	-1.24	188	-0.89	198	-0.87	205	-1.23	200	-1.06
2.5	211	-1.32	189	-0.95	199	-0.93	205	-1.31	201	-1.13
2.6	211	-1.39	190	-1.03	198	-0.99	204	-1.38	201	-1.20
2.7	212	-1.47	191	-1.10	198	-1.06	204	-1.46	201	-1.27
2.8	212	-1.55	193	-1.17	197	-1.13	204	-1.53	201	-1.35
2.9	212	-1.64	194	-1.25	197	-1.20	204	-1.61	202	-1.42
3.0	212	-1.72	194	-1.32	197	-1.27	204	-1.69	202	-1.50
3.1	213	-1.79	194	-1.40	196	-1.33	203	-1.75	202	-1.57
3.2	212	-1.88	194	-1.47	196	-1.40	203	-1.82	201	-1.64
3.3	212	-1.95	194	-1.54	196	-1.47	202	-1.90	201	-1.72
3.4	213	-2.04	194	-1.62	195	-1.54	201	-1.98	201	-1.79
3.5	212	-2.11	195	-1.69	195	-1.61	201	-2.05	201	-1.87
3.6	211	-2.20	195	-1.77	195	-1.67	200	-2.11	200	-1.94
3.7	211	-2.28	195	-1.84	194	-1.75	198	-2.19	200	-2.02
3.8	211	-2.36	195	-1.91	194	-1.82	197	-2.27	199	-2.09
3.9	210	-2.44	195	-1.99	193	-1.89	196	-2.34	199	-2.16
4.0	210	-2.52	196	-2.06	193	-1.96	195	-2.41	198	-2.24
4.1	209	-2.59	196	-2.13	193	-2.02	194	-2.47	198	-2.30
4.2	208	-2.67	196	-2.21	192	-2.09	193	-2.55	197	-2.38
4.3	208	-2.74	196	-2.27	192	-2.17	191	-2.62	197	-2.45
4.4	207	-2.82	196	-2.35	191	-2.24	189	-2.69	196	-2.53
4.5	206	-2.90	196	-2.42	191	-2.31	187	-2.76	195	-2.60
4.6	206	-2.97	196	-2.50	191	-2.37	185	-2.82	194	-2.66
4.7	205	-3.04	195	-2.57	191	-2.45	183	-2.89	194	-2.74
4.8	205	-3.11	195	-2.64	190	-2.51	181	-2.96	193	-2.80
4.9	204	-3.19	195	-2.71	190	-2.57	179	-3.03	192	-2.87
5.0	203	-3.26	195	-2.78	190	-2.64	178	-3.09	191	-2.94

Duncan and Chang (1970) Fitting

	Freeze Thaw Tests			
		S_d max	**Ea**	**Ea/sd**
1	0.7	149.07	0.53	0.003575756
	0.95	202.31	1.63	0.008068569
2	0.7	137.61	0.69	0.004990017
	0.95	186.75	2.23	0.011954399
3	0.7	138.83	0.60	0.004328932
	0.95	188.42	1.66	0.008827952
4	0.7	143.50	0.64	0.004473868
	0.95	194.75	1.60	0.008218228

	Ei	**Sd ult**	**R_f**	**Ev @ 0.7 S_d max**	**Ev at 0.95 S_d max**	**Ev at S_d max**
1	716	245	0.87	0.0875	-0.5953	-2.0039
2	527	222	0.89	0.6978	-0.3452	-2.1241
3	561	236	0.84	0.0875	-0.65	-0.9174
4	509	256	0.80	0.6978	-0.63	-0.359
Mean	**578**	**240**	**0.85**	**0.39**	**-0.56**	**-1.35**
STDEV	**82**	**12**	**0.03**	**0.31**	**0.12**	**0.74**

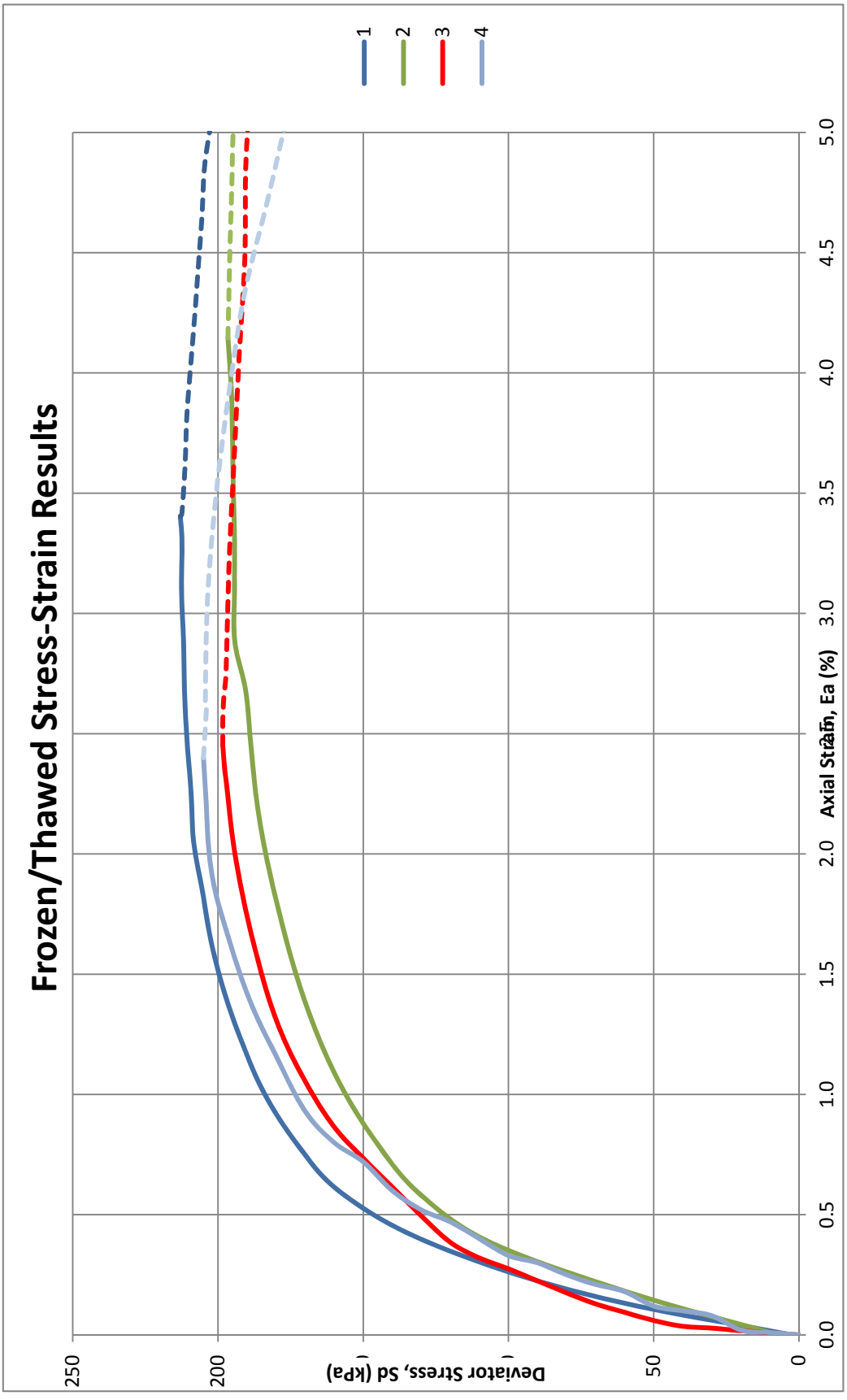
Frozen/Thawed Stress-Strain Results
1
2
3
4
Deviator Stress, Sd (kPa)
0
50
200
250
0.0
0.5
1.0
1.5
2.0
3.0
3.5
4.0
4.5
5.0
Axial Strain, Ea (%)

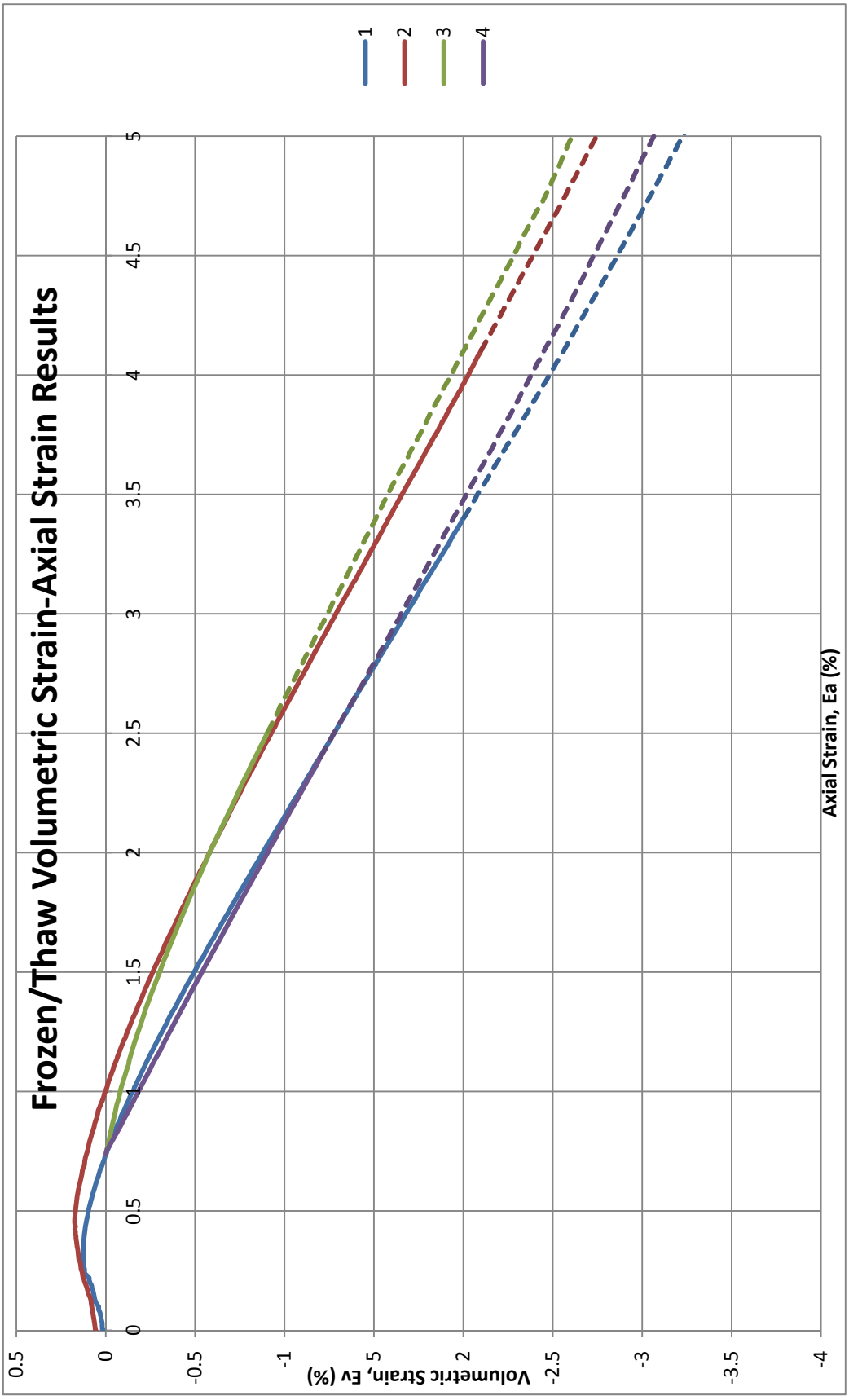
Frozen/Thaw Volumetric Strain-Axial Strain Results
1
2
3
4
Volumetric Strain, Ev (%)
0.5
0
-0.5
-1
-2
-2.5
-3
-3.5
-4
Axial Strain, Ea (%)
0
0.5
1
1.5
2
2.5
3
3.5
4
4.5
5

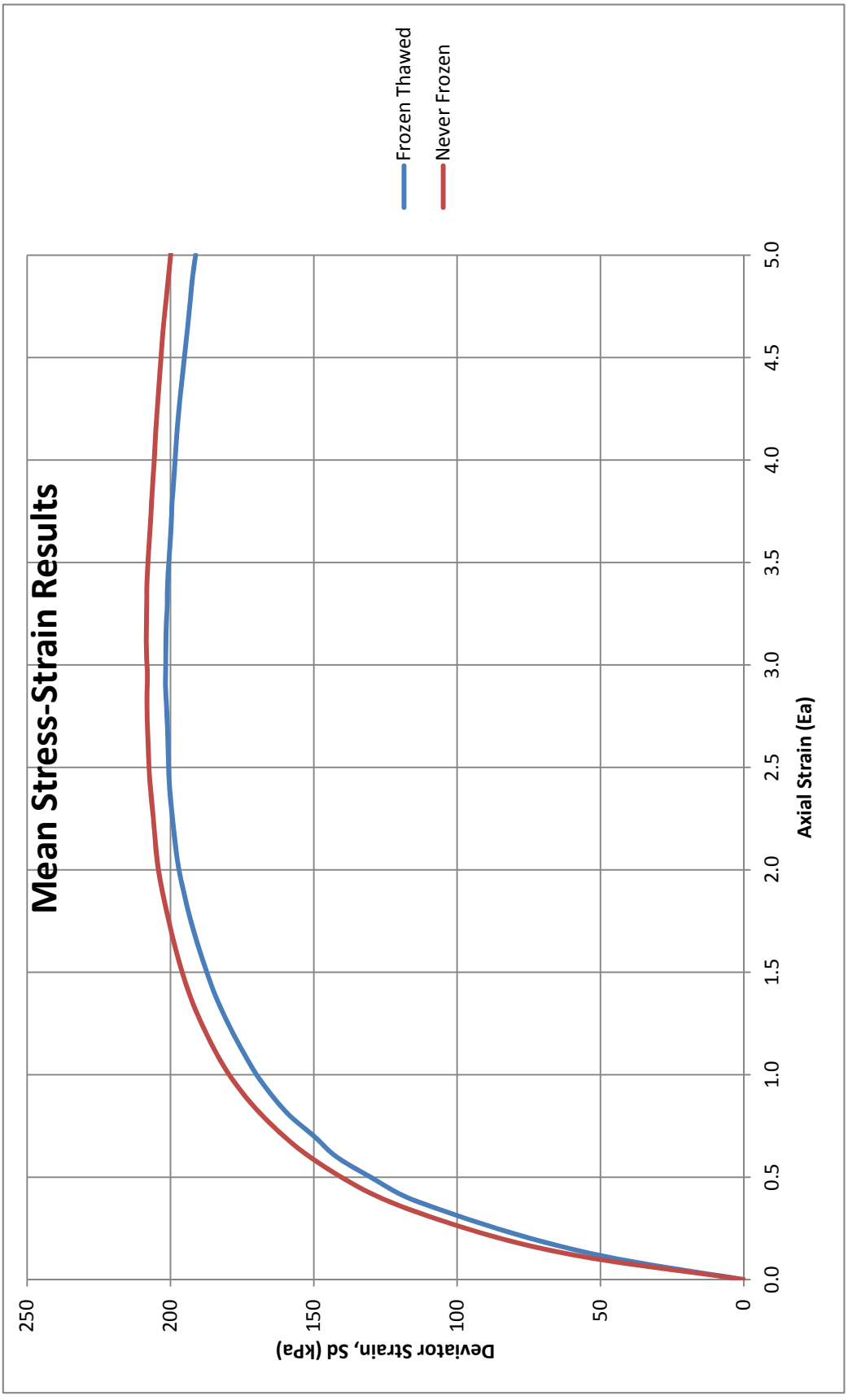
Mean Stress-Strain Results
Frozen Thawed
Never Frozen
Deviator Strain, Sd (kPa)
0
50
100
150
200
250
Axial Strain (Ea)
0.0
0.5
1.0
1.5
2.0
2.5
3.0
3.5
4.0
4.5
5.0

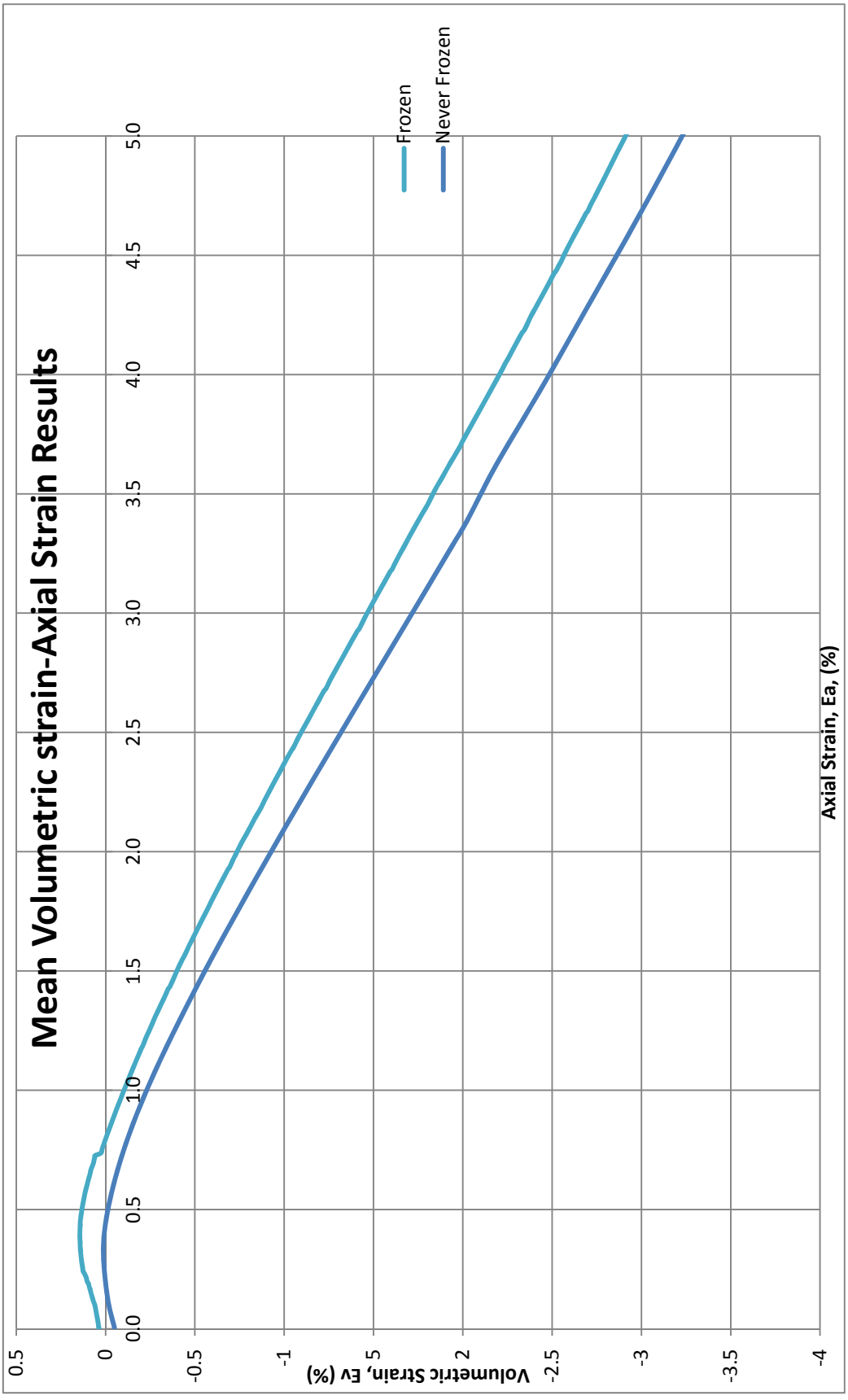
Mean Volumetric strain-Axial Strain Results
Frozen
Never Frozen
Volumetric Strain, Ev (%)
Axial Strain, Ea, (%)
0.5
0
-0.5
-1
-2
-2.5
-3
-3.5
-4
0.0
0.5
1.0
1.5
2.0
2.5
3.0
3.5
4.0
4.5
5.0

Duncan and Chang fitting

Unfrozen Sand

		Sd max	Ea	Ea/sd
83 (Test 1)	0.7	146	0.4	0.002
	0.95	198	1.4	0.007
84 (Test 2)	0.7	149	0.5	0.004
	0.95	202	1.6	0.008
86 (Test 3)	0.7	143	0.5	0.004
	0.95	194	1.7	0.009
87 (Test 4)	0.7	148	0.7	0.005
	0.95	200	1.8	0.009
88 (Test 5)	0.7	146	0.6	0.004
	0.95	198	1.6	0.008

	Ei	Sd ult	Rf	@ 0.7 Sd m	at 0.95 Sd n	Ev at Sd max
83	1153	224	0.93	-0.0367	-0.5	1.5504
84	714	245	0.87	1	-0.5	-2.0039
86	681	234	0.87	-0.05	-0.95	-1.901
87	456	264	0.80	0	-0.63	-1.7681
88	630	247	0.85	-0.05	-0.78	-1.5712
Mean	**727**	**243**	**0.86**	**0.17**	**-0.67**	**-1.14**
STDEV	**231**	**13**	**0.04**	**0.41**	**0.17**	**1.35**

Freeze Thaw Tests Duncan and Chang Fitting

		Sd max	Ea	Ea/sd
1	0.7	149.07	0.53	0.003576
	0.95	202.31	1.63	0.008069
2	0.7	137.61	0.69	0.00499
	0.95	186.75	2.23	0.011954
3	0.7	138.83	0.60	0.004329
	0.95	188.42	1.66	0.008828
4	0.7	143.50	0.64	0.004474
	0.95	194.75	1.60	0.008218

	Ei	Sd ult	Rf	@ 0.7 Sd m	at 0.95 Sd n	Ev at Sd max
1	716	245	0.87	0.0875	-0.5953	-2.0039
2	527	222	0.89	0.6978	-0.3452	-2.1241
3	561	236	0.84	0.0875	-0.65	-0.9174
4	509	256	0.80	0.6978	-0.63	-0.359
Mean	578	240	0.85	0.39	-0.56	-1.35
STDEV	82	12	0.03	0.31	0.12	0.74

Ei at 90% confidence t-Test: Two-Sample Assuming Equal Variances

	Variable 1	*Variable 2*
Mean	726.7954	578.0738
Variance	66639.44	8878.763
Observations	5	4
Pooled Variance	41884.87	
Hypothesized Mean Difference	0	
df	7	
t Stat	1.083277	
P(T<=t) one-tail	0.157291	
t Critical one-tail	1.894579	
P(T<=t) two-tail	0.314582	
t Critical two-tail	2.364624	

Sd ult at 90% confidence t-Test: Two-Sample Assuming Equal Variances

	Variable 1	*Variable 2*
Mean	243.0022	239.6897
Variance	224.315	205.8009
Observations	5	4
Pooled Variance	216.3804	
Hypothesized Mean Difference	0	
df	7	
t Stat	0.335693	
P(T<=t) one-tail	0.37347	
t Critical one-tail	1.894579	
P(T<=t) two-tail	0.746939	
t Critical two-tail	2.364624	

Rf at 90% confidence t-Test: Two-Sample Assuming Equal Variances

	Variable 1	*Variable 2*
Mean	0.862427	0.84919
Variance	0.002187	0.0014
Observations	5	4
Pooled Variance	0.00185	
Hypothesized Mean Difference	0	
df	7	
t Stat	0.458817	
P(T<=t) one-tail	0.330136	
t Critical one-tail	1.894579	
P(T<=t) two-tail	0.660272	
t Critical two-tail	2.364624	

Ev @ 0.7 Sd max at 90% confidence

t-Test: Two-Sample Assuming Equal Variances

	Variable 1	*Variable 2*
Mean	0.17266	0.39265
Variance	0.214322	0.124155
Observations	5	4
Pooled Variance	0.175679	
Hypothesized Mean Difference	0	
df	7	
t Stat	-0.78241	
P(T<=t) one-tail	0.229808	
t Critical one-tail	1.894579	
P(T<=t) two-tail	0.459616	
t Critical two-tail	2.364624	

Ev @ 0.95 Sd max at 90% confidence

t-Test: Two-Sample Assuming Equal Variances

	Variable 1	*Variable 2*
Mean	-0.672	-0.55513
Variance	0.03747	0.020097
Observations	5	4
Pooled Variance	0.030024	
Hypothesized Mean Difference	0	
df	7	
t Stat	-1.00549	
P(T<=t) one-tail	0.174072	
t Critical one-tail	1.894579	
P(T<=t) two-tail	0.348144	
t Critical two-tail	2.364624	

Ev @ Sd max at 90% confidence

t-Test: Two-Sample Assuming Equal Variances

	Variable 1	*Variable 2*
Mean	-1.13876	-1.3511
Variance	2.286033	0.732012
Observations	5	4
Pooled Variance	1.620024	
Hypothesized Mean Difference	0	
df	7	
t Stat	0.248694	
P(T<=t) one-tail	0.405368	
t Critical one-tail	1.894579	
P(T<=t) two-tail	0.810736	
t Critical two-tail	2.364624	

Initial Properties of Undrained Baseline Tests Specimens

Test #	Sample Height (mm)	Mass of Sand (g)	Initial Density (kg/m^3)	Relative Density (%)	B-Value
1	150	1019	1710	80	0.90
2	149	1013	1712	81	0.90
3	150	1012	1714	82	0.96
4	150	1019	1710	80	0.95
5	149	1012	1710	80	0.93

Baseline Undrained Test Results

	1		2		3		4		5		Mean	
Ea	Sd	Exc U	Sd	Exc U	Sd	Exc U	Sd	Exc U	Sd	Exc U	Sd	Exc U
(%)	(kPa)	(kPa)	(kPa)	(kPa)	(kPa)	(kPa)	(kPa)	(kPa)	(kPa)	(kPa)	(kPa)	(kPa)
0.0	0	0	0	0	0	0	0	0	0	0	0	0
0.1	43	0	10	6	12	9	19	0	10	-13	21	4
0.2	60	0	29	3	28	10	37	-3	25	-15	38	2
0.3	76	4	48	0	43	9	54	-6	40	-18	55	2
0.4	92	4	67	-4	57	9	70	-9	55	-19	71	0
0.5	111	2	85	-8	70	7	90	-13	70	-23	89	-3
0.6	132	-2	105	-12	84	5	110	-16	85	-26	108	-6
0.7	150	-7	125	-17	98	3	129	-21	100	-25	125	-11
0.8	167	-13	143	-22	114	0	148	-25	115	-27	143	-15
0.9	185	-18	160	-27	130	-2	166	-29	130	-31	160	-19
1.0	202	-24	180	-33	145	-5	184	-35	145	-34	178	-24
1.1	220	-30	200	-36	160	-9	202	-40	160	-37	196	-29
1.2	239	-37	219	-39	174	-12	220	-45	175	-41	213	-33
1.3	258	-44	237	-45	188	-16	239	-51	190	-45	230	-39
1.4	277	-50	256	-52	203	-19	258	-56	204	-48	248	-45
1.5	296	-57	274	-59	218	-23	276	-62	218	-52	266	-50
1.6	315	-64	292	-66	233	-27	294	-68	231	-56	283	-56
1.7	340	-71	310	-73	248	-31	319	-75	243	-60	304	-63
1.8	357	-79	330	-80	260	-35	343	-81	257	-63	322	-69
1.9	380	-86	350	-88	272	-40	357	-86	270	-67	340	-75
2.0	403	-95	374	-95	284	-43	376	-93	285	-71	359	-81
2.1	419	-102	398	-102	295	-48	395	-100	300	-76	377	-88
2.2	442	-110	420	-111	310	-53	416	-107	315	-79	397	-95
2.3	459	-118	438	-119	325	-58	435	-114	330	-84	414	-102
2.4	483	-126	460	-128	345	-63	451	-120	345	-89	435	-109
2.5	506	-134	482	-137	361	-67	471	-127	360	-93	455	-116
2.6	523	-143	502	-145	380	-73	491	-134	380	-98	474	-124
2.7	545	-150	524	-154	393	-78	511	-141	400	-103	493	-131
2.8	561	-158	547	-163	409	-84	530	-148	412	-107	512	-138
2.9	581	-165	567	-171	425	-89	544	-153	425	-113	529	-145
3.0	601	-173	587	-180	441	-94	563	-160	439	-117	548	-152
3.1	613	-180	605	-188	458	-100	581	-166	454	-122	564	-158
3.2	630	-187	623	-196	471	-105	599	-172	469	-127	581	-165
3.3	645	-193	640	-204	489	-111	614	-178	481	-132	597	-172
3.4	663	-198	655	-211	506	-117	628	-182	496	-137	613	-177
3.5	675	-204	670	-218	523	-122	641	-188	512	-142	627	-183
3.6	684	-209	682	-224	541	-127	656	-193	528	-148	641	-188
3.7	695	-213	696	-230	554	-133	669	-198	543	-153	654	-193
3.8	704	-217	708	-235	572	-139	681	-202	556	-157	666	-198
3.9	714	-221	721	-240	588	-144	691	-205	570	-162	678	-203
4.0	721	-224	731	-245	604	-148	700	-209	584	-167	689	-207
4.1	726	-227	741	-249	619	-153	711	-213	598	-171	699	-210
4.2	734	-230	750	-253	631	-158	718	-217	613	-176	708	-213
4.3	741	-232	757	-256	646	-163	728	-220	623	-180	718	-217
4.4	744	-234	765	-260	660	-168	734	-222	635	-184	726	-220
4.5	747	-236	770	-263	672	-171	741	-225	648	-188	733	-223
4.6	750	-238	775	-265	686	-176	747	-228	661	-193	739	-226
4.7	754	-239	781	-267	697	-180	754	-231	672	-197	747	-229
4.8	756	-241	784	-269	708	-184	759	-233	680	-200	752	-231
4.9	758	-242	787	-271	719	-188	762	-235	690	-203	757	-233
5.0	759	-243	790	-272	728	-191	767	-237	702	-207	761	-235
5.1	761	-244	795	-274	738	-194	771	-239	711	-210	766	-237
5.2	762	-245	795	-275	744	-197	773	-241	720	-213	768	-239
5.3	765	-246	797	-276	752	-201	778	-244	727	-216	773	-241
5.4	765	-247	798	-278	760	-203	780	-246	735	-219	776	-243
5.5	767	-248	797	-278	763	-206	782	-248	743	-221	777	-245
5.6	763	-249	799	-279	768	-209	783	-249	751	-224	779	-246
5.7	763	-249	800	-280	772	-211	784	-250	759	-226	780	-247
5.8	764	-250	802	-281	776	-214	784	-251	763	-228	781	-249
5.9	764	-251	802	-282	778	-216	784	-253	768	-231	782	-250
6.0	763	-252	801	-282	780	-217	785	-253	774	-233	782	-251
6.1	762	-252	801	-283	784	-220	783	-254	779	-235	783	-252
6.2	761	-253	802	-283	784	-222	781	-255	785	-237	782	-253
6.3	761	-254	800	-284	784	-223	782	-256	787	-238	782	-254
6.4	758	-254	799	-284	787	-225	779	-257	793	-240	781	-255
6.5	757	-255	800	-284	788	-226	778	-258	796	-242	781	-256
6.6	756	-255	801	-285	790	-228	776	-259	796	-243	781	-256
6.7	756	-256	796	-285	790	-229	771	-259	798	-245	778	-257
6.8	752	-256	793	-286	791	-230	771	-260	800	-246	777	-258
6.9	753	-257	795	-286	789	-231	766	-261	802	-247	776	-259
7.0	752	-257	792	-286	787	-233			805	-248	777	-259
7.1	750	-258	788	-287	781	-234			805	-250	773	-259

7.2	751	-258	787	-287	779	-235		807	-251	772	-260
7.3	751	-258	783	-287	772	-236		810	-252	769	-260
7.4	749	-259	782	-287	768	-236		812	-252	766	-261
7.5	747	-259	782	-288	762	-237		811	-253	764	-261
7.6	745	-259	777	-288	759	-238		813	-254	760	-262
7.7	743	-260	774	-288	755	-238		811	-255	757	-262
7.8	744	-260	770	-288	746	-239		809	-256	753	-263
7.9	743	-260	766	-288	742	-240		807	-256	751	-263
8.0	744	-261	763	-289	734	-240		805	-257	747	-263
8.1	744	-261	759	-289	731	-241		804	-257	745	-264
8.2	743	-261	760	-289	727	-241		805	-258	744	-264
8.3	744	-262	755	-289	725	-241		801	-258	741	-264
8.4	750	-262	752	-289	722	-242		802	-258	741	-264
8.5	748	-262	748	-289	710	-242		795	-259	735	-265
8.6	747	-262	746	-290	712	-243		793	-259	735	-265
8.7	749	-262	739	-290	708	-243		792	-259	732	-265
8.8	747	-263	737	-289	703	-243		788	-260	729	-265
8.9	745	-263	732	-289	697	-243		785	-260	725	-265
9.0	743	-263	731	-289	695	-243		779	-260	723	-265

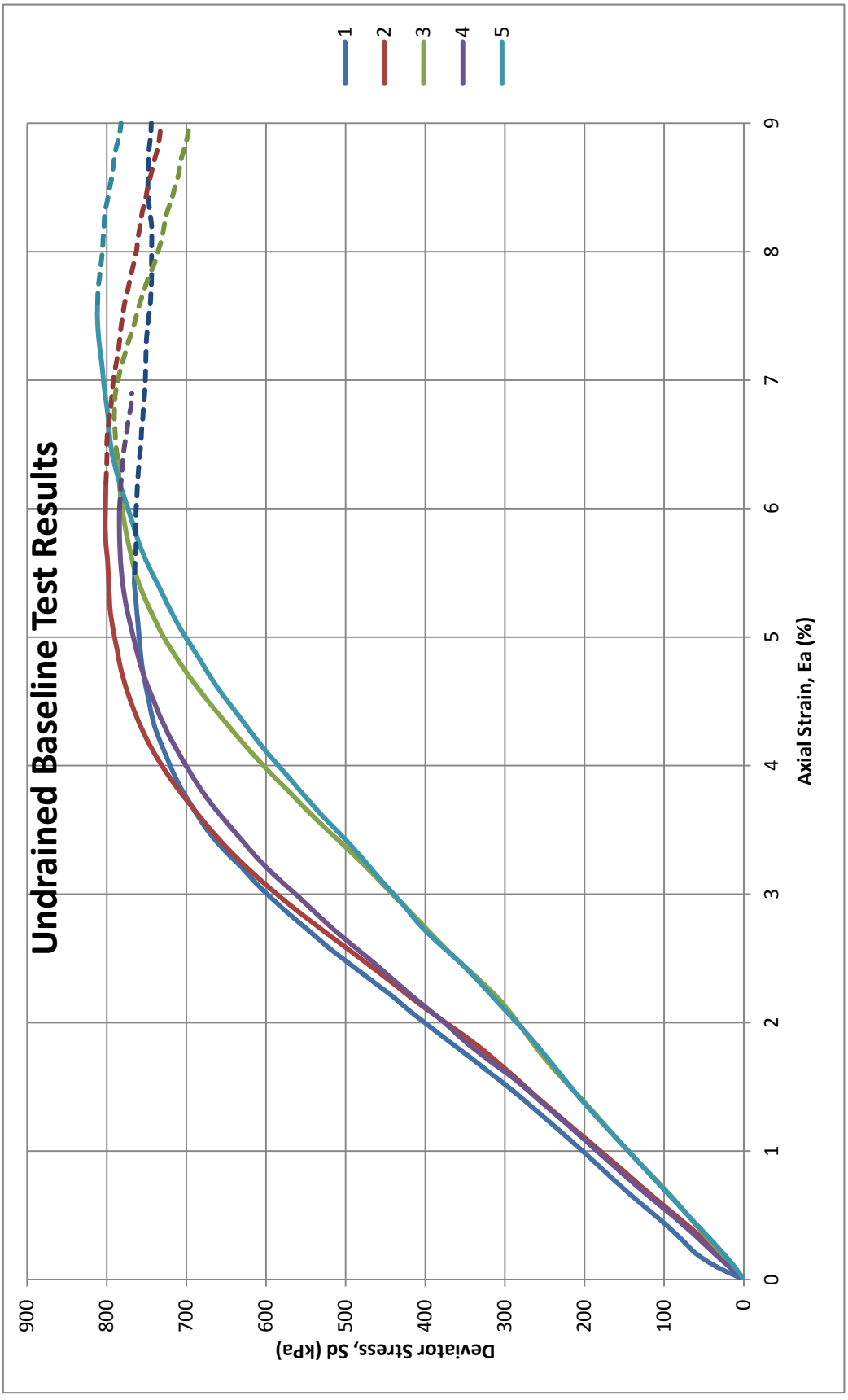
Undrained Baseline Test Results
Deviator Stress, Sd (kPa)
Axial Strain, Ea (%)
0
100
200
300
400
500
600
700
800
900
0
1
2
3
4
5
6
7
8
9
1
2
3
4
5

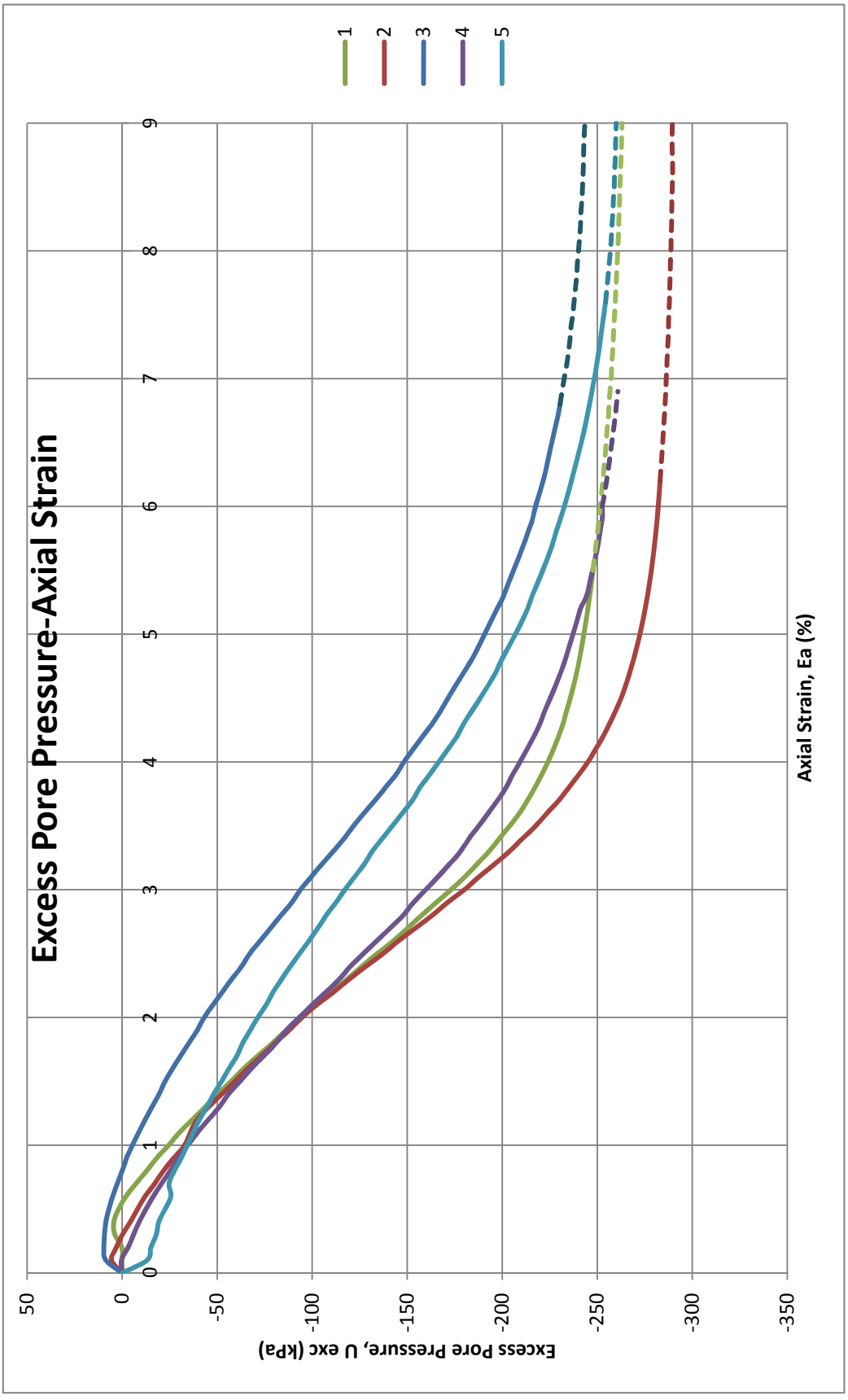
Excess Pore Pressure-Axial Strain
1
2
3
4
5
50
0
-50
-100
-150
-200
-250
-300
-350
Excess Pore Pressure, U exc (kPa)
0
1
2
3
4
5
6
7
8
9
Axial Strain, Ea (%)

Initial Properties of Frozen Core Test Specimens

Test #	Sample Height (mm)	Mass of Sand (g)	Initial Density (kg/m^3)	Relative Density (%)	B-Value
1	150	1020	1711	80	0.90
2	145	985	1708	79	0.93
3	144	979	1710	80	0.90

Frozen Core Undrained Test Results

	1		2		3		Mean	
Ea	Sd	Exc U	Sd	Exc U	Sd	Exc U	Sd	Exc U
(%)	(kPa)	(kPa)	(kPa)	(kPa)	(kPa)	(kPa)	(kPa)	(kPa)
0.0	0	0	0	0	0	0	0	0
0.1	19	6	17	4	9	2	15	4
0.2	38	8	33	19	23	5	31	11
0.3	57	9	48	20	40	5	48	11
0.4	70	10	64	20	57	4	64	11
0.5	85	10	79	20	74	2	79	11
0.6	98	9	94	19	90	0	94	9
0.7	115	7	107	17	106	-2	109	8
0.8	131	5	118	15	123	-5	124	5
0.9	149	2	131	14	141	-6	140	3
1.0	167	1	148	13	159	-5	158	3
1.1	184	-3	166	10	176	-9	175	-1
1.2	200	-7	182	9	191	-13	191	-4
1.3	215	-10	198	14	205	-16	206	-4
1.4	231	-8	214	11	221	-20	222	-5
1.5	247	-6	229	8	239	-24	238	-7
1.6	264	-9	242	5	257	-28	254	-11
1.7	280	-14	256	1	274	-33	270	-15
1.8	296	-18	271	-2	290	-36	286	-19
1.9	313	-23	287	-5	306	-41	302	-23
2.0	329	-28	303	-10	323	-45	318	-28
2.1	345	-32	319	-14	345	-50	336	-32
2.2	360	-37	336	-18	366	-55	354	-37
2.3	375	-42	352	-23	387	-59	371	-41
2.4	391	-48	368	-27	403	-64	387	-46
2.5	408	-53	383	-32	420	-69	403	-51
2.6	425	-58	398	-37	438	-74	420	-56
2.7	443	-64	414	-42	454	-79	437	-62
2.8	460	-70	429	-47	471	-83	453	-67
2.9	477	-75	445	-52	487	-88	469	-72
3.0	494	-81	460	-57	503	-94	486	-77
3.1	510	-86	475	-63	520	-99	502	-83
3.2	527	-92	489	-68	535	-104	517	-88
3.3	542	-98	504	-74	550	-108	532	-93
3.4	558	-103	517	-79	565	-113	546	-98
3.5	572	-109	530	-84	580	-118	561	-104
3.6	586	-115	543	-90	594	-123	574	-109
3.7	600	-117	556	-95	607	-127	588	-113
3.8	614	-122	567	-101	619	-131	600	-118
3.9	627	-129	579	-106	631	-136	612	-124
4.0	639	-134	590	-111	643	-140	624	-128
4.1	651	-140	602	-117	655	-144	636	-134
4.2	663	-145	613	-122	666	-148	647	-138
4.3	675	-151	624	-126	676	-151	658	-143
4.4	686	-156	634	-131	686	-155	669	-148
4.5	697	-162	643	-136	695	-159	679	-152
4.6	707	-166	651	-141	704	-163	688	-157
4.7	717	-172	660	-145	712	-166	696	-161

4.8	726	-176	668	-150	720	-169	704	-165
4.9	734	-181	675	-154	727	-172	712	-169
5.0	741	-186	682	-158	734	-175	719	-173
5.1	748	-190	688	-162	740	-178	726	-177
5.2	754	-195	695	-166	746	-181	732	-180
5.3	761	-199	700	-170	751	-183	737	-184
5.4	767	-203	706	-173	756	-185	743	-187
5.5	772	-207	711	-177	761	-188	748	-191
5.6	777	-210	716	-180	765	-190	753	-194
5.7	781	-214	719	-184	768	-193	756	-197
5.8	786	-217	722	-187	772	-194	760	-200
5.9	791	-221	725	-190	774	-197	763	-202
6.0	795	-224	728	-193	776	-199	767	-205
6.1	800	-227	731	-196	778	-201	770	-208
6.2	803	-230	732	-198	779	-202	772	-210
6.3	807	-233	734	-201	781	-203	774	-212
6.4	810	-235	735	-204	782	-205	775	-215
6.5	813	-238	737	-206	783	-207	778	-217
6.6	816	-241	739	-209	785	-208	780	-219
6.7	818	-243	741	-211	782	-209	781	-221
6.8	820	-246	741	-213	782	-210	781	-223
6.9	822	-248	740	-215	781	-212	781	-225
7.0	824	-249	739	-217	785	-212	783	-226
7.1	825	-251	737	-219	786	-213	783	-228
7.2	826	-253	734	-221	787	-214	782	-229
7.3	827	-255	732	-223	787	-215	782	-231
7.4	829	-257	727	-224	787	-217	781	-233
7.5	830	-259	724	-226	786	-218	780	-234
7.6	830	-261	720	-228	785	-219	778	-236
7.7	830	-263	717	-229	784	-221	777	-238
7.8	829	-266	713	-231	784	-221	775	-239
7.9	831	-266	708	-232	782	-222	774	-240
8.0	831	-267	704	-233	780	-222	772	-241
8.1	830	-267	700	-235	776	-223	769	-242
8.2	828	-270	695	-236	772	-224	765	-243
8.3	825	-271	690	-237	769	-226	761	-244
8.4	823	-272	684	-238	766	-226	757	-245
8.5	820	-274	678	-239	763	-226	754	-246
8.6	817	-276	674	-240	760	-227	750	-247
8.7	814	-277	668	-241	758	-227	747	-248
8.8	810	-278	666	-242	756	-228	744	-249
8.9	806	-279	663	-243	753	-229	741	-250
9.0	804	-280	663	-244	751	-229	739	-251

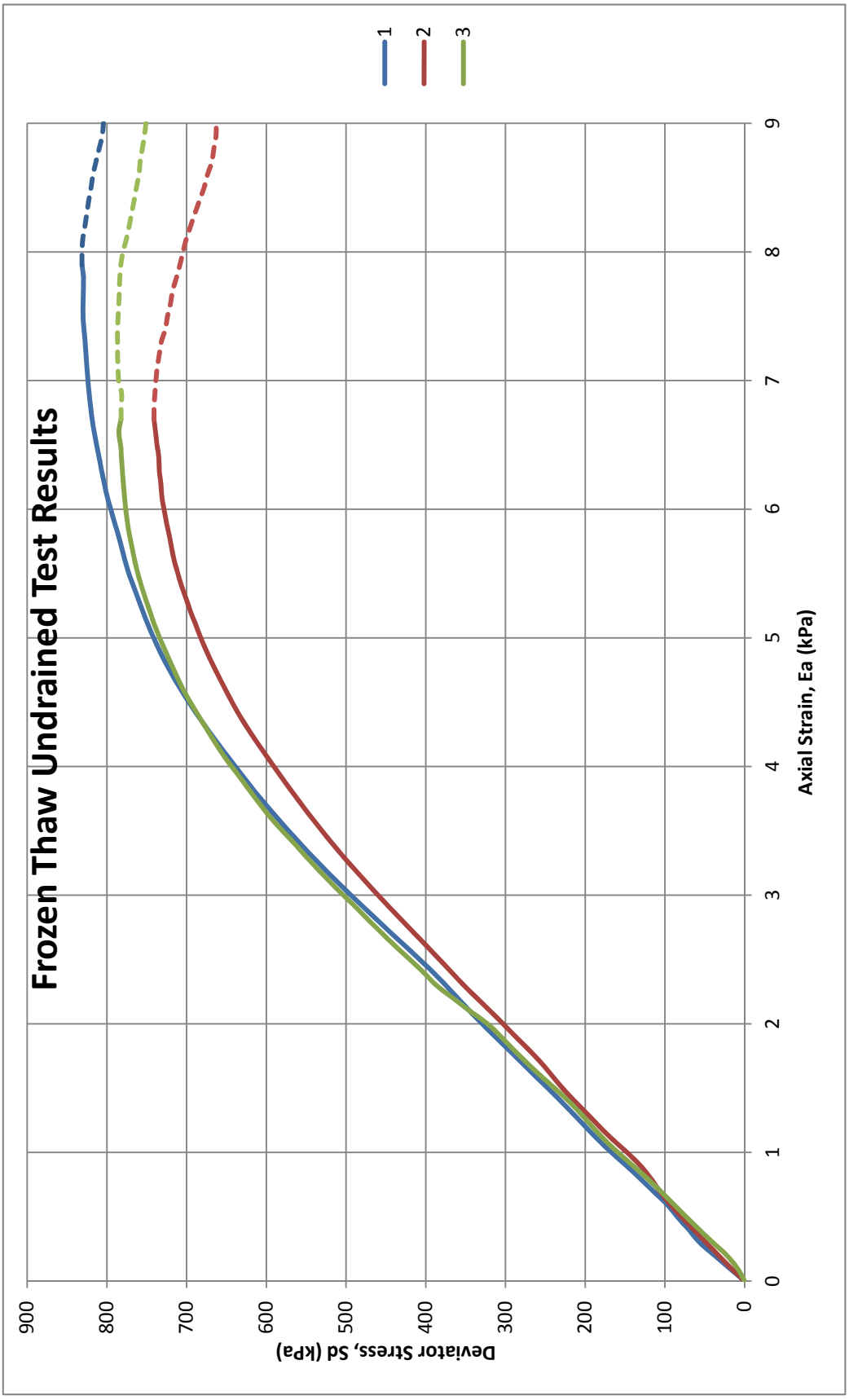
Frozen Thaw Undrained Test Results
Deviator Stress, Sd (kPa)
0
100
200
300
400
500
600
700
800
900
Axial Strain, Ea (kPa)
0
1
2
3
4
5
6
7
8
9
1
2
3

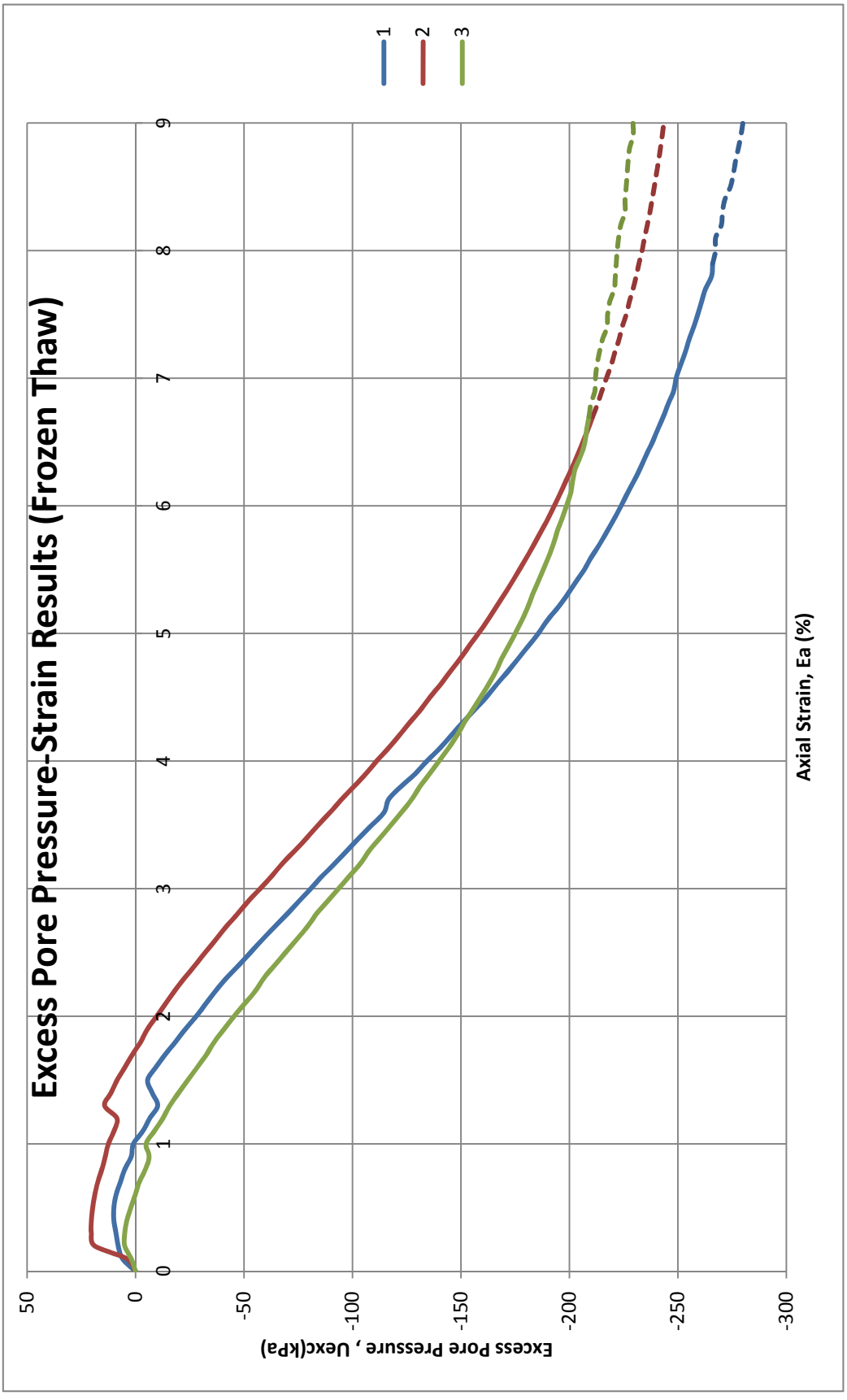
Excess Pore Pressure-Strain Results (Frozen Thaw)
Excess Pore Pressure , Uexc(kPa)
50
0
-50
-100
-150
-200
-250
-300
0
1
2
3
4
5
6
7
8
9
Axial Strain, Ea (%)
1
2
3

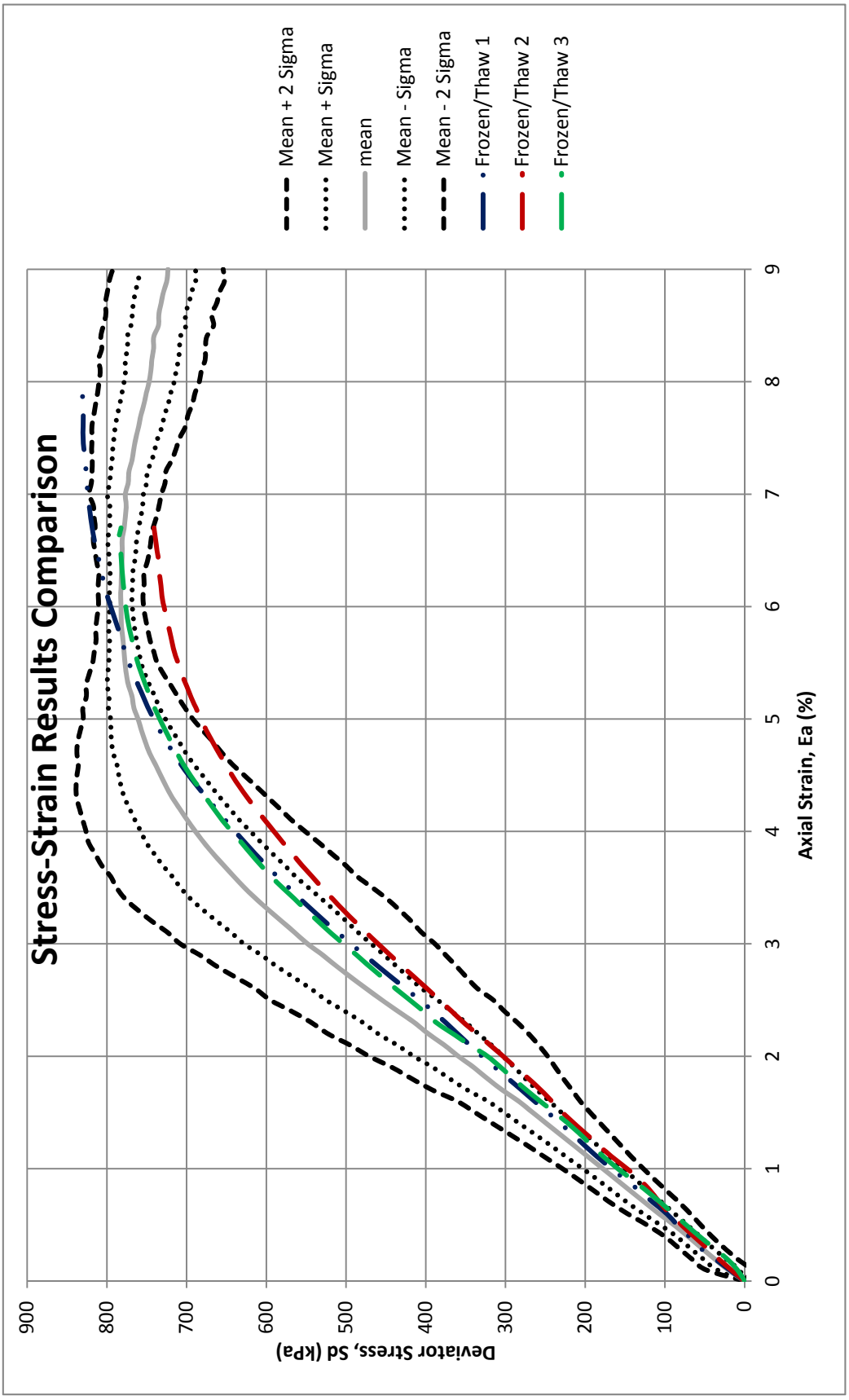
Stress-Strain Results Comparison
Mean + 2 Sigma
Mean + Sigma
mean
Mean - Sigma
Mean - 2 Sigma
Frozen/Thaw 1
Frozen/Thaw 2
Frozen/Thaw 3
Deviator Stress, Sd (kPa)
0
100
200
300
400
500
600
700
800
900
Axial Strain, Ea (%)
0
1
2
3
4
5
6
7
8
9

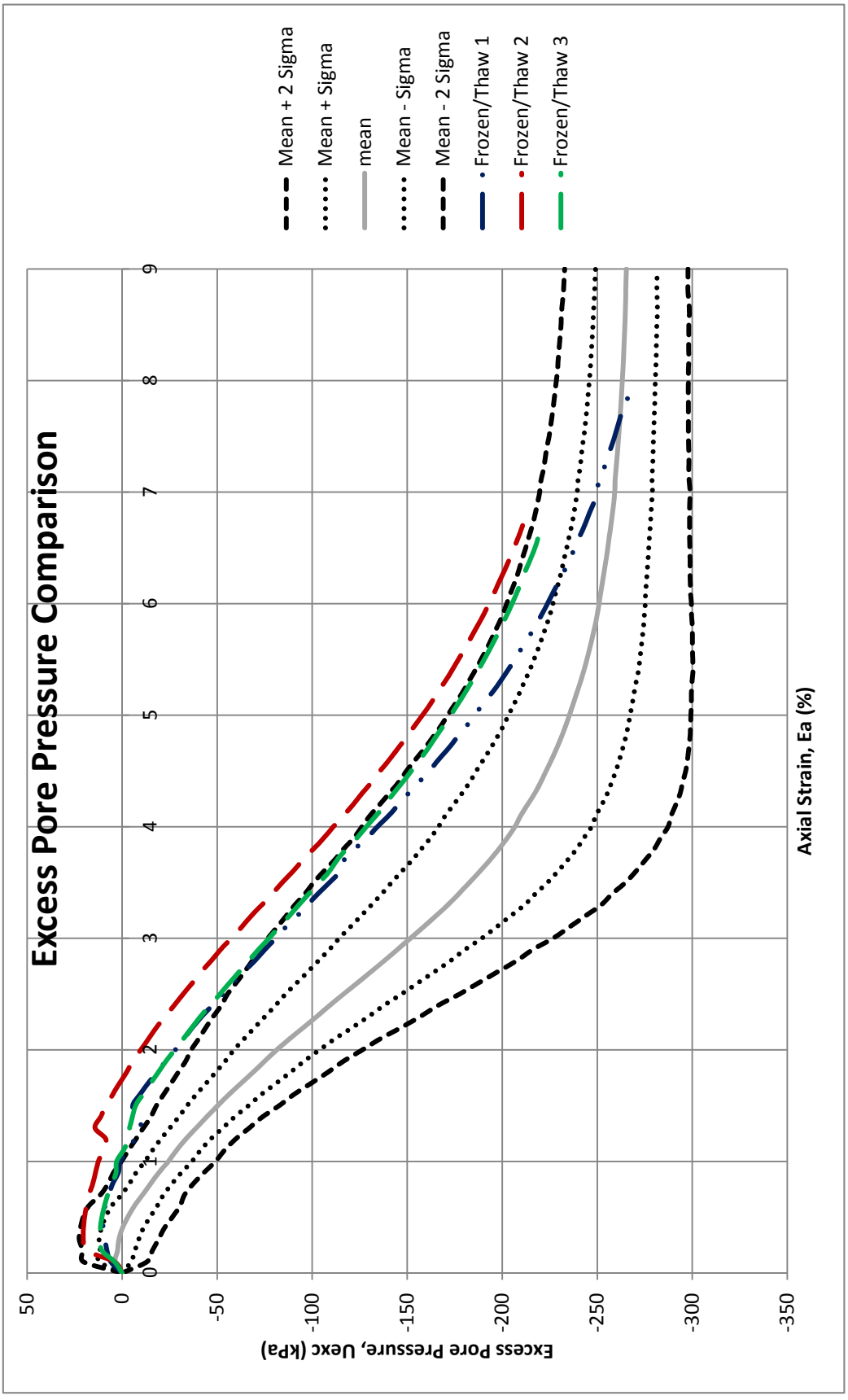
Excess Pore Pressure Comparison
Mean + 2 Sigma
Mean + Sigma
mean
Mean - Sigma
Mean - 2 Sigma
Frozen/Thaw 1
Frozen/Thaw 2
Frozen/Thaw 3
Excess Pore Pressure, Uexc (kPa)
50
0
-50
-100
-150
-200
-250
-300
-350
Axial Strain, Ea (%)
0
1
2
3
4
5
6
7
8
9

Stress-Strain Curves Comparison

		Excess pore water pressure, Uexc									
		Unfrozen sand						Frozen			
Test Number		1	2	3	4	5	Mean	1	2	3	Mean
Axial strain, Ea	1%	202	180	145	184	145	171	167	148	159	158
	3%	601	587	441	563	439	526	494	460	503	486
	5%	759	790	728	767	702	749	741	682	734	719

1% @ 90% Confidence t-Test: Two-Sample Assuming Equal Variances

	Variable 1	*Variable 2*
Mean	171.2281	157.8333
Variance	642.8654	96.08333
Observations	5	3
Pooled Variance	460.6047	
Hypothesized Mean Difference	0	
df	6	
t Stat	0.854615	
P(T<=t) one-tail	0.212783	
t Critical one-tail	1.94318	
P(T<=t) two-tail	0.425566	
t Critical two-tail	2.446912	

3% @ 90% Confidence t-Test: Two-Sample Assuming Equal Variances

	Variable 1	*Variable 2*
Mean	526.4899	485.6756
Variance	6378.175	523.2023
Observations	5	3
Pooled Variance	4426.517	
Hypothesized Mean Difference	0	
df	6	
t Stat	0.840007	
P(T<=t) one-tail	0.216547	
t Critical one-tail	1.94318	
P(T<=t) two-tail	0.433095	
t Critical two-tail	2.446912	

5% @ 90% Confidence t-Test: Two-Sample Assuming Equal Variances

	Variable 1	*Variable 2*
Mean	749.082	719.0856
Variance	945.8231	1031.372
Observations	6	3
Pooled Variance	970.2657	
Hypothesized Mean Difference	0	
df	7	
t Stat	1.361882	
P(T<=t) one-tail	0.107719	
t Critical one-tail	1.894579	
P(T<=t) two-tail	0.215438	
t Critical two-tail	2.364624	

Excess pore water pressure comparison

		Excess pore water pressure, Uexc									
		Unfrozen sand						Frozen			
Test Number		1	2	3	4	5	Mean	1	2	3	Mean
Axial strain, Ea	1%	-24	-33	-5	-35	-34	-26	1	13	-5	3
	3%	-173	-180	-94	-160	-117	-145	-81	-57	-94	-77
	5%	-243	-272	-191	-237	-207	-230	-186	-158	-175	-173

t-Test: Two-Sample Assuming Equal Variances

1% @ 90% Confidence

	Variable 1	*Variable 2*
Mean	-26.344	2.89
Variance	153.1605	78.4561
Observations	5	3
Pooled Variance	128.259	
Hypothesized Mean Difference	0	
df	6	
t Stat	-3.53464	
P(T<=t) one-tail	0.006149	
t Critical one-tail	1.94318	
P(T<=t) two-tail	0.012298	
t Critical two-tail	2.446912	

3% @ 90 % confidence

t-Test: Two-Sample Assuming Equal Variances

	Variable 1	*Variable 2*
Mean	-144.808	-77.28
Variance	1407.177	335.6899
Observations	5	3
Pooled Variance	1050.015	
Hypothesized Mean Difference	0	
df	6	
t Stat	-2.85356	
P(T<=t) one-tail	0.014523	
t Critical one-tail	1.94318	
P(T<=t) two-tail	0.029046	
t Critical two-tail	2.446912	

5% @ 90 % confidence

t-Test: Two-Sample Assuming Equal Variances

	Variable 1	Variable 2
Mean	-230.046	-172.917
Variance	1023.825	194.1294
Observations	5	3
Pooled Variance	747.26	
Hypothesized Mean Difference	0	
df	6	
t Stat	-2.8617	
P(T<=t) one-tail	0.014369	
t Critical one-tail	2.446912	
P(T<=t) two-tail	0.028738	
t Critical two-tail	2.968687	

t-Test: Two-Sample Assuming Equal Variances

1% @ 95 % confidence

	Variable 1	*Variable 2*
Mean	-26.344	2.89
Variance	153.1605	78.4561
Observations	5	3
Pooled Variance	128.259	
Hypothesized Mean Difference	0	
df	6	
t Stat	-3.53464	
P(T<=t) one-tail	0.006149	
t Critical one-tail	2.446912	
P(T<=t) two-tail	0.012298	
t Critical two-tail	2.968687	